Improving Classification System to Detect Cyclic Alternation Pattern Using Sleep EEG

by

Dina Samaha

A thesis submitted to the
School of Graduate and Postdoctoral Studies in partial
fulfillment of the requirements for the degree of

Master of Applied Science in Electrical and Computer Engineering

Electrical, Computer, and Software Engineering / Faculty of Engineering and Applied Science

University of Ontario Institute of Technology (Ontario Tech University)

Oshawa, Ontario, Canada

August 2023

THESIS EXAMINATION INFORMATION

Submitted by: **Dina Samaha**

Master of Applied Science in Electrical and Computer Engineering

Thesis title: **Improving Classification System to detect Cyclic Alternation Pattern Using Sleep EEG**

An oral defense of this thesis took place on August, 2023 in front of the following examining committee:

Examining Committee:

Chair of Examining Committee	Dr. Khalid Elgazzar
Research Supervisor	Dr. Mikael Eklund
Examining Committee Member	Dr. Ruth Milman
University Examiner	Dr. Jing Ren

The above committee determined that the thesis is acceptable in form and content and that a satisfactory knowledge of the field covered by the thesis was demonstrated by the candidate during an oral examination. A signed copy of the Certificate of Approval is available from the School of Graduate and Postdoctoral Studies.

ABSTRACT

Cyclic alternative patterns (CAP) became an important tool to diagnose sleep disorders. This study aims to have a better understanding of CAP, as the clinical applications remain limited as CAP analysis is a time-consuming activity; the goal of this thesis research is to improve the automatic classification system used to detect CAP in sleep. To determine the highest accuracy at detecting CAPs, MATLAB's classification learner app trains and tests the extracted features' characteristics against different classifiers. The combination of these selected characteristics and proposed classifiers can effectively measure the degree of change in brain state between non-CAPs and Caps. Time domain characteristics are computed from the signal amplitude values like Tsallis entropy, Renyi entropy, and Shannon entropy. In this study, the Hilbert-Huang Transform (HHT) and FFT characteristics provide information about the frequency characteristics of CAP phases. A cross-validation procedure is used in MATLAB model validation to estimate the performance of the classifier. CAP detection in healthy patients was more effective using time-based entropy features and KNN classifiers than frequency-based ones. With higher accuracy up to 90%, time-based entropy features performed better for insomnia patients.

Keywords: Cyclic Alternating Pattern; FFT; Classification; EEG signal; Sleep

AUTHOR'S DECLARATION

I hereby declare that this thesis consists of original work of which I have authored. This is a true copy of the thesis, including any required final revisions, as accepted by my examiners.

I authorize the University of Ontario Institute of Technology (Ontario Tech University) to lend this thesis to other institutions or individuals for the purpose of scholarly research. I further authorize University of Ontario Institute of Technology (Ontario Tech University) to reproduce this thesis by photocopying or by other means, in total or in part, at the request of other institutions or individuals for the purpose of scholarly research. I understand that my thesis will be made electronically available to the public.

Dina Samaha

STATEMENT OF CONTRIBUTIONS

In this thesis, I certify that I am the sole author and that no part of this thesis has been published or submitted for publication. I have cited ideas, research techniques, or other materials that are the property of others using standard referencing practices. In addition, I hereby certify that the creative works and/or inventive knowledge described in this thesis are my own original creations.

ACKNOWLEDGEMENTS

I would like to take this opportunity to express my deepest gratitude to the individuals who have supported me throughout my thesis work. Without their encouragement, assistance, and unwavering support, this accomplishment would not have been possible.

First and foremost, I would like to extend my heartfelt appreciation to Dr. Mikael Eklund for his invaluable guidance and mentorship. His insights, suggestions, and constructive feedback were instrumental in shaping this thesis and improving its quality. I am truly grateful for the time and effort he invested in my work.

I also want to extend my sincere thanks to my beloved family, especially my dad and mom, for their unconditional love, encouragement, and support. Their unwavering faith in me gave me the strength and motivation to overcome the challenges that I encountered during this journey. I am blessed to have them in my life.

Furthermore, I want to express my gratitude to my loving husband and kids, who have been my pillars of strength and support throughout this journey. Their unwavering patience, understanding, and encouragement provided me with the motivation and inspiration to pursue my academic goals while also fulfilling my family responsibilities.

Last but not least, I would like to thank all of my friends and colleagues who have been there for me during this time. Their words of encouragement, support, and friendship have been a source of strength and inspiration throughout my academic journey.

In conclusion, I would like to express my heartfelt gratitude to all those who have supported me throughout this thesis journey. Your contributions have been invaluable, and I am deeply grateful for your presence in my life.

TABLE OF CONTENTS

LIST OF TABLES

LIST OF FIGURES

LIST OF ABBREVIATIONS AND SYMBOLS

ANN	Artificial Neural Network
AASM	American Academy of Sleep Medicine
BCI	Brain computer interface
CAP	Cyclic Alternating Pattern
DWT	Discrete Wavelet Transform
ECG	Electrocardiogram
EEG	Electroencephalogram
EMG	Electromyogram
EOG	Electrooculogram
FFT	Fast Fourier Transform
FMRI	Functional Magnetic Resonance Imaging
FN	False Negative
FP	False Positive
HHT	Hilbert-Huang Transform
IFCN	International Federation of Clinical Neurophysiology
KNN	K-Nearest Neighbor
LDA	Linear Discriminant Analysis
MRMR	Minimum Redundancy Maximum-Relevance
NREM	Non-rapid eye movement
PCA	Principal Component Analysis
PET	Positron Emission Topography
R&K	Rechtschaffen and Kales rules
REM	Rapid eye movement
RF	Random Forest

SDB	Sleep Disorder Breathing
SSM	Sequential Selection Method
SVM	Support Vector Machine
SWS	Slow Wave Sleep
TN	True Negative
TP	True Positive
WT	Wavelet Transfor

Chapter 1: Introduction

Human sleep during various stages of life has gained extensive attention from researchers. Scientists can diagnose and treat physiological and neurological disorders by analyzing sleep stages. These disorders include for example apnea and insomnia. Sleep analysis is usually done based on polysomnographic recordings of the patient, such as electroencephalogram (EEG), electrooculogram (EOG), Chin electromyogram (EMG), and electrocardiogram (ECG), during their sleep. The identification of the sleep stages (scoring) is performed manually by experts (electroencephalographers) by dividing the entire sleep record into epochs of 30s and assigning each epoch a certain sleep stage. The scoring procedure is characterized by the presence of certain waves embedded in the recorded ECG signal [20].

Each sleep stage is characterized by the presence of the EEG waves and events as well as their duration. The sleep architecture is based on the cyclic alternation of two major neurophysiological states NREM which is non-rapid eye movement and REM which is the rapid eye movement during sleep.

1.1 Objective

The CAP sequence is made up of CAP cycles. Each cycle includes two main phases A and B; the CAP cycle usually starts with phase A and ends with the second phase B, and each phase is about 2-60 seconds in duration. CAP detection aids in the diagnosis of sleep disorders such as insomnia, depression, periodic limb movements, and epilepsy. In the literature, there exist many studies available to companies developing CAP scoring systems; this thesis approach is to build on the previous research and use it as a foundation for the development of a new improved algorithm for identifying CAPs in the sleeping brain. This study aims to improve the classification methods studied in the original paper [35] in order to increase the accuracy of CAP detection by using different features' characteristics with different classification methods in order to offer an alternative approach with higher accuracy. It is imperative to determine the accuracy of

the algorithm-produced data compared to that generated by the currently available solution. The dataset chosen from the research resource for complex physiologic signals of PhysioNet [16], this website offers an extensive list of projects with their databases. The CAP annotations (i.e. extracted from PhysioNet) are not simulated but rather utilized as a time frame to determine the CAP event in the EEG signal and the CAP duration.

1.2 Problem Domain

Recent research shows CAP represents an unstable NREM component of the sleep EEG. CAP is seen both in adults and children's sleep. It is therefore used not only for sleep disorders but also for the diagnosis of many other brain diseases. To understand CAP, the EEG signal and its details are discussed. In addition, a brief description of EEG uses and the methods of its recording will be provided in later chapters.

There has been extensive evidence that CAP parameters offer more comprehensive information and are considerably more sensitive than conventional sleep measures. CAP scoring is time-consuming and compromises the method's effectiveness. In other words, only the availability of an adequate system for CAP automatic detection can make it an easily consumable tool [43]. Classifying CAP EEG analysis is a valuable tool for assessing sleep quality and identifying sleep disorders. It has the potential to improve the diagnosis and treatment of sleep disorders and has shown promising results in research studies.

1.3 Methodology

In this study, EEG CAPs are used to detect characteristics related to Normal, Sleep Disorder Breathing (SDB), and Insomnia subjects, by building machine learning multiple classifiers taking many features' characteristics measure as predictors. These features include FFT and four entropy methods including Shannon, Tsallis, Renyi, Sample Entropy, and the last feature is Hilbert-Huang Transform (HHT). Using multiple classifiers with a variety of features increases the validation accuracy of the proposed classification model. In addition, it shows that combining many features as predictors with various classifiers will result in a higher validation and accuracy score than other research studies applied.

This can be achieved by extracting the desired time-based and frequency-based features from the EEG sleep data set, in the latest stage of the research to select appropriate machine learning algorithms for developing a new model and testing them for accuracy, errors, and precision, if possible. The study is applied to 11 subjects, 4 have normal sleep, 4 with SDB, and 3 with insomnia. The research process starts with determining the types of data and information available for research as follows.

Feature extraction is possibly the most critical step in signal processing. This step aims to create a manageable and meaningful representation of the original EEG signal (although clean), to maximize the potential success of qualifiers and in turn the overall system performance. Implementation of different machine learning algorithms to estimate which one is best adapted to this problem. After running feature codes, then compile the results in a table to be sent to the Classifier App. The data is trained to obtain a confusion matrix. The analysis is run multiple times for different features. The idea is to utilize results from the feature extraction step to detect or target CAP event signals for healthy and non-healthy patients by analyzing the features codes to see which features best locate the CAP events and compare the machine learning classifiers. Many classifiers are tested for signal classification, and although these methods succeed in many classification problems, in this study four methods have been applied. These methods are K-Nearest Neighbor (KNN) and Random Forest (RF), SVM, and LDA classifiers. The software used to analyze the records is MATLAB. The code was written from scratch and can be found at the end of the thesis document.

1.4 Contribution of thesis work

One key improvement in this thesis work is the incorporation of frequency-based features using a fast Fourier transform (FFT) in the feature extraction process. This allows for a more comprehensive analysis of EEG signals and captures the cyclic patterns more accurately. It provides a detailed representation of the signal's frequency components and magnitudes. By utilizing frequency domain information, the classification model can better differentiate between CAP and non-CAP segments in EEG signals.

Furthermore, the thesis aims to develop a learning model that could be flexibly applied to train subjects with different time and frequency-based characteristics. The proposed learning model is automating the system mode which enables the development of a versatile learning model that can be customized to handle various EEG CAP recording characteristics. This adaptability, achieved through the automation of individual modules, empowers the model to effectively learn from range of datasets, generalize across different subjects, and accurately classify CAP patterns. As a result of this flexibility, the model will be able to be applied to a variety of datasets and its generalizability will be improved. By training the model on different subjects, it becomes robust and capable of accurately classifying CAP patterns in diverse EEG recordings.

Overall, the thesis contributes by enhancing the classification accuracy of detecting cyclic alternating patterns in EEG through the addition of the Random Forest Classifier. It also includes frequency-based characteristics extracted using a fast Fourier transform. The flexibility of the learning model also enabled the training of more subjects with different time and frequency-based characteristics, expanding its applicability and potential impact in EEG analysis.

1.5 Conclusion

Overall, chapter 2 covers the theoretical background and motivation for this study, and provided a literature review of different key components of EEG signal analysis and CAP detection. Chapter 3 illustrates CAP EEG detection processing consists of five significant stages; preprocessing, feature extraction, feature selection, and feature classification which are explained in detail with results and discussions in chapter 4. By assessing more patients, using more classifiers, and comparing time-frequency-based features to conventional and non-conventional features, this study can be improved. Chapter 5 highlights the key conclusions drawn from the study and outlining potential avenues for future work. It typically brings together the findings, implications, and limitations of the research while also suggesting directions for further exploration.

Chapter 2: Theoretical background and Literature review

Sleep is crucial to an individual's performance and development; approximately 50 – 70 million people experience a type of sleep disorder in the United States [1-2]. Cyclic Alternative Patterns (CAP) have become a crucial tool used in sleep analysis to diagnose sleep disorders. The purpose of this chapter is to present a detailed background review of Electroencephalography (EEG), the role of CAP in sleep analysis, and the various methods for CAP detection.

In Chapter 2, the theoretical background and literature review of the study are presented. The chapter starts with an introduction to EEG and recording techniques. The various frequency bands of EEG signals are discussed in detail, along with the mathematical model of EEG signals. The chapter then delves into Sleep Stages Architecture, providing an overview of the different sleep stages and their characteristics. The focus then shifts to Cyclic Alternating Patterns (CAP) and its EEG features, CAP sequence, cycles, non-CAP, and measurements of CAP. Next, general features and classifiers for EEG signals from the literature are presented. These include popular proposed methods and procedures for CAP detection in EEG. Finally, the chapter concludes with an overview of the various classification tools used in EEG signal analysis, including Linear Discriminant Analysis (LDA), Support Vector Machine (SVM), K-Nearest Neighbor (KNN), and Random Forest (RF). Overall, this chapter provides a comprehensive understanding of the theoretical background and literature review of EEG signal analysis and CAP detection.

2.1 – Background Electroencephalography (EEG)

EEG records the electrical activity of the brain which refers to recordings that are captured over a period of time [1]. Hans Berger measured EEG for the first time in 1929[1]. EEG became an all-important medical tool to visualize and record electrical activities in the human brain [1-3]. Technologies such as Positron Emission Topography (PET) and Functional Magnetic Resonance Imaging (FMRI) also capture various brain activities but differ from EEG as they illustrate variations in blood flow or metabolic activities rather

than direct electromagnetic signaling [2-3]. EEG is sometimes called the brain wave test and is a non-invasive test for patients with several brain disorders [3].

The stimulation of brain cells results in a flowing current, and the flowing current in turn generates electrical dipoles with a potential difference between them. The electrical dipoles are between apical dendrites which mostly branch from neurons. In addition, the electromagnetic current produced in the brain is comprised of basic elements such as Chloride, Potassium, and Sodium ions [1]. EEG has been recognized as a well-established methodology for studying brain waves and activities. By using EEG, neuroscientists realized that the human species produces electromagnetic activities around the 20th day of development. A typical healthy and normal amplitude exasperating from a human body is around 10 and 100 microvolts and a frequency of about 1 HZ to 100 HZ [52].

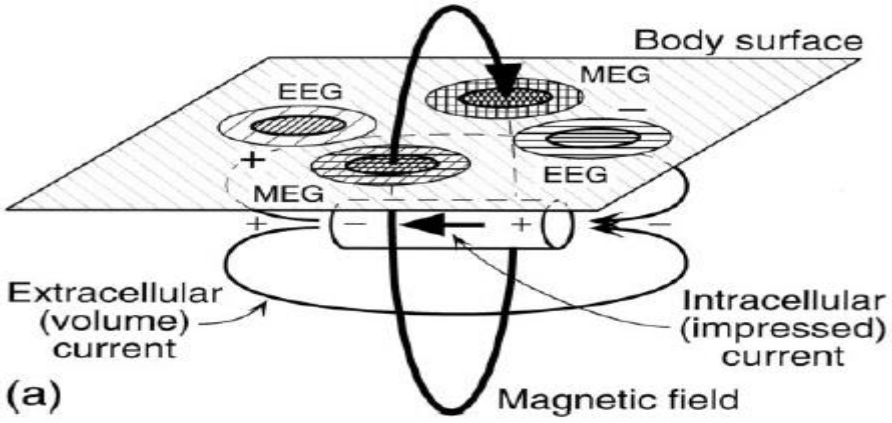

Figure 2-1 Illustration of current flowing and producing an electric dipole with a potential difference [4].

The recording of neuron activities in the brain through EEG uses potential differences between two electrodes, the reference electrode and the signal electrode. These electrodes are essentially placed on the scalp of the subject in order to retrieve signals from the scalp.

In 1958 a standardization for electrode placement known as the 10-20 system was recognized by the International Federation of Clinical Neurophysiology (IFCN) of the EEG Society [3]. Through the standardized system, the head is divided into two equal parts to ensure all brain regions are equally covered.

The electrodes are labeled according to the parts of the brain covered. Segment names are assigned using the first letter of the segment. For example, F is for frontal, O is for occipital, P is for posterior, C is for central, and T is for temporal. The right-hand side of the brain is marked with even numbers while the left-hand side is marked with odd numbers, as shown in Figure 2-2a. The scalp is divided into four categories; the naison, the inion, the left preauricular points, and the right preauricular points [54]. The area between the nose and the forehead is called the naison and the bottom area of the scalp is the inion in Figure 2-2b. The letters and numbers utilized refer to the part of the brain where the activity is occurring and on which side (right or left hemisphere). The EEG electrodes are placed in a 10-20 system at the scalp surface. The 10-20 system is defined as the placement of EEG electrodes in a 10% or 20% diagonal pattern from front to back

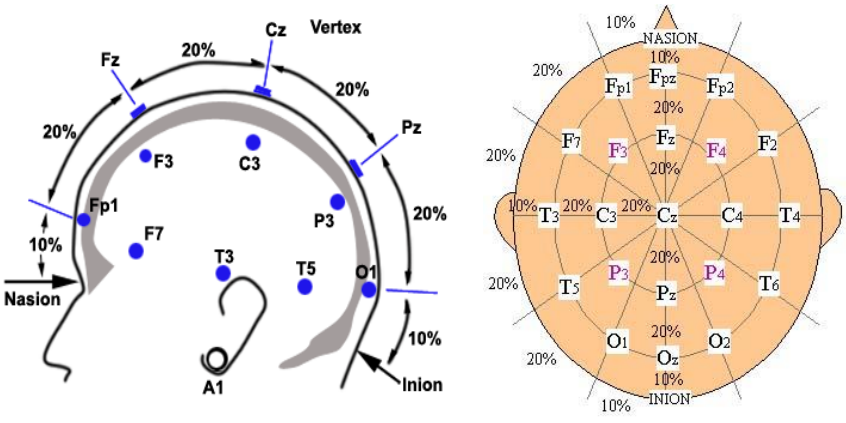

Figure 2-2 EEG electrode placement a: Electrodes labeled according to brain parts [36] b: 10-20 system electrodes placed at scalp surface with labels [3,54]

or left to right area of the skull. When brain signals and waves are prepared to be recorded, electrodes are carefully placed on the scalp in special locations, and in a particular manner. It is important to clean the scalp prior to EEG electrode placement to optimize conduction [4]. These locations and placement orientations are determined by the recording technician who measures the scalp using the 10-20 system. This is shown in Figure 2-3 [3].

Reference electrodes are relevant to mention, as they are commonly used as relative points to all other electrodes while measuring electric brain activities. Typically, inactive

sites on the scalp are selected as reference zones; the left-right earlobes. Reference electrodes are highly utilized in focusing pathological brain activities [1,34].

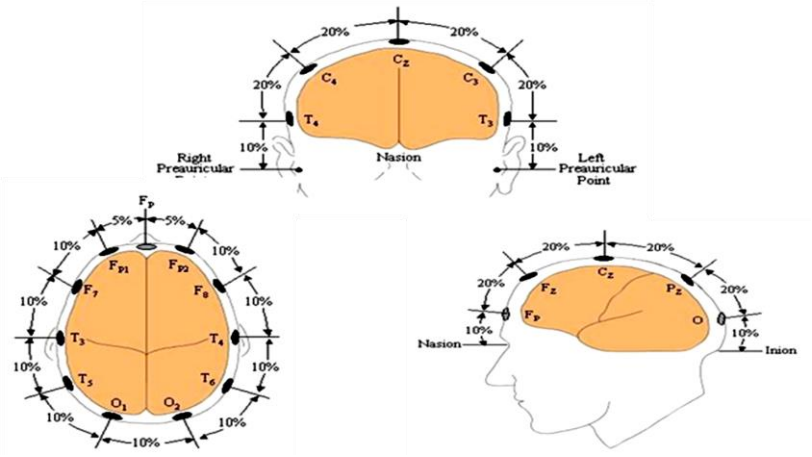

Figure 2-3: The international 10–20 system. The image of the right and left hemisphere of the brain [54]

2.1.2 - EEG Signal Recording Technique

EEG electrodes are a necessity for getting good-quality signals for recording and subsequent interpretation. Based on the characteristics of the electrodes, several electrodes are used in the EEG technique. These electrodes include needle electrodes, saline-based electrodes, headband electrode caps, and reusable disk electrodes. In order to record EEGs, the recording system will consist of the following: electrodes with conductive media, amplifiers with filters, an A/D converter, and a recording device. The electrodes placed in a 10-20 system on the patients' scalp will read the microvolt signal that is then amplified by the amplifiers. The gel acts like a malleable extension of the electrode so that artifacts are less likely to be produced by electrode movement [3].

The gel maximizes skin contact and allows low-resistance recording through the skin. Once the signal is amplified, it is digitalized. The analog-to-digital converter transforms the signal electronically, as shown in figure 2-4.

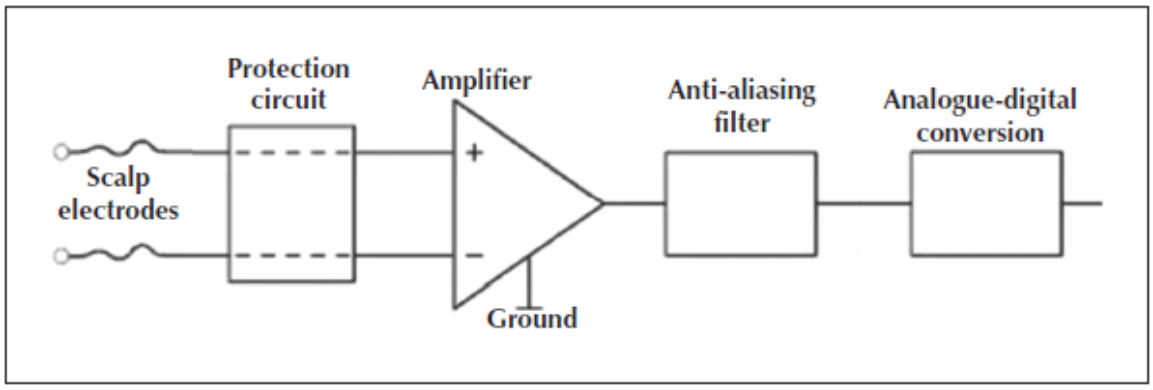

Figure 2-4: Conversion of analogue signal to digital [2]

The hardware components of the analog filters are integrated during the amplification process; the low-pass filters prevent signal distortion by interface effects with sampling rates. This is called aliasing and occurs when frequencies greater than one-half of the sample rate survive without reducing. The data is then stored on a recording device (computer) [3] as shown in Figure 2-5.

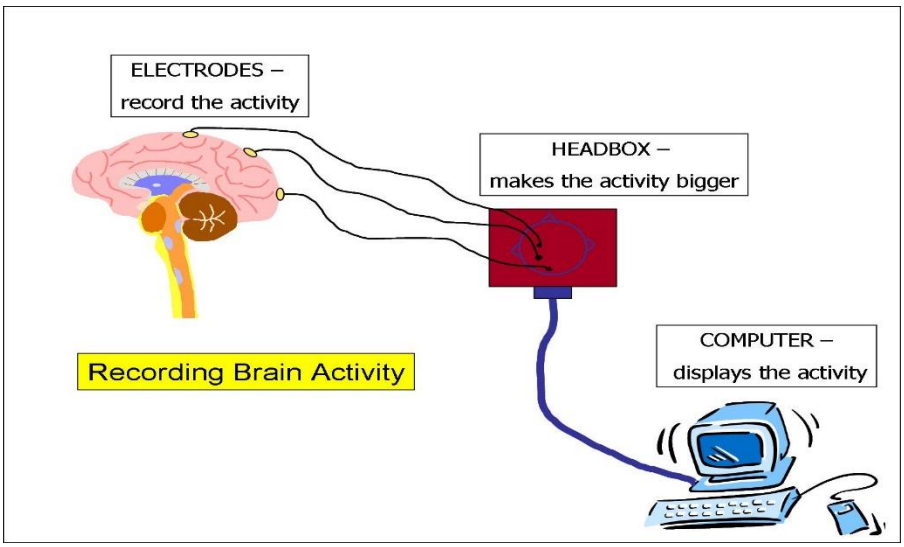

Figure 2-5: The Electroencephalogram (EEG) Test. http://www.bcchildrens.ca/our-services/hospital-services/diagnostic-neurophysiology-eeg-emg/electroencephalography-(eeg)

The analog signal is frequently sampled over a fixed time interval and each sample is converted to a digital sample by an A/D converter. The converter is the interface between the sample and the computer. The converter resolution is obtained by dividing the converter voltage by 2 and raising it to the power of the number of bits associated with the converter. Typical A/D converters utilize 12 bits and resolve 0.5 microvolts. Below

Figure 2-6 shows a flow chart outlining the general steps required to translate raw electrical signals picked up by the EEG electrodes to an understandable output.

Figure 2-6: Different Steps of EEG Signal Processing

The first step is to record raw signals, which undergo pre-processing. Depending on the brain study performed, the most significant features will be extracted for classification. The EEG signal is the foundation of a brain-computer interface (BCI), and proper feature selection and classification are highly important. Figure 2-7 illustrates different recordings of raw EEG signals from set A healthy volunteers with eyes open, set C from the hippocampal formation of the opposite hemisphere of the brain, and set E epilepsy patients during epileptic seizures.

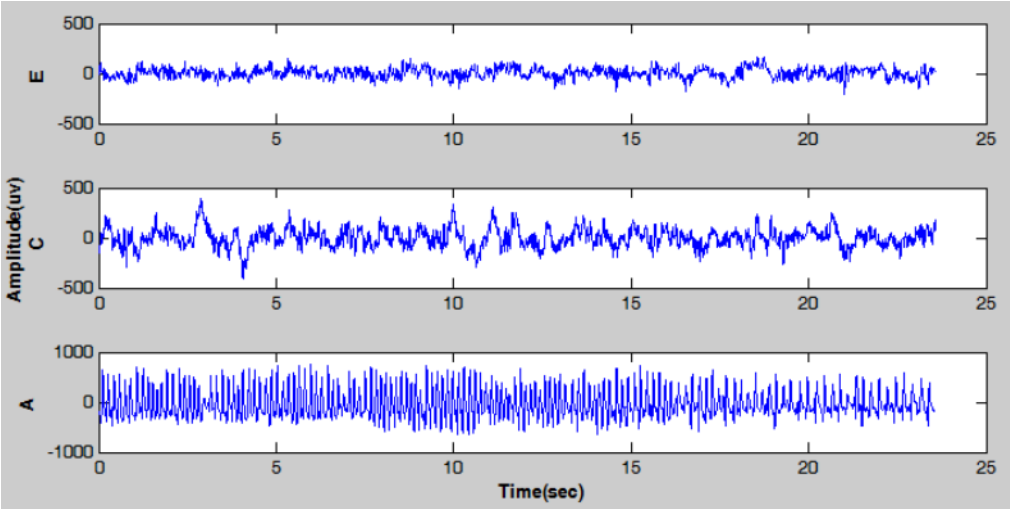

Figure 2-7: Raw EEG signal obtained from three different classes of EEG signals from different subjects A, C,E [57].

2.1.3 EEG Signal Frequency Bands

EEG waveforms are classified according to frequency, amplitude, shape, and the sites on the scalp at which they are recorded. Most of the useful information about the human brain's functional state lies in five major brain rhythms distinguished by their different frequency bands. These frequency bands are delta, theta, alpha, beta, and gamma. Figure

2-8 shows the types of waves picked up by EEG. These waves constitute the EEG background and vary according to overall neurophysiological state; that is, wakefulness, non-rapid eye movement (NREM), and rapid eye movement during sleep (REM) as clarified in Table 2-1.

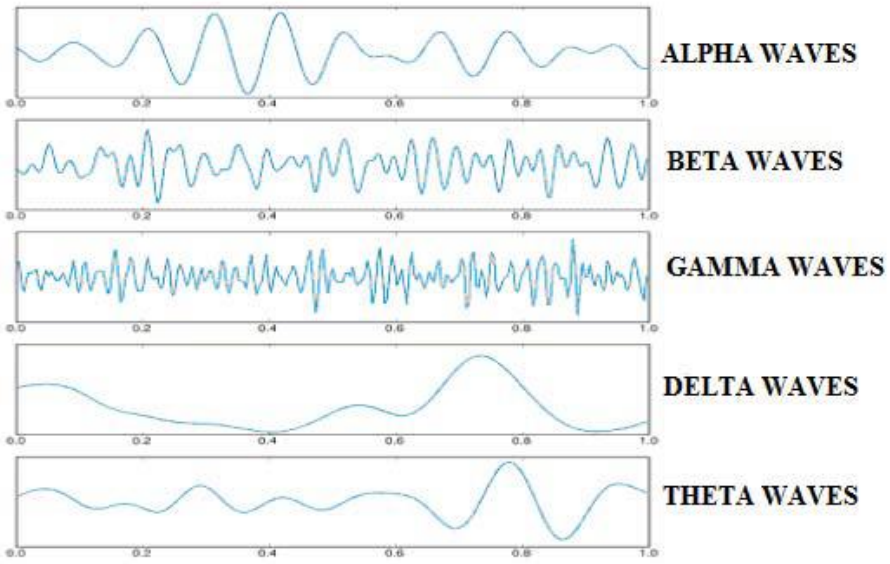

Figure 2-8: Wave shapes for different frequency bands of EEG signal in the brain [56]

Brain waves are often measured from peak to peak and utilizing the Fourier transform spectrum, where sine waves with various frequencies are visible, can derive a raw EEG signal.

EEG frequency is a measurement of repeated activity within the brain spectrum over time. Frequency domain analysis encompasses how a signal is represented by frequency components. The frequency domain is preferred over the time domain for EEG signal measurement. This is because the frequency domain provides temporal information about window size in contrast to the time domain where it does not. Better results can be extracted from window estimation. The time domain is sometimes known as time-dependent analysis and uses mean, energy, and power formulas. Table 2-1 below shows the EEG waveforms subdivided into five frequency band categories. The frequency bands aid in monitoring and diagnosing different sleep disorders and are useful for CAP

detection in EEG. Typically, α bands illustrate how calm an individual is, while β frequency bands illustrate attention

Waves	**Frequencies per second**	**Amplitude in µV**	**Characteristics**
Delta-waves ς - Delta	0,5 - 3	5 - 250	Abnormality in waking adults. In healthy people don't exit Accompaniment of deep sleep
Theta-waves θ - Theta	4 - 7	20 - 100	Strictly rhythmic or highly irregular Awake & drowsiness or light sleep stages
Alpha-waves α - Alpha	8 - 13	30-50, mainly below 50	Awake, eyes closed, mental inactivity, physical relaxation,
Beta-waves β - Beta	14 - 30	5 - 30, mainly below 30	Produce high and intense spike-waves over 35 Hz, Active thinking, active attention

			Categorized as of light sleep stages (wakefulness)
Gamma-waves γ - Gamma	31 - 60	Less than 5	Legality of appearance and site not well established Highly related to the decision-making mode

Table 2- 1 EEG Frequency Spectrum [56]

2.1.4 Mathematical model of Electroencephalograph Signal

EEG data analysis presents a challenge because it is recorded at low resolution. Therefore, the signal recorded may be corrupted with a certain degree of uncertainty. EEG signal is significant both for neural and cognitive engineering because of its ability to measure brain activities at various sites on the scalp. The EEG signal can be analysed in various dimensions. Since the EEG signal is continuous, temporal activity can be identified by signals from multiple locations over a given period “t”.

If the sampling is done at intervals of T then the EEG approximation becomes:

$$X[n]=X(nT); \qquad n=1;2;3\ldots\ldots. \qquad (2\text{-}1)$$

Where X[n] is the discrete time signal recorded at intervals of t=T, 2T…….; nT and is measured directly from the brain. The behaviour of the signal over a period of time is called the dynamic of the signal and is labelled z[n] [41]. The resultant behaviour can be calculated by summing up the true signal and noise due to other factors. Mathematically this becomes;

$$X[n]=X[n]+\dot{\eta}[nT]; \qquad n=1,2,3\ldots\ldots\ldots\ldots \qquad (2\text{-}2)$$

Where X(nT) is the value of the true signal when t=nT and $\dot{\eta}[nT]$ is the contamination due to factors such as noise. In cases where $\dot{\eta}[nT]$ is very small, X[n]= X(nT). True signals can be isolated from measured EEG signals as presented in Figure 2-6. The analysis process of a signal over a set range with time dependencies is called “Time Domain Analysis”.

During the EEG analysis process, the parameters include signal power, signal amplitude (energy) |X[n]|, the same as the signal period [41]. If an average of all the parameters is calculated according to time, the mean sequence will equal the EEG signal required. The average produces an estimate of the EEG signal over the time domain. Better resolution can be further produced using short window duration and extended behaviour from long window duration.

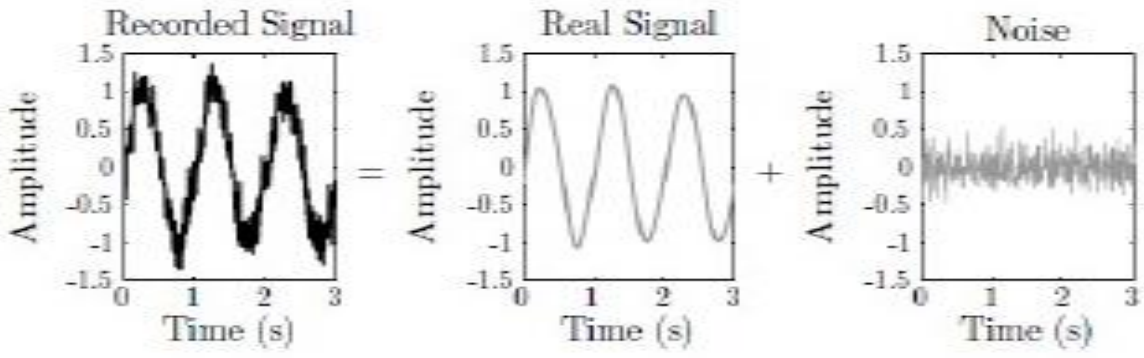

Figure 2-9 Recorded signal decomposed in true signal and noise [41]

2.2 – Sleep Stages Architecture

Human sleep patterns, configurations, and phenomena became research topics for researchers. Scientists and researchers realized that they could diagnose and treat some physiological and neurological abnormalities by analyzing the patient's sleep stages. These abnormalities include disorders such as sleep apnea, insomnia, and narcolepsy. The analysis can be conducted in various ways, including a method that uses a

polysomnographic recording of the patient, such as EEG. An example of a test to record patients' sleep and record EEG signals is shown in Figure 2-10.

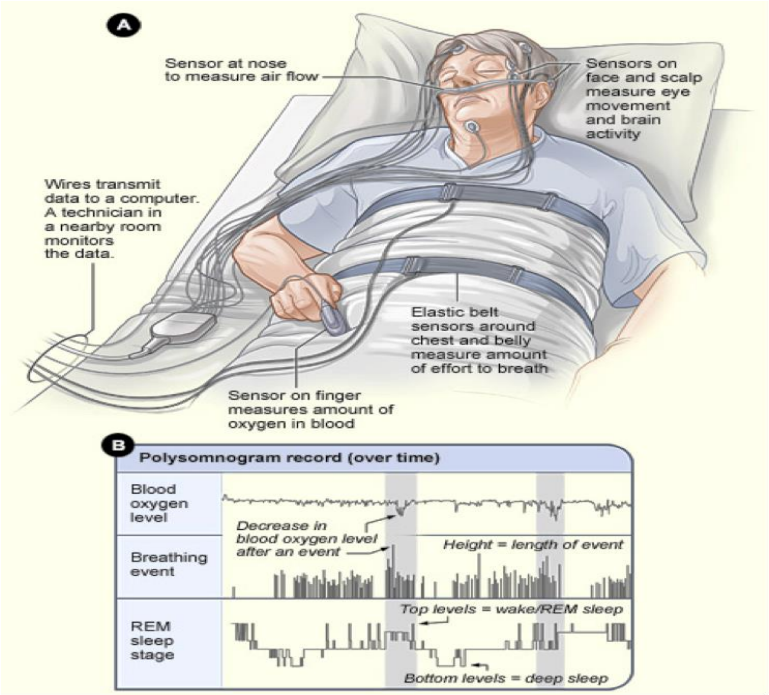

Figure 2-10 EEG Signal detection configuration of test subject. (a) components attached to sleeping subject (b) example of recordings [58].

Sleep architecture is based on the cyclic alternation of two major neurophysiological states; non-rapid eye movement (NREM) and rapid eye movement during sleep (REM). Sleep stage scoring has become the optimum standard for human sleep analysis.

A standardized manual for sleep scoring was developed in 1968 by Rechtschaffen and Kales (R&K) rules. The R&K rules divide sleep into 6 distinct stages: W (wake); non-rapid eye movement (non-REM [NREM]) stages S1, S2, S3, and S4; and REM sleep stages, stages 3 and 4, are called Slow Wave Sleep (SWS) [59]. In 2007, the American Academy of Sleep Medicine (AASM) updated the scoring manual, known as the AASM scoring manual. The AASM rules recognize five main sleep stages: wakefulness (Stage W), Stage N1, Stage N2, Stage N3, and Stage R (REM sleep). Figure 2-11 shows the difference in sleep-scoring terminologies used by R&K and AASM rules.

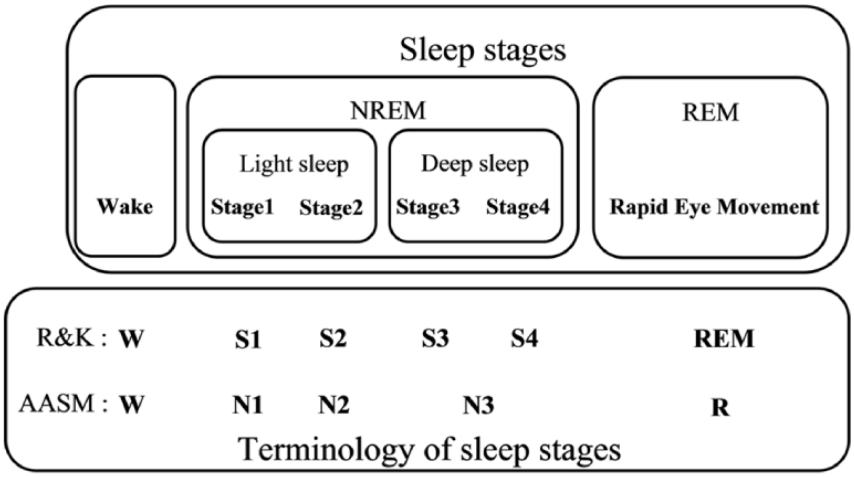

Figure2-11 Terminology used by R&K and AASM for sleep stages scoring [59]

According to the RK method, sleep-scoring trained individuals categorize each 20–30 second fraction into one of five primary sleep stages. This standardized manual is utilized for grading sleep stages that incorporate parameters and recordings of distinct brain rhythms shown through an EEG signal. These distinct brain rhythms are only visualized when the subject sleeps. In the R&K standardized manual, the EEG signal is separated into 30-second epochs. These epochs are selected and utilized based on their speed of 10 alpha spindles and their ability to be displayed on one page. The previously mentioned epochs are typically categorized into one stage. For two or more stages present during a singular epoch, the stage encompassing the majority of the epoch is the stage graded.

The greatest amplitude of an EEG signal, between 2 and 9 Hz, is found in the S1 stage. Furthermore, the alpha waves found in the EEG signal represent half of the total duration of the epochs. Slow rolling eye movements are evident. Sleep spindles and K complexes that range between frequencies 12 – 14 Hz are present in the S2 stage, whose presence classifies it as the second stage [48].

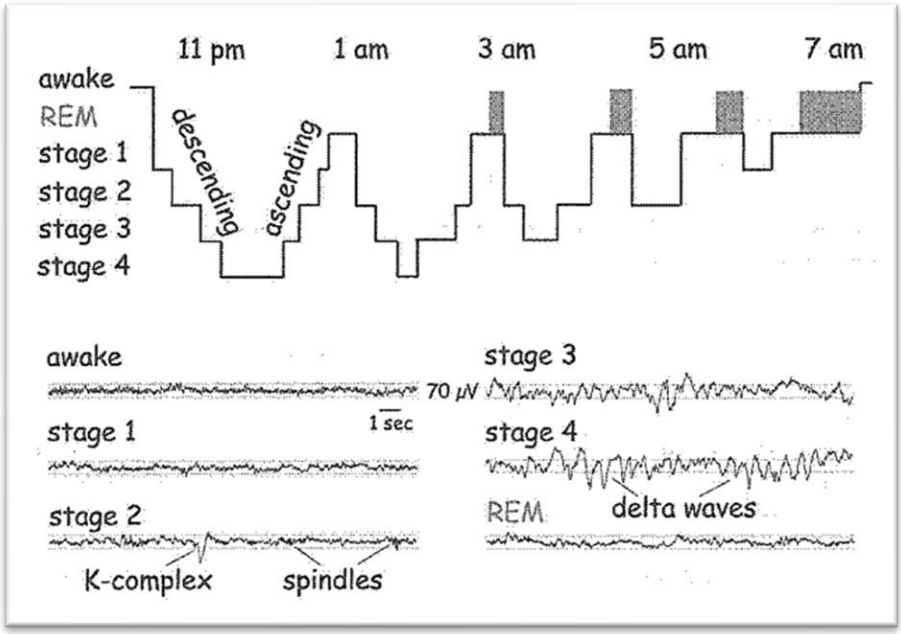

Figure 2-12 Different Stages of Sleep [55]

The grading for stage S2 is as follows: a total of two subsequent incidences of sleep spindles and K complexes lasting less than 3 minutes would result in a stage 2 grading. Stage S3 is referred to as the deepest sleep stage and has a frequency lower than 2 Hz associated with it. This is due to the possibility of sleep spindles and K complexes occurring during this stage. Typically, in stage S3, an EEG recording will encompass approximately 20%–50% of waves with a frequency of 2 HZ, and an amplitude exceeding than 75 μV. Figure 2-9 illustrates sleep stages. Following stage 3, stage 4 will encompass 50% of waves with a 2 Hz frequency and amplitudes higher than 75 μV. The rapid eye movement (REM) stage displays a mixture of frequencies and low voltages of an EEG signal. The conditions of the REM stage are most similar to stage 1, which is a sawtooth pattern of waves [53].

Throughout the sleep cycle, the EEG is broken down into four different waveforms in relation to their frequencies, as demonstrated in Figure 2-13

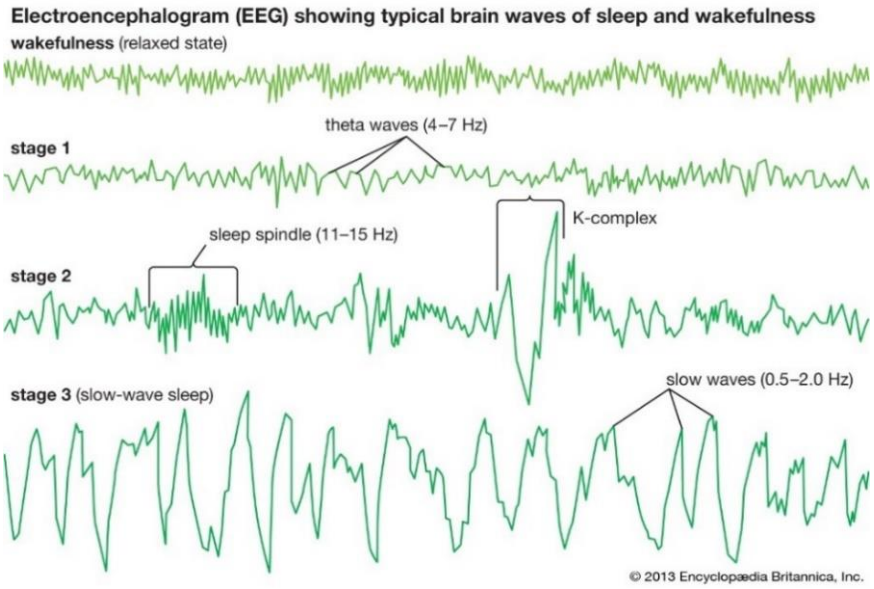

Figure 2-13 Zoom image showing EEG brain waves of sleep and wakefulness [adapted from Encyclopedia Britannica)]

Furthermore, at the REM stage, the EMG is at its lowest level. An EEG case where no arousal movements exist is comprised of comparatively low voltage and a mixture of frequencies. In addition, sleep spindles and K complexes, which are characteristics of stage 2, alternate between common features found in the REM stage, which is the lowest EMG level. The grading or scoring rubrics depend on the EMG or REM level being at the lowest stage.

2.3 Cyclic Alternating Patterns (CAP)

The Cyclic Alternative Pattern (CAP) is an EEG indicator of sleep disorders that measures sleep flexibility [43]. CAPs are repetitive patterns exhibited in the EEG during NREM sleep. They involve an initial phase of brain activation, known as Phase A, followed by a second phase of return to background activity, known as Phase B [21].

2.3.1 The EEG features of CAP

In normal sleep, regular EEG features of CAP are highly complex and typically multi-phased compared to coma-made sleep and fluctuations in various stages of sleep. CAP is apparent for all the sleep stages throughout the NREM stage. As mentioned, the first phase (A) is categorized via transient events, which are highlighted in the second phase's (B) contextual rhythmic cycle. In comparison to the period's phase B, the first phase may

be comprised of sluggish rhythms with higher voltages, a faster lower voltage, or a mixture of both patterns [22].

Physiologic CAP is observed to be different under certain conditions, which are health problems experienced by the patient. These may include insomnia, depression, epilepsy, and eating disorders. Furthermore, external factors can be an issue when performing or observing Physiologic CAP. External factors may include noise, temperature, etc. [16]. Sleep instability is associated with external and internal challenges in the sleep process and slow wave activity results in the brain's attempts to preserve sleep [38].

The EEG signal is used to quantify the electrical brain activity during the sleep stages of the subject. In addition to quantifying electrical brain activity, EEG offers the CAP feature, which is a microstructural feature.

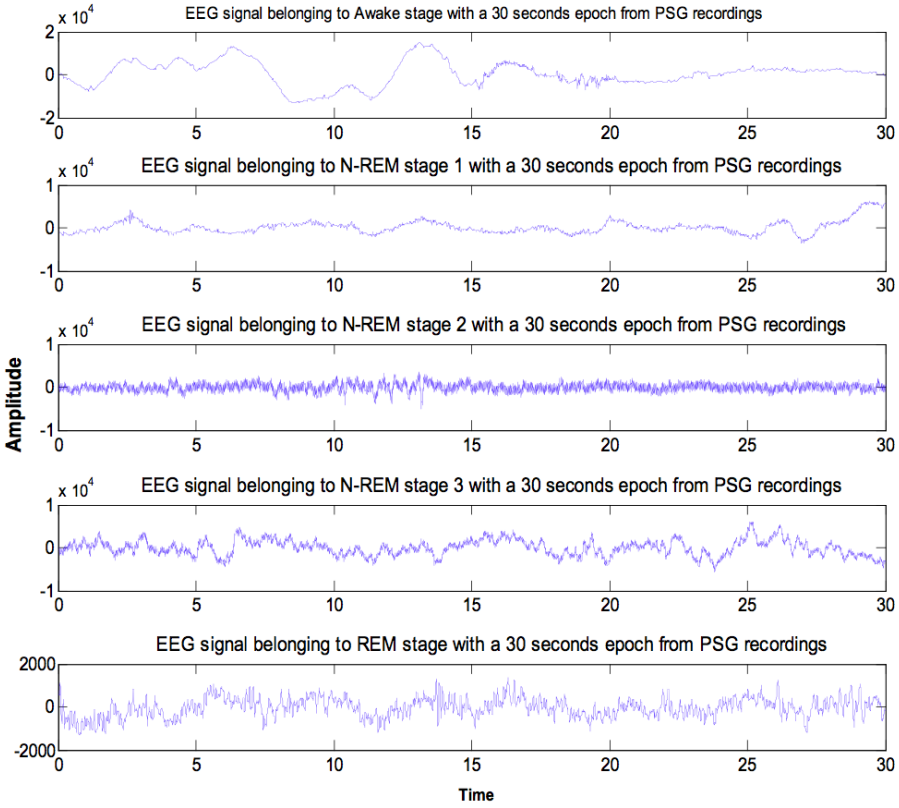

Figure 2-14 EEG signals recorded over a 30 seconds time interval for N-REM stage 1,2, and 3, along with REM stages recorded on a healthy subject [60]

Figure 2-14 illustrates the recorded EEG signals belonging to the previously mentioned sleep stages. This figure will help visualize where CAP occurs in EEG.

Analyzing the CAP feature is not intended to replace sleep stage or arousal grading. Instead, it is rather intended to expand quantifiable sleep analysis, in addition to proving a potentially new instrument to better comprehend sleep stages. CAP characterizes the NREM portion, or uneven sleep, found in children and adults during their sleep. It detects numerous brain and sleep disorders [19].

2.3.2 CAP Sequence

The CAP's periodic movement, which is made up of phases A and B, ranges between 2 seconds and 60 seconds per cycle (C), as demonstrated in Figure 2-12. CAP's phase A is detected by the observed occurrences in the non-REM stage and distinguishable in the contextual rhythmic cycle, which may include the following EEG patterns: Polyphasic and Delta bursts, intermittent and K-alpha, and vertex sharp transients. As previously stated, two sequences make up CAP and have no upper constraints on the total period or CAP cycles. In typical young adults, the estimated mean time for a typical CAP sequence with an average of six CAP cycles is 2 minutes and 30 seconds. For a CAP sequence with phase A, a grade is assigned only if a preceding phase A with a temporal range between 2 seconds – 60 seconds is present; this is to avoid a non-CAP categorization of the cycle [43]. Through plotting the statistical distribution of events at the commencement of subsequent A phases, the CAP time structure can be obtained; this is illustrated in Figure 2-15, where phases A and B in the CAP sequence are visually distinguished from one another with respect to time. A closer look at the A1 distribution illustrates a straightforward pattern with interval peaks of approximately 25 seconds. There is no clear emerging peak for subtypes phases A2 and A3.

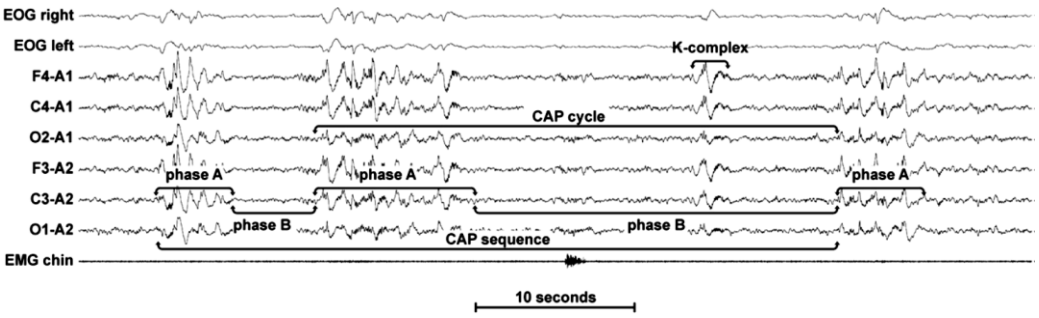

Figure 2-15 CAP Sequence [43]

Periodic EEG events include CAPs of sleep instability that fluctuate between two phases: A and B. Phase A includes three categories: A1, A2, and A3. CAPs occur when two consecutive sequences of phases A and B are present. This results in various sleep disorders such as insomnia, depression, irregular limb movements, and epilepsy. There are three different parameters for periodic activities, as follows:

1. Beginning with the repeating element, which is the period's phase A which is embodied by the repeated EEG feature.
2. The second element is the period's phase B which is the overriding background recognized by the interval separating the repeating elements.
3. The last element is the combination of phase A and phase B durations, which is known as the cycle that prescribes the repetition rate. Phase A and phase B are both composed of their own CAP cycles, which are related to higher or lower levels of arousal. This is shown below in Figure 2-16.

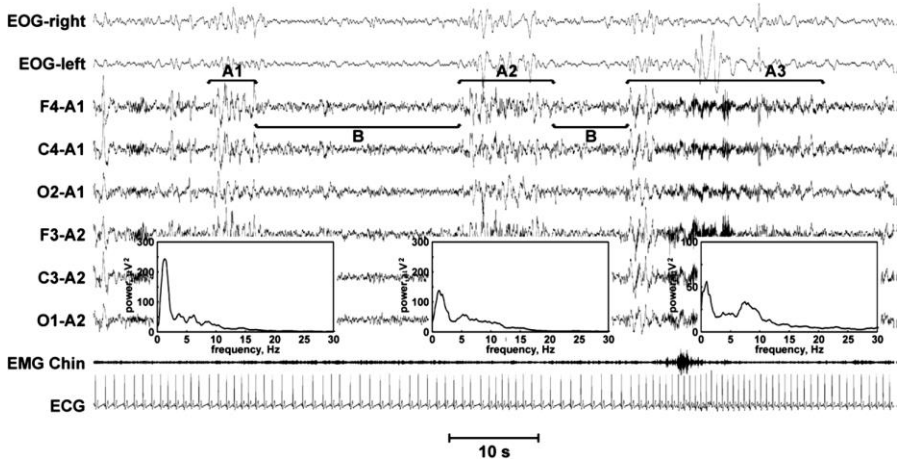

Figure 2-16 CAP two main phases A and B [15]

In order for the period's phase A to be determined, the transient events detected in the non-REM stage that regularly change in frequency and amplitude must be obtained Furthermore, these transient events typically stand out in the background rhythm [15]. Sleep records from multiple patients are needed to identify CAP under physiological conditions. In hindsight, studies performed on patients (e.g., stimulation to detect CAP patterns) are relevant based on the knowledge that CAP is the EEG conversion of the asleep brain restructuring tested by alterations to environmental factors [23].

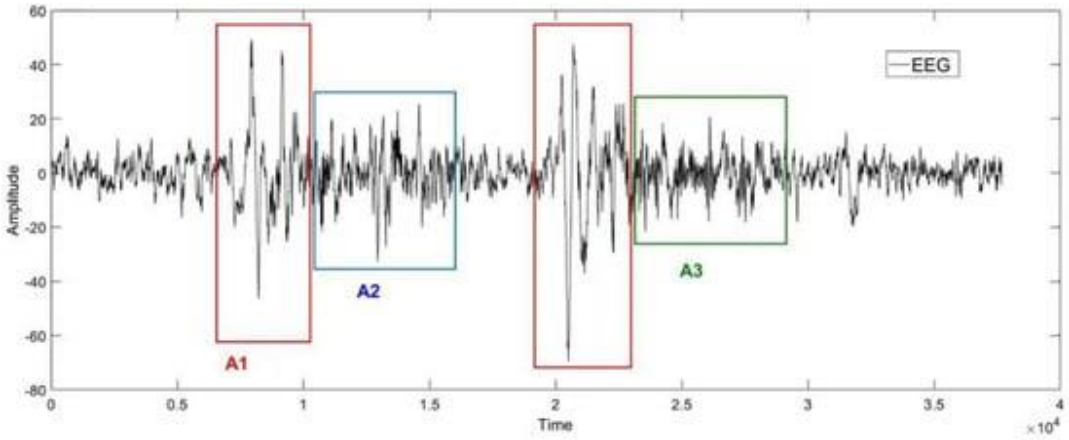

Figure 2-17 An example of the EEG (CAP phases) in sleep stage 2 [40]

Figure 2.17 is obtained for n1 data plots (the C4-A1 signal with respect to time is obtained). The horizontal axis represents the sampling point, and the vertical axis represents the signal amplitude. The shapes of the EEG signals in the red, blue, and green boxes correspond to CAP-A1, CAP-A2, and CAP-A3, respectively.

The CAP parameters used for diagnosis are more sensitive than other (conventional) sleep parameters. The disadvantage of using CAP to grade brain and sleep disorders is often the cost associated with the time it takes. This can result in inconsistent results. Hence, a reliable, efficient classification method is required to automatically detect CAP.

The outcomes of the automatic breakdown for CAP resulted in false negatives and false positives significantly greater in comparison to CAP visual grading.

Figure 2.18 below illustrates an EEG signal and where CAP would be located in healthy subjects and subjects with sleep disorders (SDB). As shown, CAP is captured in phase A of the non-REM sleep stage. The figure was created from the preprocessing EEG data used in this thesis study.

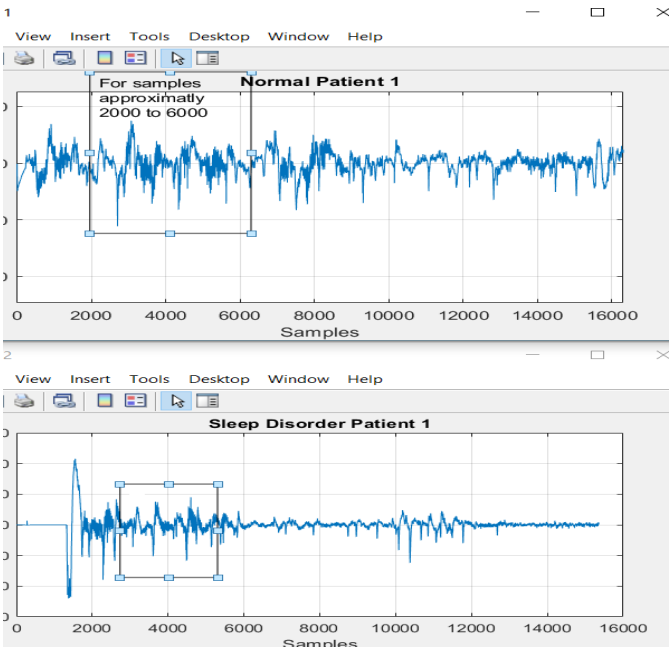

Figure 2-18 CAP detection in Phase A in non-REM sleep stage 2 utilizing healthy subject (first diagram) compared to subject with SDB (second diagram) in EEG taken over 30 second interval.

2.3.3 CAP Cycles

CAP cycle is composed of two phases, the first phase A is determined by certain frequency and amplitude components and these components determine the transient brain activation. The second phase B follows phase A, where no significant patterns are analyzed and it is indeed different from phase A shown in Figure 2.19, meaning that one

can determine the two phases simply by examining a sleep pattern visually [16].

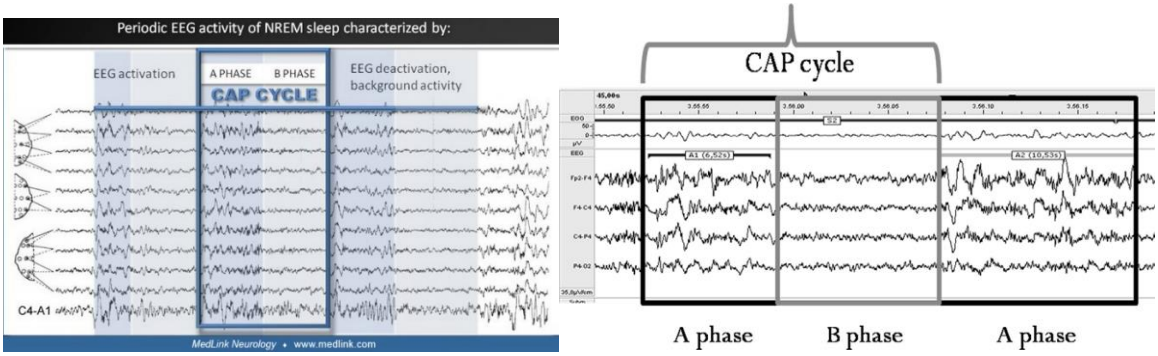

A B

Figure 2-19 CAP Cycle [44,21] Image B shows zoom in for two different subtypes of phase A one belonging to the A1 subtype and the other to the A2 subtype

During the infancy period, the average duration for a CAP cycle is approximately 30 seconds whilst in young children it is approximately 30.5 seconds, in young adults that time is 25.2 seconds, in young adults that number is 28 seconds, and for the elderly, that number is 31 seconds. The common length of the CAP cycles specifies the stability of the CAP cycles during a subject's life [37].

2.3.4 Non-CAP

When a CAP is undetected for more than 60 seconds, it is registered as Non-CAP (NCAP). In addition, phase A is followed by another phase A but separated by more than 60 seconds (which would be classified as (NCAP) [39]. The proper definition of a Non-CAP, as shown in Figure 2-20 the A phases that terminate a CAP sequence (light black boxes) are counted as non-CAP.

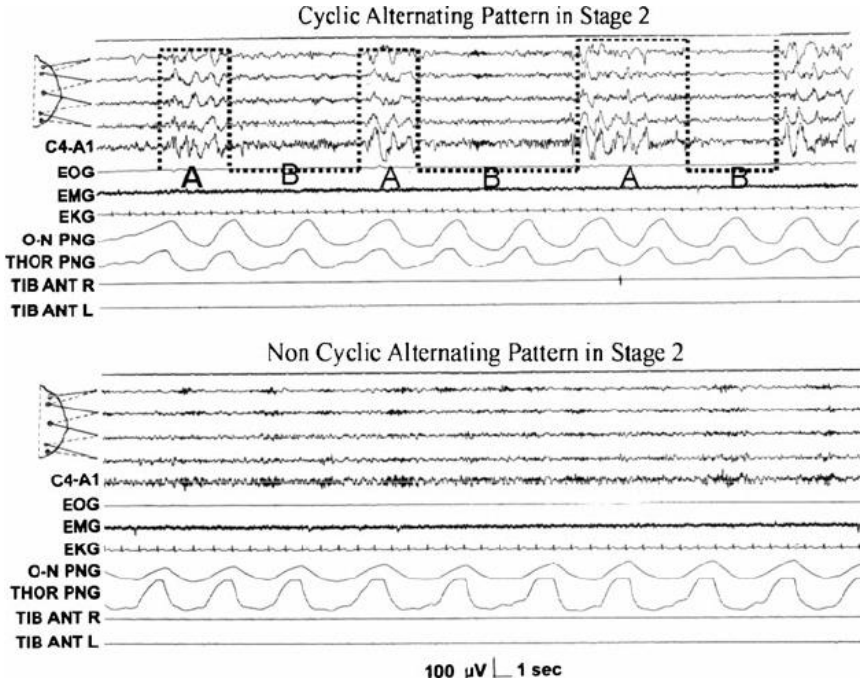

Figure 2-20 CAP/Non-CAP Sequence in Stage 2 [45]

2.3.5 The measurements of CAP

EEG structures are extremely complex indicators of brain development. Sleeping patterns and behaviors reflect physical and neural changes associated with natural human aging. Figure 2-21 below demonstrates EEG cap channel locations. Different colors indicate different impedances on the corresponding electrodes with blue

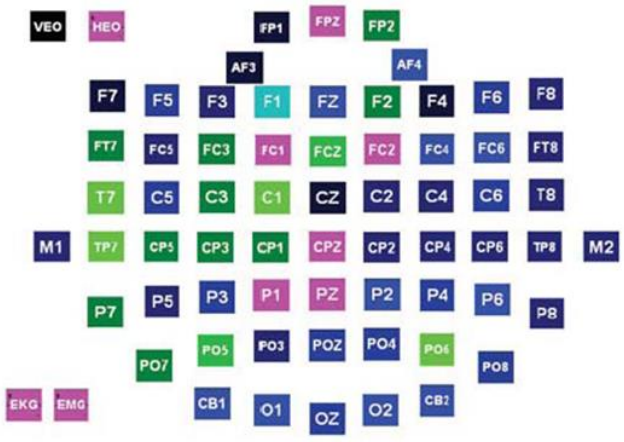

Figure 2-21 EEG cap channel locations [51]

representing good impedance and pink indicating bad impedance.

CAP time is the temporal sum of all CAP sequences. CAP time can be calculated throughout total NREM sleep and within single NREM stages. The percentage ratio of CAP time to sleep time is called CAP rate in equations from 2-5 to 2-7.

CAP rate is a dynamic parameter that measures the effort of the cerebral centers to maintain a compatible organization of sleep. CAP rate can be measured in NREM sleep (percentage ratio of total CAP time to total NREM sleep time) and in single NREM stages (percentage ratio of CAP time in a given stage to the entire duration of that stage throughout sleep) [19].

CAP can be measured by obtaining the average cycle length, the average duration for each phase, the average ratio of phase by cycle, the CAP index represented by the number of CAPs occurring per minute in the non-rapid eye movement (NREM) stages, and the CAP rate. The previously mentioned CAP parameters are expressed in the following equations. Furthermore, Equation 3 will be utilized to obtain Equations 4, 5, and 6 [24].

$$.\frac{Average\ ratio\ phase}{cycle\ duration} = \frac{Phase\ A\ duration}{cycle\ duration}\ x\ 100\ and\ \frac{Phase\ B\ duration}{cycle\ duration}\ x\ 100 \qquad (2-3)$$

$$CAP\ index\ (stages\ 1-4) = \frac{number\ of\ CAPs\ in\ stages\ 1-4}{total\ duration\ stage\ 1-4\ (\min)} \qquad (2-4)$$

$$CAP\ rate\ (per\ sleep\ record) = \frac{CAP\ time}{Sleep\ time} \qquad (2-5)$$

$$NREM\ sleep = \frac{Total\ CAP\ time}{NREM\ sleep\ time}\ x\ 100 \qquad (2-6)$$

$$total\ sleep\ time = \frac{Total\ CAP\ time}{total\ sleep\ time}\ x\ 100 \qquad (2-7)$$

$$NREM\ total\ sleep\ stage\ (each\ one) = \frac{CAP\ time\ in\ stage\ 1-4}{total\ stage\ 1-4\ (\min)}\ x\ 100 \qquad (2-8)$$

The average cycle length, the average duration for each phase, the number of CAPs in stages 1-4, the total duration of stages 1-4, the CAP time, the sleep time, and the NREM sleep time can be obtained from sleep records. In conclusion, the CAP rates may point to the number of operations required by the sleeping brain to regulate back to regular environmental conditions (i.e. the flexibility of organizational sleep) [43]. Although there are several CAP parameters, the CAP rate is the most important of them all as it is utilized the most for clinical purposes. CAP rate is a measure of arousal instability in the human brain. It can be further enhanced if sleep is disturbed by internal and external factors. It is calculated as the percentage ratio of total CAP time to Non-REM time.

2. 4 General features and Classifiers for EEG signal from literature

This section illustrates the different feature types and classification methods studied in the literature applied to EEG signals in general. The following section will present specific techniques, features, and classification methods used for CAP detection in EEG. These methods are more related to this thesis study. In the literature, when features are extracted from EEG signals are subsequently classified utilizing a signal classification method to differentiate the CAP fragments. These procedures obtain a specific feature from the EEG recording that is then used in a classification algorithm to diagnose sleep disorders [7,9,11,12].

Frequency Domain	Non-parametric analysis Parametric analysis Coherence analysis Spectral entropy Itakura distance Harmonic Parameter Median frequency

Time- Frequency Domain	Wavelet Transform (WT) Short Time Fast Fourier (STFT) Ensemble Empirical Mode Decomposition (EMD) entropy features of the Wigner–Ville Distribution (WVD) Choi-Williams
Complexity measures and non-linear factors	Correlation dimension Lyapunov exponent Fractal dimension Approximate Entropy Sample Entropy Autoregressive Phase space Hurst exponent Energy operator Permutation entropy Multiscale Entropy

Table 2-2 Various time domain, frequency domain, time-frequency domain, complexity measures and non-linear parameters techniques and their respective features and features extraction in literature [1]

Table 2-3 and 2-4 summarize the different classification techniques and feature selection in EEG established processing, respectively [1,14,20]. For the more conventional classifiers such as K nearest neighbor and support vector machine, they are explained in more detail in sections 3.3.4.2 and 3.3.4.3.

Method	**Classifiers found in Literature**
Artificial Neural Networks (ANN)	-
Statistical	Linear Discriminant Analysis (LDA)

	Support Vector Machine (SVM) [5] Hidden Markov Model Bayesian Quadratic
Instance base	K Nearest Neighbor (KNN)
Decision tree	DT
Ensemble	Adaboost Bagging RF
Clustering	K Means Classifier

Table 2-3 Classification methods and their respective features found in literature [1,14,20].

Method alternatives
Minimum Redundancy Maximum-Relevance (mRMR)
Sequential methods
Best Subsets Procedure
t-test
SVM - Recursive Feature Elimination
Differential Evolution Feature
Fisher score
Relief F method
Fast correlation-based filter
Principal component analysis
Method alternatives (cont.)
Linear Discriminant Analysis
Large Margin NN
Fuzzy C-means clustering
Artificial Immune Clustering

Table 2- 4 Different methods of feature selections.

2.5 Popular Proposed Methods and Procedures for CAP Detection in EEG in Literature

The purpose of this section is to provide an overview of the techniques and procedures used in the process of CAP detection in EEG, from the raw signal to the classification and output. The first step is to record the EEG signal as described in section 2.1.2. The second stage is to separate the EEG signal based on different frequency bandpass filters (delta, theta, alpha, beta, and gamma) [1,5,6,10,14,22]. The third stage is to classify the different sleep stages (W, REM, and non-REM) using the illustrated machine learning classifiers shown in section 2.2.1, Table 2-3 [1,5,6,10,14,22].

2.5.1 Database (Physio net) and EEG Signal Preprocessing

EEG signals are often obtained from recognized databases such as PhysioNet. PhysioNet is an online platform that houses a large group of 61 PSGs acquired from 1987 – 2002. For signal processing, it is critical to determine any noise and artifacts found in the raw signals. The preprocessing stage removes or reduces noise and artifacts present in the EEG signal prior to CAP feature extraction. Some popular methods for pre-processing procedures include Discrete Wavelet Transform (DWT), frequency selective filtering, Infinite Impulse Response (IIR), or Finite Impulse Response (FIR) [1,5,6,10,14,22]. The output of EEG preprocessing is smooth and has little to no ripple signal that is ready for feature selection and extraction.

2.5.2 Feature Extraction for CAP Detection in EEG

Section 2.4 Table 2-2 shows that there are many methods for extracting the desired features from the EEG signal and applying different classifiers to differentiate between the CAP fragments [10,14,22,23]. There are several commonly used feature extraction techniques: time domain, frequency domain, and time-frequency-based domain.

2.5.2.1 Time Based Feature

For automatic CAP detection in EEG, a popular feature is a variance. This feature is determined by the variance of 1-s opening traveling on a raw EEG signal [10,14,22]. This feature accounts for sudden frequency changes. Another commonly observed feature in CAP detection is Hjorth activity. This is utilized to measure the total rise of the delta band power that takes place during Phase A in CAP [10,14,22]. In [35], it proposes a method that utilizes entropy-based features for distinguishing CAP parts from non-CAP parts, and it evaluates the performance of this method using different classifiers such as Support Vector Machine (SVM), K-nearest neighbor (KNN), and Linear Discriminant Analysis (LDA).

2.5.2.2 Frequency Based Feature

Frequency based Characteristics are used to remove the EEG sleep signals with their respective frequency bands. In this feature, the EEG signal is distinguished in the five different frequency stages [10,14]. A band feature is utilized by dividing the two travelling short and long duration magnitudes by the respective band. The CAP sections are obtained by relating the band features to a set threshold [22].

2.5.2.3 Time-Frequency Based Feature

Wavelet Transform (WT) is a common and highly utilized time-frequency-based feature. It is a signal processing technique that allows for the decomposition of EEG signals into different frequency bands at various time scales. WT is a dominant tool for feature extraction from an EEG signal [10,14]. The WT method delivers precise frequency knowledge at small frequencies and accurate time information during peak frequencies. This feature benefits spectral analysis and detects different mental orders (resting and figure rotation) [9]. The WT feature decomposes the input signal into its respective frequency bands. It also obtains the input to the classifier using multi-resolution methods. The Hilbert-Huang transform is a signal processing technique that decomposes a signal into a set of intrinsic mode functions (IMFs) and a residual component. IMFs are extracted using empirical mode decomposition and represent the underlying oscillatory modes of

the signal. Hilbert-Huang-based feature extraction methods, such as instantaneous frequency and amplitude, have been proposed to quantify dynamic changes in CAP EEG activity [50].

2.5.3 Feature Selection for CAP Detection in EEG

Feature selection is used to obtain elite features to optimize the classification process. For CAP detection in EEG, feature selection often follows an algorithmic process. Feature selection is used to lower any complexity in the classifier and to select a suitable set of features to send to the classifier. Principal Component Analysis (PCA) and Sequential Selection Methods are the most commonly applied techniques. This technique is a linear conversion to decrease the dataset size while keeping the most contributing features [10,14,22,23]. Also, feature selection maintains a low order of the main components. PCA illustrates d-vectors while performing in a low dimension; this will reduce time-space complexity. There are several different feature selection methods, but the most common and simplest is the subset selection method (SSM), which follows a set algorithm. Figure 2-22 shows a comparison of methods for EEG signal features extraction using Linear Analysis in Frequency and Time-Frequency Domains.

The SSM begins by applying one feature to an empty feature sub-set; this will clearly show a desired function. The SSM then undergoes a second step; in this second step, a desired feature that can be compared to the first feature is selected. The SSM feature selection algorithm repeats the first and second steps until the most effective features are selected.

Method name	Advantages	Disadvantages	Analysis method	Suitability
Fast fourier transform	(i) Good tool for stationary signal processing (ii) It is more appropriate for narrowband signal, such as sine wave (iii) It has an enhanced speed over virtually all other available methods in real-time applications	(i) Weakness in analyzing nonstationary signals such as EEG (ii) It does not have good spectral estimation and cannot be employed for analysis of short EEG signals (iii) FFT cannot reveal the localized spikes and complexes that are typical among epileptic seizures in EEG signals (iv) FFT suffers from large noise sensitivity, and it does not have shorter duration data record	Frequency domain	Narrowband, stationary signals
Wavelet transform	(i) It has a varying window size, being broad at low frequencies and narrow at high frequencies (ii) It is better suited for analysis of sudden and transient signal changes (iii) Better poised to analyze irregular data patterns, that is, impulses existing at different time instances	Needs selecting a proper mother wavelet	Both time and freq. domain, and linear	Transient and stationary signal
Eigenvector	Provides suitable resolution to evaluate the sinusoid from the data	Lowest eigenvalue may generate false zeros when Pisarenko's method is employed	Frequency domain	Signal buried with noise
Time frequency distribution	(i) It gives the feasibility of examining great continuous segments of EEG signal (ii) TFD only analyses clean signal for good results	(i) The time-frequency methods are oriented to deal with the concept of stationary; as a result, windowing process is needed in the preprocessing module (ii) It is quite slow (because of the gradient ascent computation) (iii) Extracted features can be dependent on each other	Both time and frequency domains	Stationary signal
Autoregressive	(i) AR limits the loss of spectral problems and yields improved frequency resolution (ii) Gives good frequency resolution (iii) Spectral analysis based on AR model is particularly advantageous when short data segments are analyzed, since the frequency resolution of an analytically derived AR spectrum is infinite and does not depend on the length of analyzed data	(i) The model order in AR spectral estimation is difficult to select (ii) AR method will give poor spectral estimation once the estimated model is not appropriate, and model's orders are incorrectly selected (iii) It is readily susceptible to heavy biases and even large variability	Frequency domain	Signal with sharp spectral features

Figure 2-22 Methods of EEG Signal Features Extraction [49]

2-6 Classification Tools:

Machine learning techniques offer significant advantages due to their automated nature. These techniques are capable of analyzing vast amounts of complex data more accurately than traditional methods. In the literature approach taken to classify EEG data during the sleep cycle into two categories: phase A and non-phase A [34]. The classification was performed using a simple binary logistic regression classifier using of raw EEG data without the need for frequency-domain transformation, the results suggest that the binary logistic regression classifier applied directly to raw time-domain EEG data was not effective enough to accurately distinguish between phase A and non-phase A. Another approach to create an automated algorithm that can identify the activation phases (A phases) of the CAP in sleep EEG data was proposed in [40], An Artificial Neural Network

(ANN) was employed to learn from the extracted features and make automatic predictions about the A phases of CAP.

One powerful tool for data classification in the context of machine learning is MATLAB's classification learner application. The primary purpose of the classification learner application in MATLAB is to streamline the process of data classification. It automates the various steps involved in classification, including feature selection, model selection, model training, and performance evaluation. The application supports a wide range of well-known classification algorithms, such as decision trees, discriminant analysis, logistic regression, Naive Bayes, support vector machines (SVM), K-Nearest Neighbor (KNN), and Random Forest (RF).

One of the key features of the application is its interactive nature. Users can explore data, train different models, and compare their performances within the application itself. Furthermore, the application generates MATLAB code that can be used to reproduce the results obtained. This not only saves time but also allows for easy sharing and replication of the analysis. The classification learner application supports two main approaches for model training: validated model and full model. In the validated model approach, the model is trained using a validation scheme, while the full model approach involves training the model using the entire dataset without validation

2.6.1 Linear Discriminant Analysis (LDA)

LDA was developed by Fisher in 1936 and optimized by the Fisher criterion function**.** This method is statistically based and optimized by the ratio of the covariance matrix. This means the probable space samples in each class develop a dense center and other samples separated by class fall away from that center [4]. LDA makes predictions by estimating the probability that each set of inputs belongs to each class. The class that gets the highest probability is the output class and a prediction is made as shown in Figure 2-23

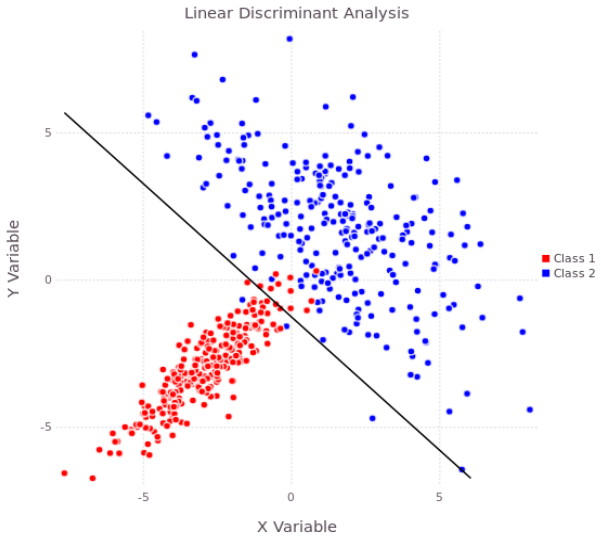

Figure 2-23 Simple probabilistic classifiers intended for two-class or binary classification problems

The LDA classifier optimizes the ratio between the class covariance matrices [46]. Meaning that differing class samples remain as far away from one another and those with similar classes condense in the center, the LDA is shown in the equation below, where the parameters SW and SB represent the scattering matrices of classes [48]: The Fisher criterion is described as:

$$J(W) = \max\left(\frac{W^T S_B W}{W^T S_W W}\right) \qquad (2\text{-}9)$$

where W is potentially a hyperplane (in two-class problems) or a matrix of hyperplane (in multi-class problems) Incidentally.

2.6.2 Support Vector Machine (SVM)

Vapnik's classifier reduces structural risk (any test errors). The method is to optimize margins and minimize risk. It contains a user-selected bound that governs the margin width. SVM is categorized as linear binary and can be applied to input data with the leading SVM, which delivers a non-linear margin between different class models [46]. The SVM simply attempts to minimize the test errors and or expected risk associated with the errors, this is done by training the errors which in turn minimized the empirical risk.

Furthermore, this is done while controlling the margin width via a user-defined parameter [35].

2.6.3 K-Nearest Neighbor (KNN)

This classifier is extremely flexible and performs best when the data distribution is multi module. KNN makes choices for different class samples and acts as a local classifier. This classifier operates by finding the KNNs and labeling them based on the majority of KNNs found [46].

2.6.4 Random Forest (RF)

The Random Forest (RF) classifier consists of an ensemble of tree structures. It is based on a random vector sampled value and serves as a classifier for each individual tree. The main difference between RF to other classifiers is that feeding the input samples to the trees is performed as randomly as possible. The broader the number of trees in the forest, the higher the robustness of prediction is; meaning the increased the accuracy will be. It is commonly said that random forest methods can grow several trees [48]. The RF classifier handles missing values and maintains accuracy for missing data. It can also be used for extremely large data sets, which is what we use to analyze Sleep Data.

Chapter 3 (Methodology)

This study explores various sleep disorders, including insomnia and sleep-disordered breathing, to determine a specific combination of features with classifiers for the detection of Cap events in EEG signals.

Chapter 3 provides the approach utilized in this thesis to detect CAP events. A proposed classification model incorporates additional features to train a classifier to detect CAP sequences. Furthermore, the five phases implemented in this study are expanded upon. This is the collection of raw data, the conversion of the EEG signal to a physical signal, feature extraction, feature selection, and classification of CAP.

3.1 Introduction

In the literature, efficient features for automatic CAP detection in sleep EEG signals explore the utilization of conventional characteristics through a proposed method. In comparison with conventional and statistical signal processing methods, the non-conventional features (i.e. entropy-based features), are highly dependent on the size of the data, poor spectral estimation and degree of roughness of the transitional CAP phases, and non-CAP events. Conventional signal processing features include frequency-based (bandwidth) features such as the fast Fourier Transform [34].

The study is exploratory in nature, which means that the primary goal is to explore patterns, trends, and potential relationships within the data. It serves as a starting point for generating hypotheses and identifying areas for further investigation. Given the small sample size and the exploratory nature of the study, it's important to interpret the findings cautiously. Total of a five-phase approach is implemented to detect CAP with conventional and non-conventional features with different classifiers in this thesis.

The first phase is the collection of raw data obtained from PhysioNet. The second phase in detecting CAP is the conversion of the raw EEG signal to a physical signal; this is accomplished through the Waveform Database (WFDB) Toolbox for MATLAB.

The third phase is feature extraction for CAP detection in EEG. Renyi's entropy, Tsallis entropy, Shannon entropy, Sample entropy, Hilbert-Huang Transform (HHT), and Fast Fourier Transform (FFT) are the selected features for various reasons such as their ability to differ between EEG waveforms and CAP events in addition to their speed over other available methods in real-time applications.

The fourth phase is feature selection; feature selection is used to obtain elite characteristics to optimize the classification process. Time-based and frequency-based characteristics are selected for the next phase. Furthermore, feature selection aims to lower classifier complexity.

The fifth phase is data classification. The aim of the classification application is to produce a hyperplane decision surface that divides the feature space, maximizing the ratio of between-class variance and within-class variance. The class variance represents different inputs/features. Classifiers such as Support Vector Machine (SVM), Linear Discriminant Analysis, K-Nearest Neighbor (KNN), and random forest are utilized.

The entropy-based features (non-conventional features) used with the classifiers SVM, KNN, LDA, and RDT are proven through literature study comparison to produce higher accuracy results when used for CAP detection in EEG. The reason the results yield higher accuracy is due to the degree of roughness accommodated in the entropy-based features.

Figure 3.1 illustrates the implementation of the proposed system beginning with the collection of raw EEG data. This is followed by pre-processing of the physical EEG signal, feature time-frequency analysis, feature extraction, and classification. The extracted features are trained in a MATLAB classification app, in which different classifiers are tested to determine their accuracy in detecting CAP. The confusion matrix was generated through MATLAB's classification app to compare different classifiers in detecting CAP based on the extracted features. Figure 4.1 shows steps to run and analyze in MATLAB.

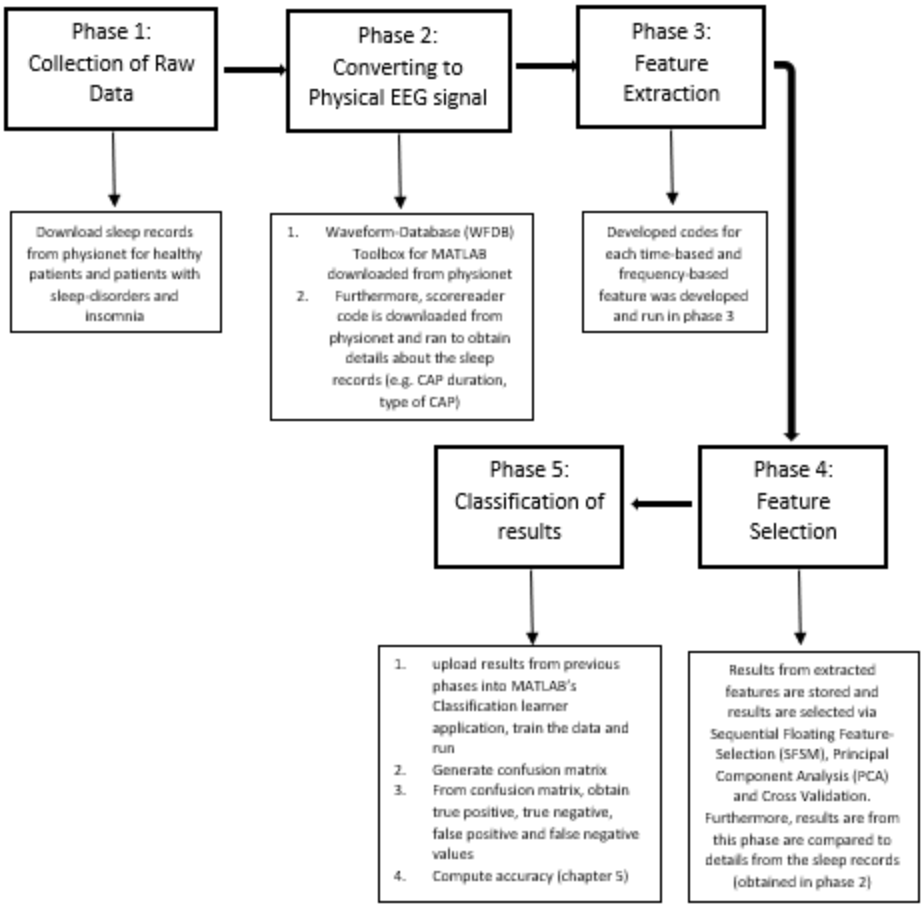

Figure 3-1 Processing steps necessary to detecting CAP in an EEG signal collected from PhysioNet.

3.2 Collection of Raw EEG Data

Pre-processing EEG signals are very sensitive to external factors independent of the brain, for example, broken EEG electrodes, blinking and movement of eyes, dried electrodes, stretching of muscles, excessive electrode gel, etc. EEG signals are often obtained from recognized databases such as PhysioNet. The database PhysioNet is an online platform that houses a large group of 61 PSGs acquired from 1987–2002 [17]. Several channels are available, such as F3 or F4, C3 or C4, and O1 or O2, referred to as A1 or A2, detailed in the following sections [14]. As shown in Figure 4.2 below, the sleep recordings obtained from PhysioNet vary in type of disorder and are described with related acronyms and label

numbers. This is for clarification in a later phase of data pre-processing. Furthermore, PhysioNet offers annotation text files for each recording.

CAP parameters such as sleep stage (W=wake, S1-S4=sleep stages, R=REM, MT=body movements), body position, time of day, event (e.g. phase A), duration (in seconds), and event location can be obtained.

n1-n16	No pathology (controls)
brux1-brux2	Bruxism
ins1-ins9	Insomnia
narco1-narco5	Narcolepsy
nfle1-nfle40	Nocturnal frontal lobe epilepsy
plm1-plm10	Periodic leg movements
rbd1-rbd22	REM behavior disorder
sdb1-sdb4	Sleep-disordered breathing

Figure 3-2 Sleep recordings obtained from PhysioNet vary in type of disorders conditions.

For signal processing, it is imperative to determine any noise and artifacts found in the raw signals. As CAP detection is the focus of the thesis, the raw data used for the analysis is obtained from the PhysioBank Database. The required raw data is exported from Physio Bank ATM, which is a toolbox for data exploration.

3.2.1 Subjects and Annotations

The CAP Sleep Database in PhysioNet houses 108 polysomnographic recordings identified at the Sleep Disorders Center (Ospedale Maggiore of Parma, Italy) [14].CAP sleep data access is open to the public without specific authorization. This database contains records of 16 healthy subjects that did not display any neurological disorders and were not under influences (drugs, alcohol) that could affect the central nervous system. Out of the remaining 92 pathological recordings, 40 represent patients diagnosed with nocturnal frontal lobe epilepsy (NFLE), 22 represent patients with REM behavior disorder (RBD), 10 are patients with periodic leg movement (PLM), 10 are patients with insomnia, 5 are

patients with narcoleptic, 4 are patients with sleep-disordered breathing (SDB) and 2 are patients with bruxism.

In this thesis, the polysomnographic recordings of four healthy patients, three patients diagnosed with insomnia, and four patients diagnosed with sleep-disordered breathing obtained from the CAP Sleep Database are considered for this thesis as described in Table 3-1 below. Insomnia and sleep-disordered breathing are chosen as the type of sleep disorder because it is the most common form of sleep disorder.

Type of patients	**Recording file name from Physionet**	**Age**
Healthy patients	N1	54
	N2	55
	N3	54
	N5	56
Patients diagnosed with insomnia	INS1	54
	INS3	82
	INS8	64
Patients with sleep disordered breathing	SDB1	65
	SDB2	68
	SDB3	78
	SDB4	65

Table 3-1 Type of patients, recording obtained from Physionet and age of patients utilized in this proposed study.

Male patients older than 54 years of age represent most insomnia recordings in the CAP Sleep Database. Patients diagnosed with a disorder are evaluated for the detection of CAP in an EEG signal depending on the disorder. CAP events are recorded there – rather than extracting the CAP event from the FP2-F4 channel and matching it to the CAP event in the C4-A1 channel and so on (less work and more efficient). PhysioNet provides CAP annotations in text format along with the channel where the event is taking place. For all subjects, channels FP2 – F4 and C4-A1 are used for EEG analysis. Signals for healthy patients are sampled at 512 Hz. Signals for patients with sleep disorders are sampled at 256 Hz and taken and recorded every 0.0019531 seconds. The sampling frequency is determined by the info.txt file provided for each patient from PhysioNet [14]. It is common to find one or more annotation sets for each polysomnographic recording in the PhysioBank database. These annotations represent labels that point to certain locations within the recording and describe the events occurring at those specific locations.

3.3 Preprocessing of the EEG Physical Signal

From PhysioBank ATM, All the signals were visualized and the scorings were performed using REMlogic™ software (Embla). The scores for each recording are provided as .txt files in REMlogic report format in PhysioBank-compatible format. The .txt score files have the following fields:

- Sleep stage (W=wake, S1-S4=sleep stages, R=REM, MT=body movements)
- Body position (Left, Right, Prone, or Supine; not recorded in some subjects)
- Time of day [hh:mm: ss]
- Event (either a sleep stage (SLEEP-S0.S4, REM, MT), or a phase A of CAP)
- Duration (in seconds)
- Location (the signal(s) in which the event can be observed)

Figure 3.3 illustrates the columns found in the annotations text file downloaded from PhysioNet data. These columns include Cap events, event duration, sleep stage, and location. The downloaded data file is a MATLAB file, in addition to. edfm and. hea

extension files. As instructed by PhysioNet, to convert raw EEG data, the WaveForm DataBase (WFDB) Toolbox for MATLAB enables integrated access to PhysioNet's software and databases. The WFDB toolbox is a collection of reading, writing, and processing functions for physiological signals and time series. In the WFDB toolbox, the rdmat function reads the raw EEG data from the MATLAB file and returns the EEG signal in physical units. In addition, a MATLAB code is created to plot the converted EEG signals in either the time or frequency domain.

Time	Date	Sample #	Type	Sub	Chan	Num	Aux
[21:50:52.000	01/01/2008]	0	"	0	0	0	## time resolution: 256
[21:50:52.000	01/01/2008]	0	"	0	0	0	
[21:56:22.000	01/01/2008]	84480	"	0	0	0	SLEEP-S0 30 W ROC-LOC
[21:56:52.000	01/01/2008]	92160	"	0	0	0	SLEEP-S0 30 W ROC-LOC
[21:57:22.000	01/01/2008]	99840	"	0	0	0	SLEEP-S0 30 W ROC-LOC
[21:57:52.000	01/01/2008]	107520	"	0	0	0	SLEEP-S0 30 W ROC-LOC
[21:58:22.000	01/01/2008]	115200	"	0	0	0	SLEEP-S0 30 W ROC-LOC
[21:58:52.000	01/01/2008]	122880	"	0	0	0	SLEEP-S0 30 W ROC-LOC
[21:59:22.000	01/01/2008]	130560	"	0	0	0	SLEEP-S0 30 W ROC-LOC
[21:59:52.000	01/01/2008]	138240	"	0	0	0	SLEEP-S0 30 W ROC-LOC
[22:00:22.000	01/01/2008]	145920	"	0	0	0	SLEEP-S0 30 W ROC-LOC
[22:00:52.000	01/01/2008]	153600	"	0	0	0	SLEEP-S0 30 W ROC-LOC
[22:01:22.000	01/01/2008]	161280	"	0	0	0	SLEEP-S0 30 W ROC-LOC
[22:01:52.000	01/01/2008]	168960	"	0	0	0	SLEEP-S0 30 W ROC-LOC
[22:02:22.000	01/01/2008]	176640	"	0	0	0	SLEEP-S1 30 S1 ROC-LOC
[22:02:44.000	01/01/2008]	182272	"	0	0	0	MCAP-A3 12 S1 EEG-Fp2-F4
[22:02:52.000	01/01/2008]	184320	"	0	0	0	SLEEP-S1 30 S1 ROC-LOC
[22:03:15.000	01/01/2008]	190208	"	0	0	0	MCAP-A3 14 S1 EEG-Fp2-F4
[22:03:22.000	01/01/2008]	192000	"	0	0	0	SLEEP-S1 30 S1 ROC-LOC
[22:03:52.000	01/01/2008]	199680	"	0	0	0	SLEEP-S1 30 S1 ROC-LOC
[22:04:00.000	01/01/2008]	201728	"	0	0	0	MCAP-A3 5 S1 EEG-Fp2-F4
[22:04:13.000	01/01/2008]	205056	"	0	0	0	MCAP-A3 17 S1 EEG-Fp2-F4
[22:04:22.000	01/01/2008]	207360	"	0	0	0	SLEEP-S1 30 S1 ROC-LOC
[22:04:37.000	01/01/2008]	211200	"	0	0	0	MCAP-A3 5 S1 EEG-Fp2-F4
[22:04:50.000	01/01/2008]	214528	"	0	0	0	MCAP-A3 6 S1 EEG-Fp2-F4
[22:04:52.000	01/01/2008]	215040	"	0	0	0	SLEEP-S1 30 S1 ROC-LOC
[22:05:06.000	01/01/2008]	218624	"	0	0	0	MCAP-A3 7 S1 EEG-Fp2-F4
[22:05:20.000	01/01/2008]	222208	"	0	0	0	MCAP-A2 7 S1 EEG-Fp2-F4
[22:05:22.000	01/01/2008]	222720	"	0	0	0	SLEEP-S1 30 S1 ROC-LOC
[22:05:31.000	01/01/2008]	225024	"	0	0	0	MCAP-A2 8 S1 EEG-Fp2-F4
[22:05:52.000	01/01/2008]	230400	"	0	0	0	SLEEP-S1 30 S1 ROC-LOC
[22:06:07.000	01/01/2008]	234240	"	0	0	0	MCAP-A2 8 S1 EEG-Fp2-F4
[22:06:22.000	01/01/2008]	238080	"	0	0	0	SLEEP-S2 30 S2 ROC-LOC
[22:06:27.000	01/01/2008]	239360	"	0	0	0	MCAP-A3 10 S2 EEG-Fp2-F4

- Sleep stage (W=wake, S1-S4=sleep stages, R=REM, MT=body movements)
- Body position (Left, Right, Prone, or Supine; not recorded in some subjects)
- Time of day [hh:mm:ss]
- Event (either a sleep stage (SLEEP-S0..S4, REM, MT), or a phase A of CAP)
- Duration (in seconds)
- Location (the signal(s) in which the event can be observed)

Figure 3-3 Sample of columns from annotation text file from PhysioNet that demonstrate the CAP events, their duration and the channel location

This raw data represents samples that are expressed in an analog-to-digital unit. Downloaded files need to be converted to physical units prior to resuming analysis. This task is performed by the WFDB Toolbox downloaded from Physionet. The function rdmat

reads the signal stored in the MATLAB file and converts it to physical units. The following subsections and figures explain the methodology for converting raw EEG data to a physical EEG signal. An additional note to make, PhysioNet contains data for the various channels (e.g. C4-A1). For this study, channels C4-A1 and FP2-F4 are selected due to the annotation files that show the duration of the CAP event and in which channel they occur.

3.3.1 – Converting to Physical EEG signal

This section focuses on the methodology used to convert raw EEG data downloaded from PhysioNet to a physical EEG signal. The physical EEG signal will be prepared so that feature selection and extraction can be achieved in later steps. In order to analyze the EEG data and identify specific patterns or events, it is necessary to first make the data stationary by removing the time-varying mean and variance. This helps to ensure that any conclusions drawn from the data are accurate and not affected by the changing nature of the EEG signal. Data for healthy patients and patients diagnosed with sleep disorders (i.e. insomnia and sleep-disordered breathing) are the focus of patients to be considered. In addition, multiple 1-minute to 12 hours' worth of data can be downloaded at a time.

Fig. 3.4 shows the physical signal of normal subjects n1, n2, n3, and n5. The y-axis represents the signal response and the x-axis is the time in seconds. In Figure 3.5, the physical signal of subjects with sleep-disordering breathing (SDB), which are sdb1, sdb2, sdb3, and sdb4, is shown. Figure 3.6 illustrates the physical signals of subjects with insomnia used in this study which are Ins1, Ins3, and Ins8.

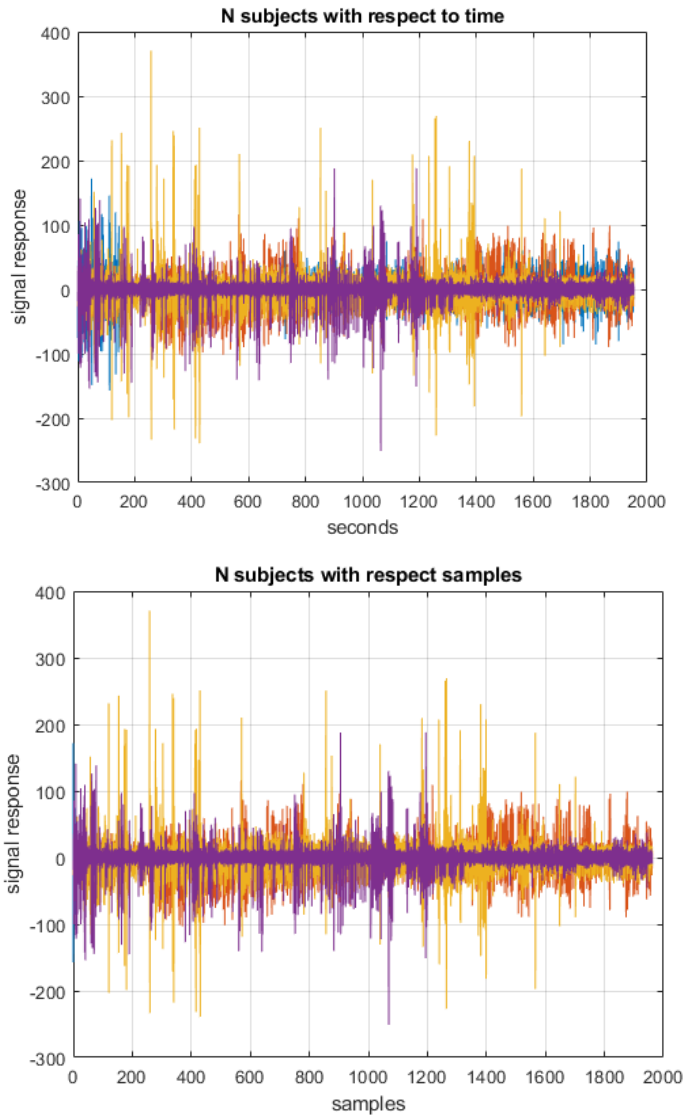

Figure 3-4 Physical signal response of a normal subjects with related to time and samples

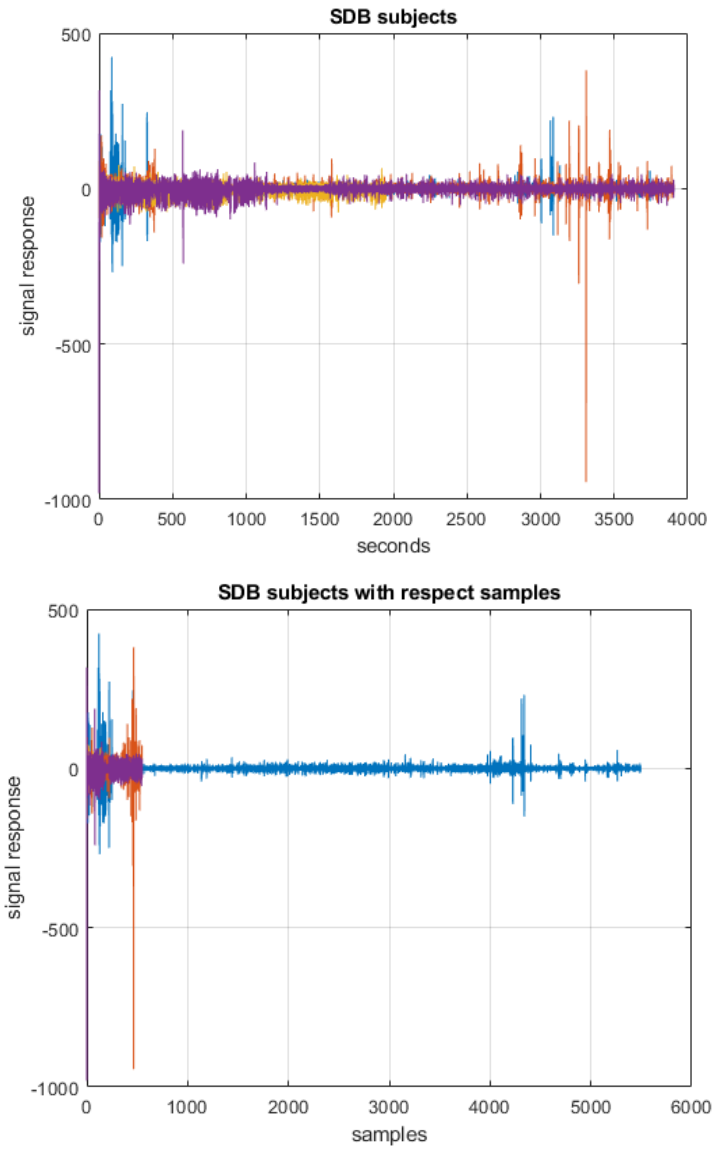

Figure 3-5 Physical signal response of sleep disorder patients with related to time and samples

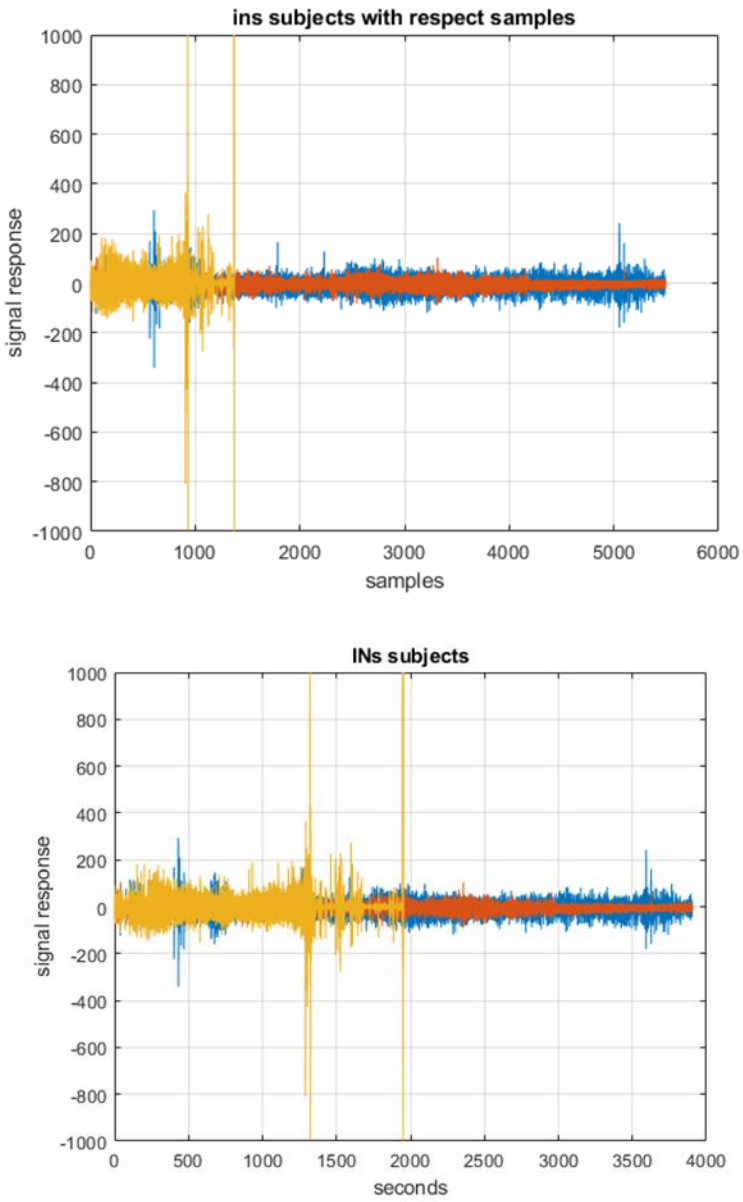

Figure 3-6 Physical signal response of Insomnia patients with related to time and samples

3.3.2 – Extracting CAP Annotations

The next step in preprocessing is to convert MCAP annotations to “physical responses” with respect to time. In order to accomplish this, the function ‘rdmat’ need to be called from the WFDB toolbox provided by PhysioNet. The output of ‘rdmat’ is the physical properties of the input signal. Furthermore, by utilizing the annotation files, the scorereader MATLAB file can be downloaded and run. The scorereader file converts annotation files from .txt to a workspace variable in MATLAB hence optimizing the

process. The CAP parameters (e.g. CAP duration, time, phase...etc.) extracted from the annotation files via scorereader will be utilized to select the extracted features that illustrate the CAP event taking place in the EEG signal.

In order to analyze the CAP annotations found in a .txt file in PhysioNet, a MATLAB code is developed to retrieve the CAP annotations for various patients. It stores them in a cell array ready to be converted to their "physical EEG response" with respect to time. The MATLAB code for extracting CAP annotations takes the physical EEG signal of the patient and loops around the peaks of the signal to determine the CAP location; this is accomplished by comparing event peaks. The physical response plots and the extracted CAP events plots are plotted in MATLAB.

Figure 3.7 below illustrates different plots for the physical EEG response, in blue, for normal subjects (left) and the red plots (right) represent the extracted CAP annotations from the EEG signal for the normal subjects considered in this study. The right red plot represents the variations in CAP physical response extracted from the EEG signal with an event duration of 20 seconds. The red plots below are obtained by looping through a 2000-second EEG signal for different normal subjects.

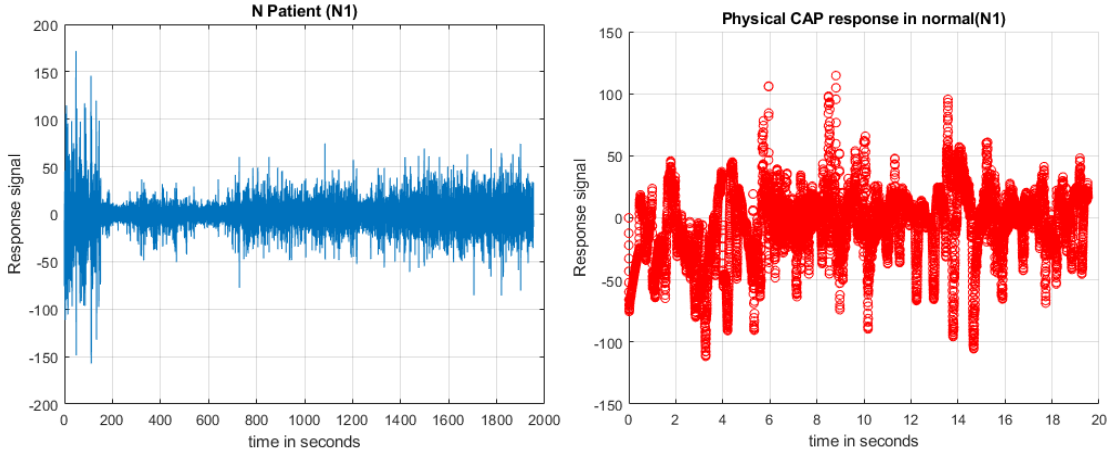

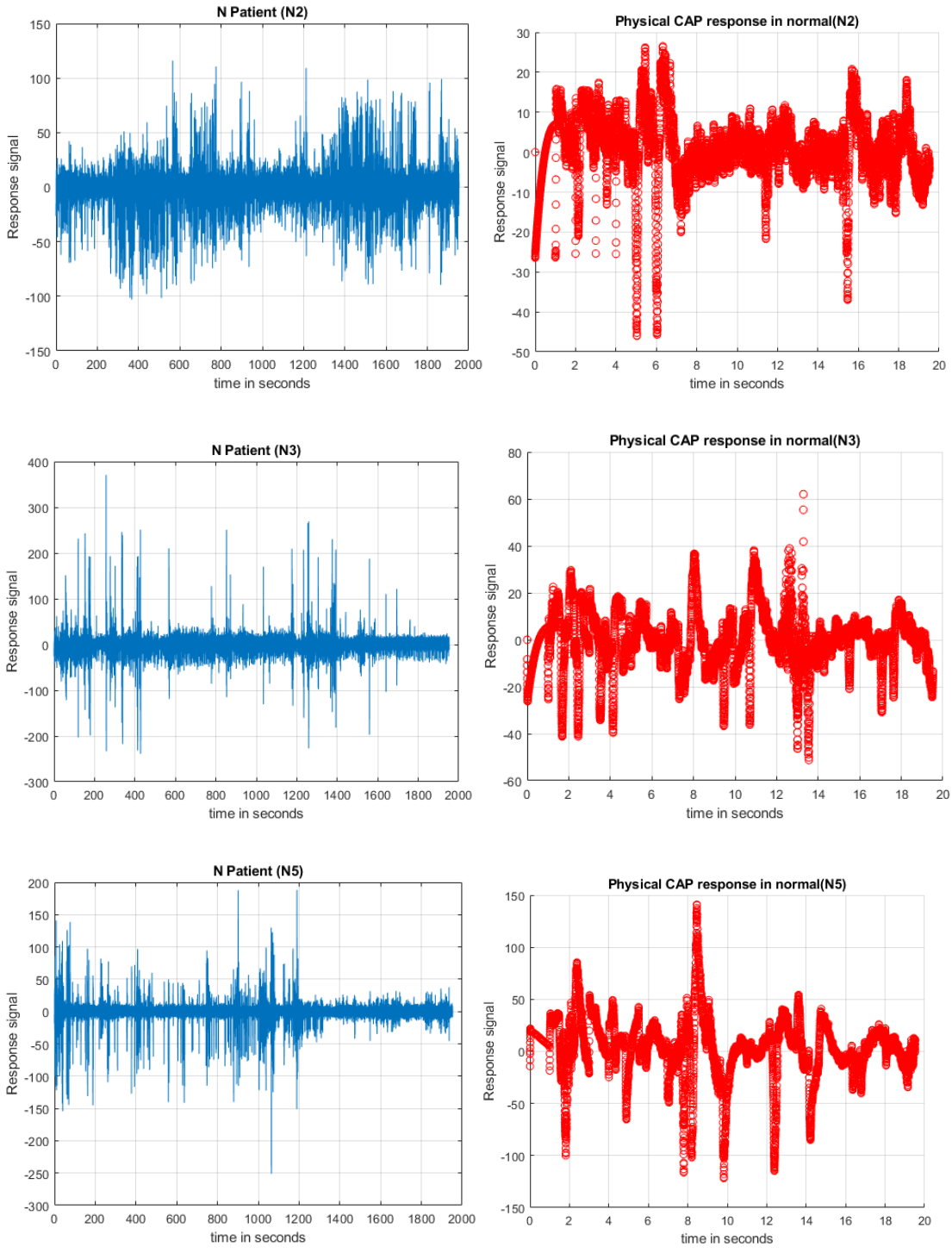

Figure 3-7 Physical EEG response plot blue (left) and extracted CAP plot (red) for normal subjects

The code to extract CAP annotations can be provided with various signals with differing time lengths. The CAP annotations from PhysioNet help pinpoint the channel where the CAP event is taking place. CAP events were observed in channels FP2 - F4 and C4-A1 in

this study. Figure 3.8 below illustrates the physical EEG response plot, in blue, for a patient with sleep-disordered breathing (left) and the red plots (right) represent the extracted CAP annotations from the EEG signal for the sleep-disordered subjects.

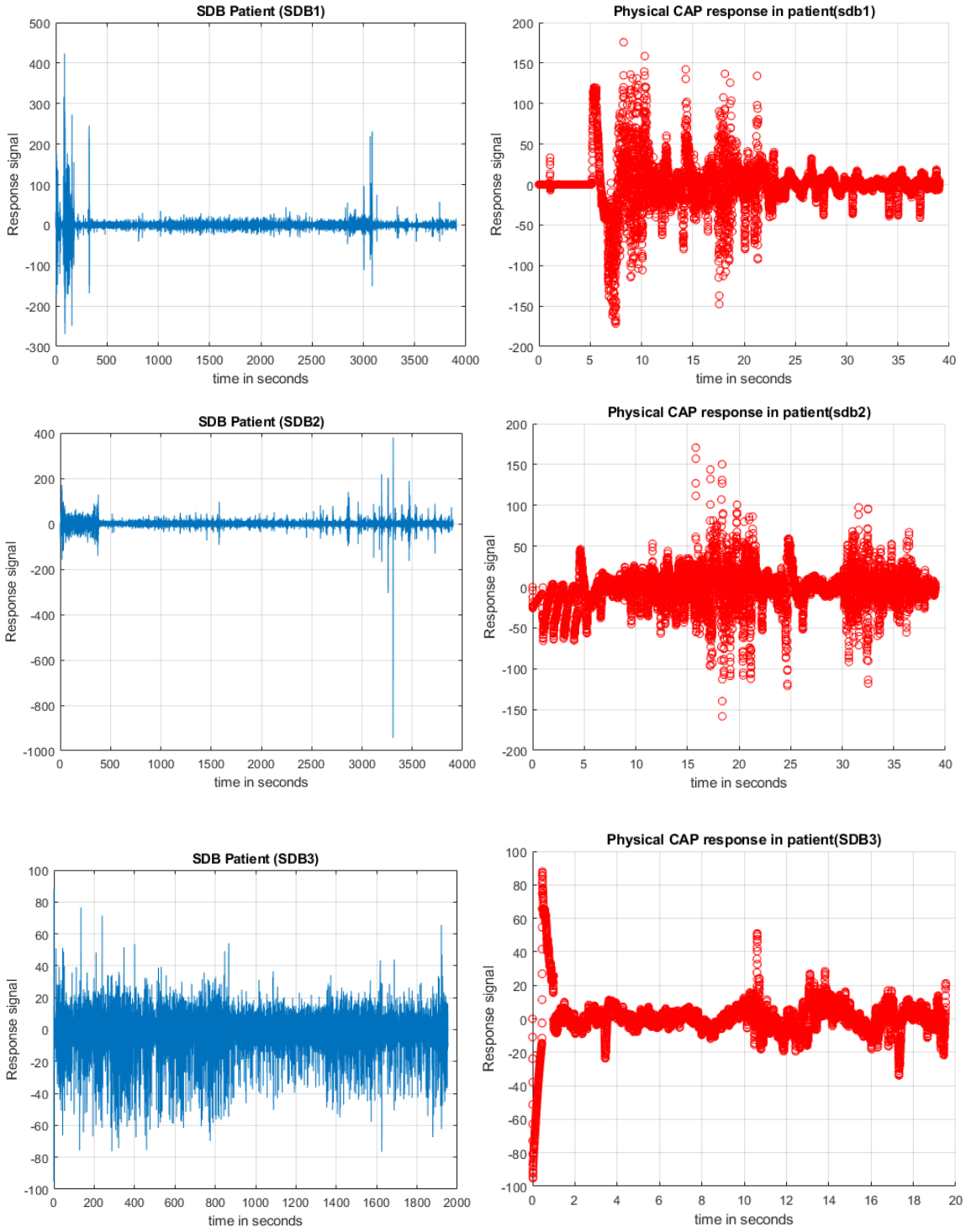

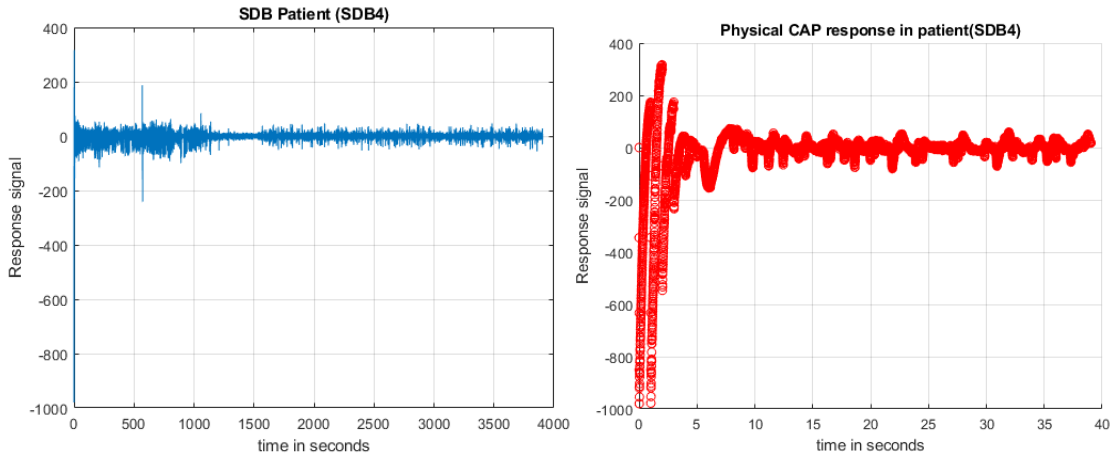

Figure 3-8 Physical EEG response plot blue (left) and extracted CAP plot (red) for SDB subjects

Figure 3.9 below illustrates the physical EEG response plots, in blue, for a patient with Insomnia (left) and the red plots (right) represent the extracted CAP annotations from the EEG signal.

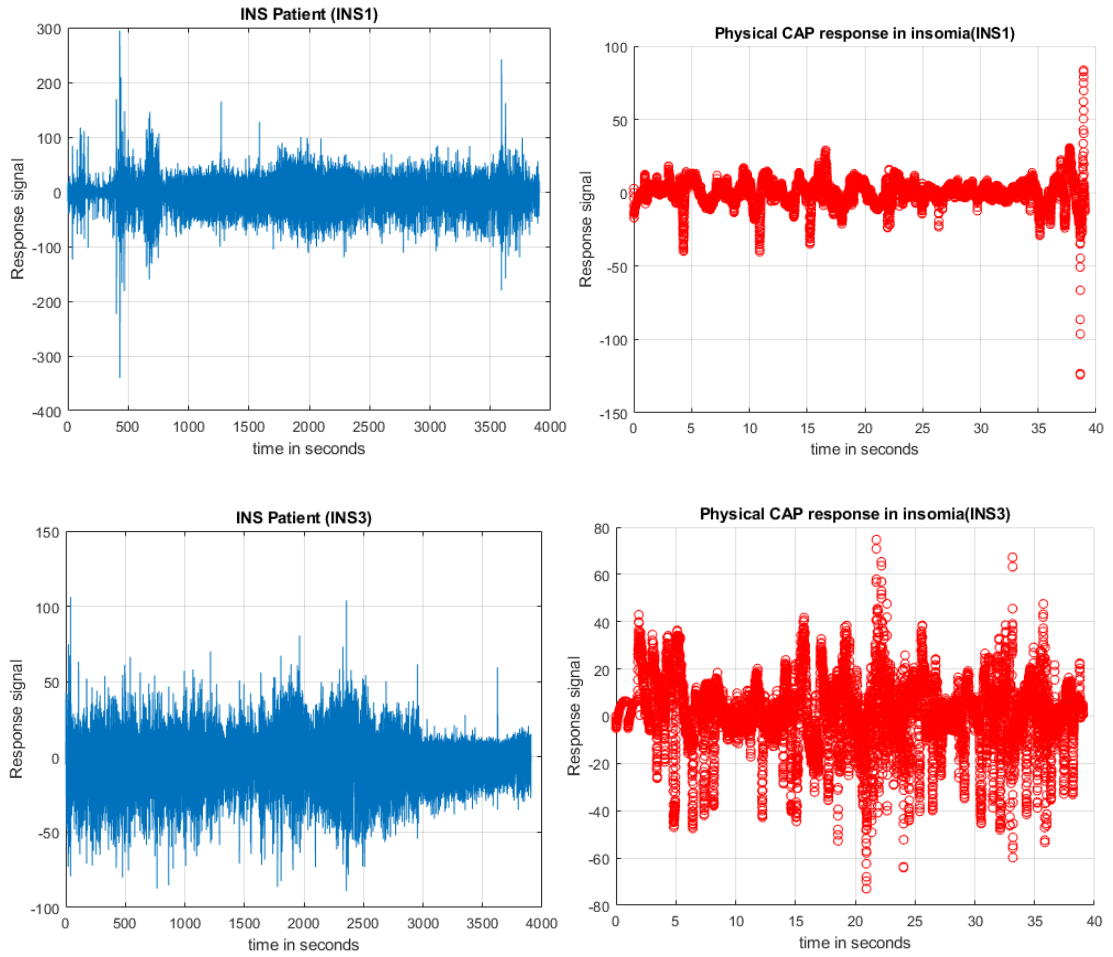

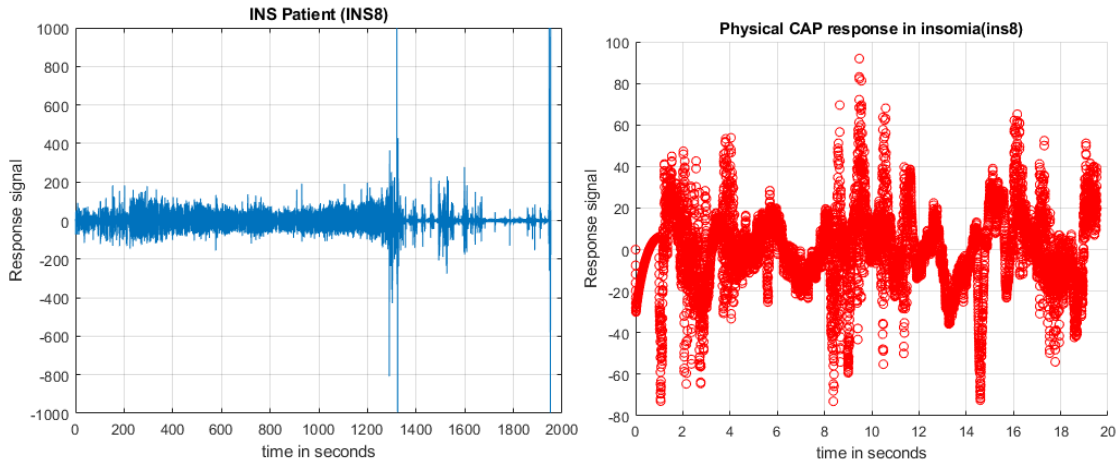

Figure 3-9 Physical EEG response plot blue (left) and extracted CAP plot (red) for Insomnia subjects

3.4 – Feature Selection

A feature is a measurable property or characteristic extracted from EEG data. Features can represent different aspects of the data, such as frequency distribution, amplitude, temporal patterns, statistical properties, and more. These features are calculated from the raw EEG signals and are used to create a numerical representation of the data that can be input into a classification algorithm. In the time domain, there is a significant disadvantage because the signal's statistical properties have changed over time [34]. Time domain features are computed from the signal amplitude value. On the other hand, frequency domain features are extracted using Power Spectral Density (PSD). Frequency domain features are highly appropriate for narrowband signals and have an enhanced speed over other methods in real-time applications. Analyzing non-stationary signals and suffering from large noise sensitivity are weaknesses of frequency domain features.

Subsections 3.4.1 to 3.4.2 provide an overview of the time- and frequency-based approaches proposed in this study. In addition, a feature selection process is used to select the most effective features for the classification process. It is used to lower the classifier complexity and choose the right set of features. The results of the extracted features can be selected through cross-validation.

Subsections 3.4.1 to 3.4.2 describe the time- and frequency-based approaches proposed in this study. In addition, a feature selection process is used to determine the highest-quality features for the classification process. This is done to lower classifier complexity and select the right set of features. The results of the extracted features can be selected through cross-validation.

Method	**Features Proposed in this thesis**
Time Domain	Sample entropy Tsallis entropy Renyi entropy Shannon entropy
Frequency Domain	Hilbert–Huang transform (HHT) Fast Fourier transform (FFT)

Table 3- 2 Time and frequency domain features considered in this thesis study

3.4.1 Time Domain Characteristics

Time domain features can provide significant information about signal morphological characteristics, such as shape, duration, and amplitude. These features can be computed directly from the signal's time series data, without more complex analysis techniques. Entropy is a statistical measure of randomness or uncertainty. In EEG, entropy features can be extracted from EEG signals to quantify the degree of randomness or complexity in the brain signals. These features can be used for various purposes, such as identifying EEG patterns associated with certain cognitive or physiological states, detecting changes in brain activity over time, or distinguishing between healthy and abnormal EEG signals. Entropy measures used in EEG analysis in this thesis include:

3.4.1.1 Shannon Entropy

Shannon entropy is categorized under a degree of ambiguity regarding the rate of the result which measures of the data spread. The greater the entropy is the higher the ambiguity and the difficulty factor in predicting the results increases. Shannon entropy is typically used by considering all the data surrounding specific points. Information regarding specific events, such as CAP, can be obtained from this method. Equation 1 below defines the Shannon entropy equation, $p(x_i)$ represents the probability of acceptance off the random variable X data [30] and *n* is the number of samples.

$$H(x) = \Sigma_{i=1}^{n} p(x_i) log_a \frac{1}{p(x_i)} \qquad (3-1)$$

3.4.1.2 Tsallis Entropy

Tsallis entropy is considered to be a generalized form of Shannon entropy. Entropy evaluates the quantity of information of a random variable in regard to the minimum number of bits with respect to the symbol required to code the variable. Entropy is generally used to compute the theoretical minimum capacity or bandwidth necessary for storage or transmission of an information source. Tsallis entropy encompasses the diagonalization technique, which extracts all the relevant peak limitations, the complex frequencies and various amplitudes. Tsallis uses a windowing process n the EEG signal, hence the time signal is composed of N points and the sampling time (τ). The time signal is processed to obtain a low-resolution spectrum. For the purpose of this study, the entropic index (q) is the resulting measure of Tsallis entropy which ultimately has the effect to impose on a control will be greater than 1. The default value for q that was used is 2. Equation 2 below defines Tsallis entropy [35].

$$H_q(p_i) = \frac{k}{q-1}\left(1 - \Sigma_i p_i^q\right) \qquad (3-2)$$

3.4.1.3 Renyi Entropy

Renyi entropy is another generalized form of Shannon entropy. The probability of a distribution on a finite set depends on the parameter α (represents the order of Renyi entropy). Equation 3 illustrates the mathematical equation for Renyi's entropy. Renyi's entropy has certain limiting cases that represent the most convincing results; $R_0 = \lim_{\alpha \to 0} R_\alpha$ and $R_\infty = \lim_{\alpha \to \infty} R_\alpha$. These limiting conditions are known as max-entropy and min-entropy [50,]. The Renyi entropy $H_{re} =$ is of order α where $\alpha > 0$ and ¸ $\alpha \neq 1$. If ¸is equal to 2, then the measurement equally emphasizes the sub-gaussian and the super-gaussian components [23].

$$H_{re} = \frac{1}{1-\alpha} ln \Sigma_{i=1}^{n} p(x_i)^{\alpha} \qquad (3-3)$$

3.4.2 Frequency Domain Characteristics

Frequency domain features are widely used in EEG signal analysis to characterize spectral content changes. The EEG signal is distinguished in the five different frequency stages, a band feature is utilized by dividing the two traveling short and long-duration magnitudes by the respective band. The CAP sections are obtained by relating the band features to a set threshold. This study aims to detect CAP in EEG and explore different methodologies, features, and classifiers.

3.4.2.1 Hilbert–Huang transform

HHT is put forward for the analysis of nonlinear and non-stationary signals. Unlike FFT, HHT is unique in not requiring a priori functional basis. Meaning HHT can be utilized for the analysis of both non-stationary and nonlinear signals and can be adapted to local characteristically time scales for the desired data. HHT a computational method for analyzing and decomposing signals into intrinsic mode functions (IMFs) which is based on the empirical mode decomposition (EMD) algorithm. The HHT is particularly useful for analyzing signals with non-stationary and non-linear characteristics, as it can extract and separate different components of the signal in both time and frequency domains). The

most telling way of describing this system is in terms of instantaneous frequency. From the instantaneous frequency, the intra-wave frequency can be displayed. The output of HHT is a time series that is complexly valued with its amplitude and phase dependent on time, introducing the concept of instantaneous frequency. Equation 3-4 illustrates the instantaneous version of HHT [50].

$$H(t) = \frac{1}{\pi} lim_{\epsilon \to 0^+} \left(\int_{t-\frac{1}{\epsilon}}^{1-\epsilon} \frac{x(\tau)}{t-\tau} d\tau + \int_{t+\frac{1}{\epsilon}}^{1+\epsilon} \frac{x(\tau)}{t-\tau} d\tau \right) \qquad (3-4)$$

3.4.2.2 Fast Fourier Transform

Fast Fourier Transform (FFT) is utilized to convert the EEG signal from the time domain to the frequency domain in this thesis. Key improvement in the thesis work: the incorporation of frequency-based features through the use of a fast Fourier transform (FFT) in the process of extracting features from EEG signals, by applying the FFT to EEG signals, the time-domain signals are transformed into the frequency domain. This transformation allows for a more comprehensive analysis of the signals, which can be particularly beneficial for capturing CAPsEEG signals are first transformed into frequency domain using FFT which calculates the Discrete Fourier Transform (DFT) of a specific sequence or the inverse of that sequence [9]. Typically, one can obtain the DFT by disintegrating the data sequence intro variables with different frequencies. In other words, the original signal can be separated into its sub spectral components by using spectral analysis methods. The equation of FFT defined as

$$F_r = \sum_{u=0}^{M-1} x_n e^{-2\pi r \frac{u}{M}} \qquad (3\text{-}5)$$

where *Fr* is the FT coefficients, *M* is the length of input EEG [42]. FFT is an algorithm that computes the discrete Fourier transform (DFT) of a sequence, or its inverse (IDFT). Fourier analysis converts a signal from its original domain (often time or space) to a representation in the frequency domain and vice versa. The DFT is obtained by decomposing a sequence of values into components of different frequencies. As

previously mentioned, the signal is decomposed into components with different frequency, in this case the CAP components will be different that the non-CAP components.

FFT variations in for CAP and Non-CAP components in different normal subjects

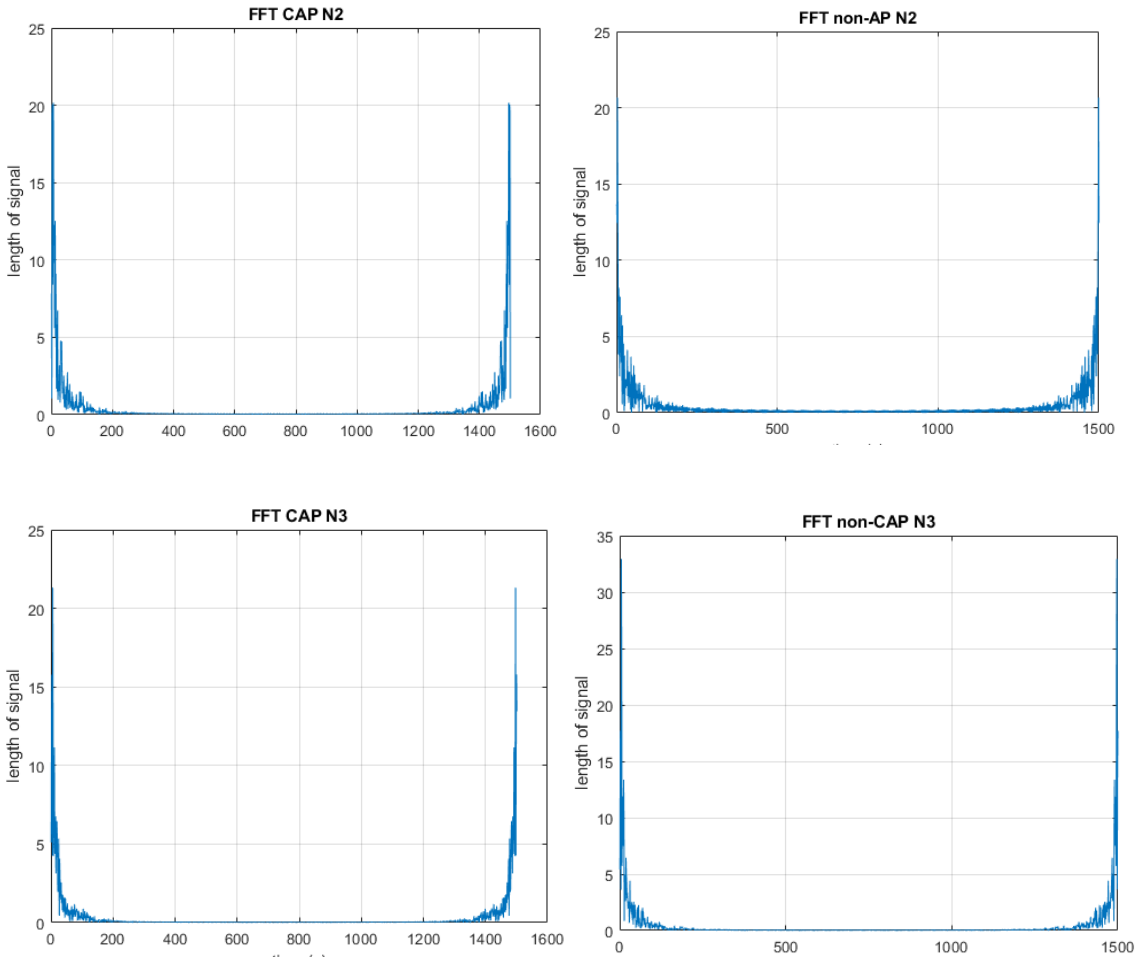

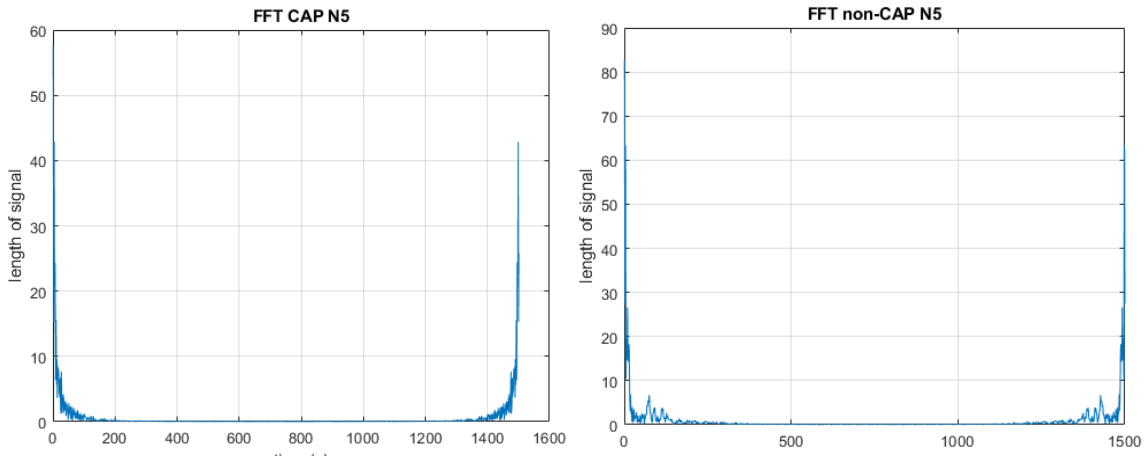

Figure 3-10 FFT features for Normal subjects

FFT variations in for CAP and Non-CAP components in different SDB subjects

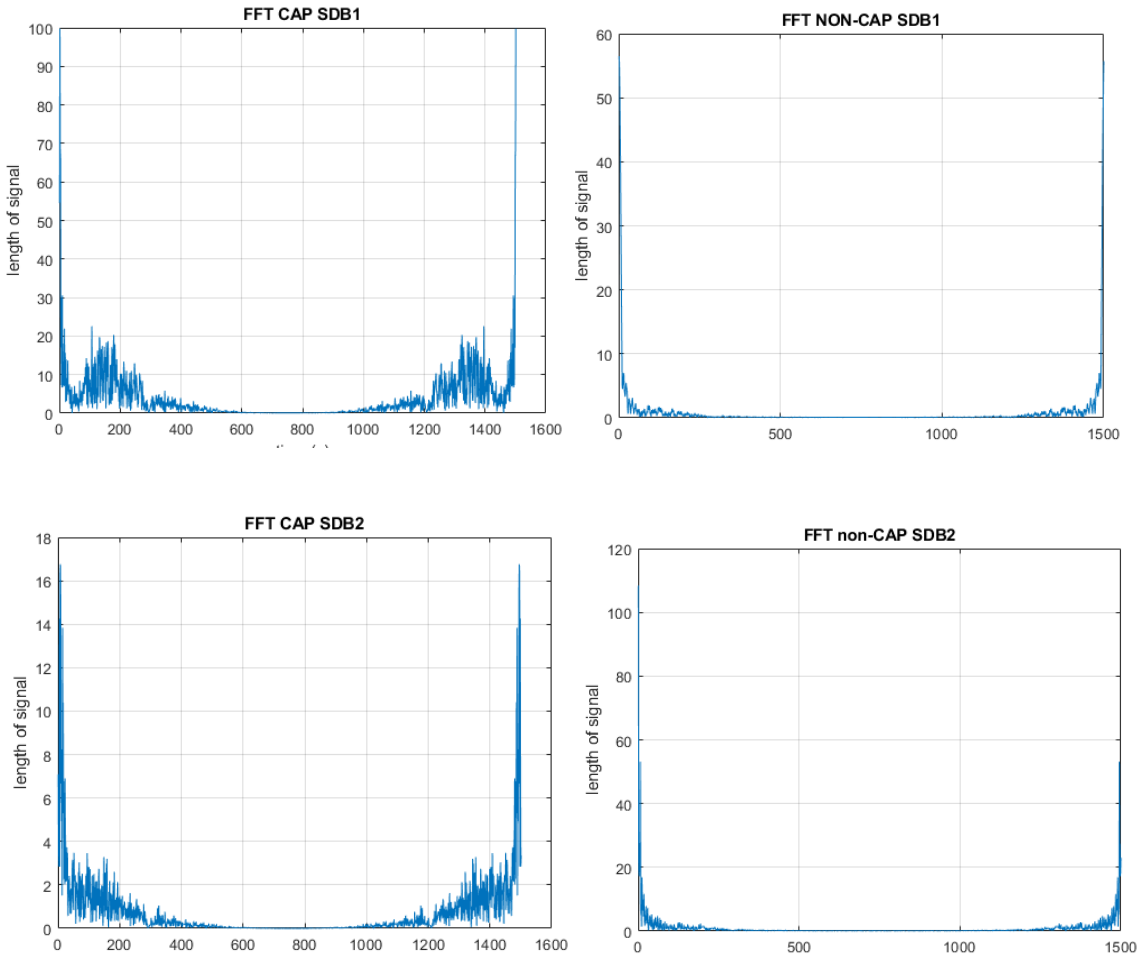

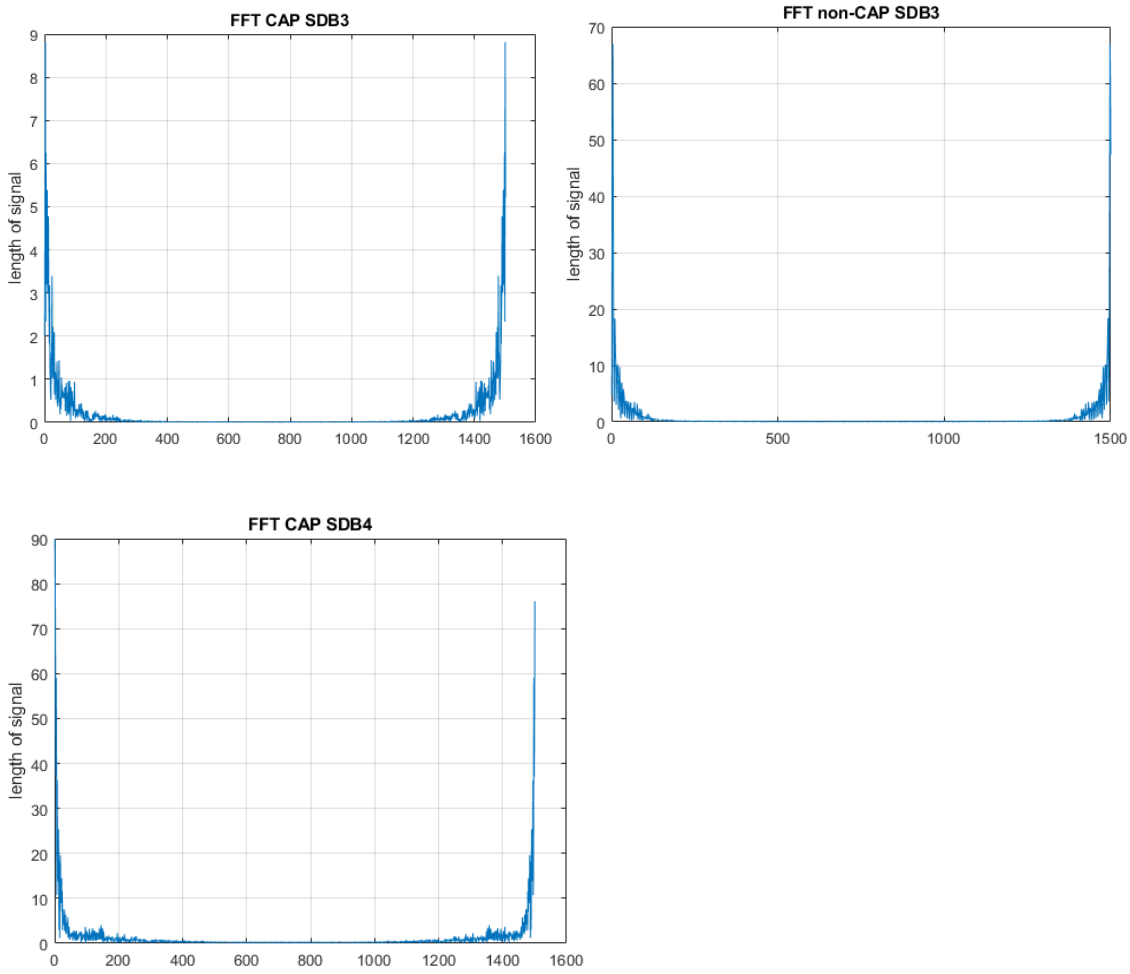

Figure 3-11 FFT features for SDB subjects

FFT variations in for CAP and Non-CAP components in different INS subjects

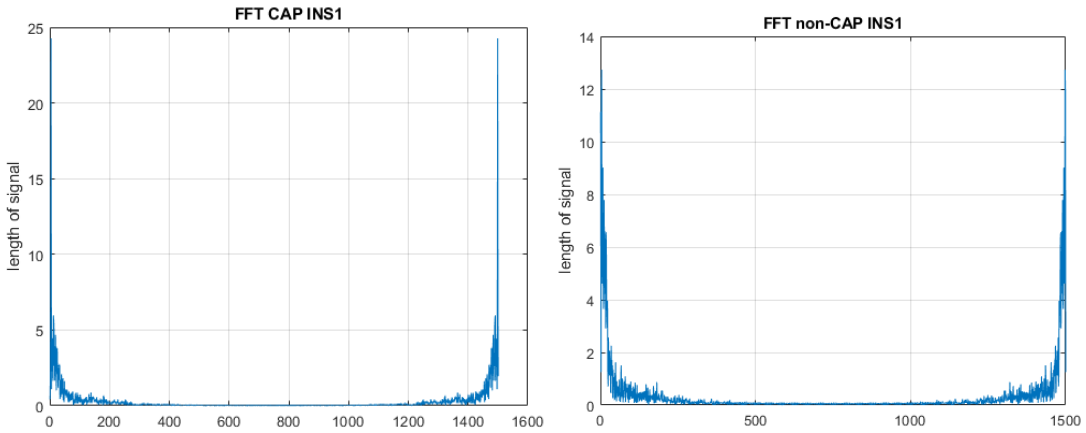

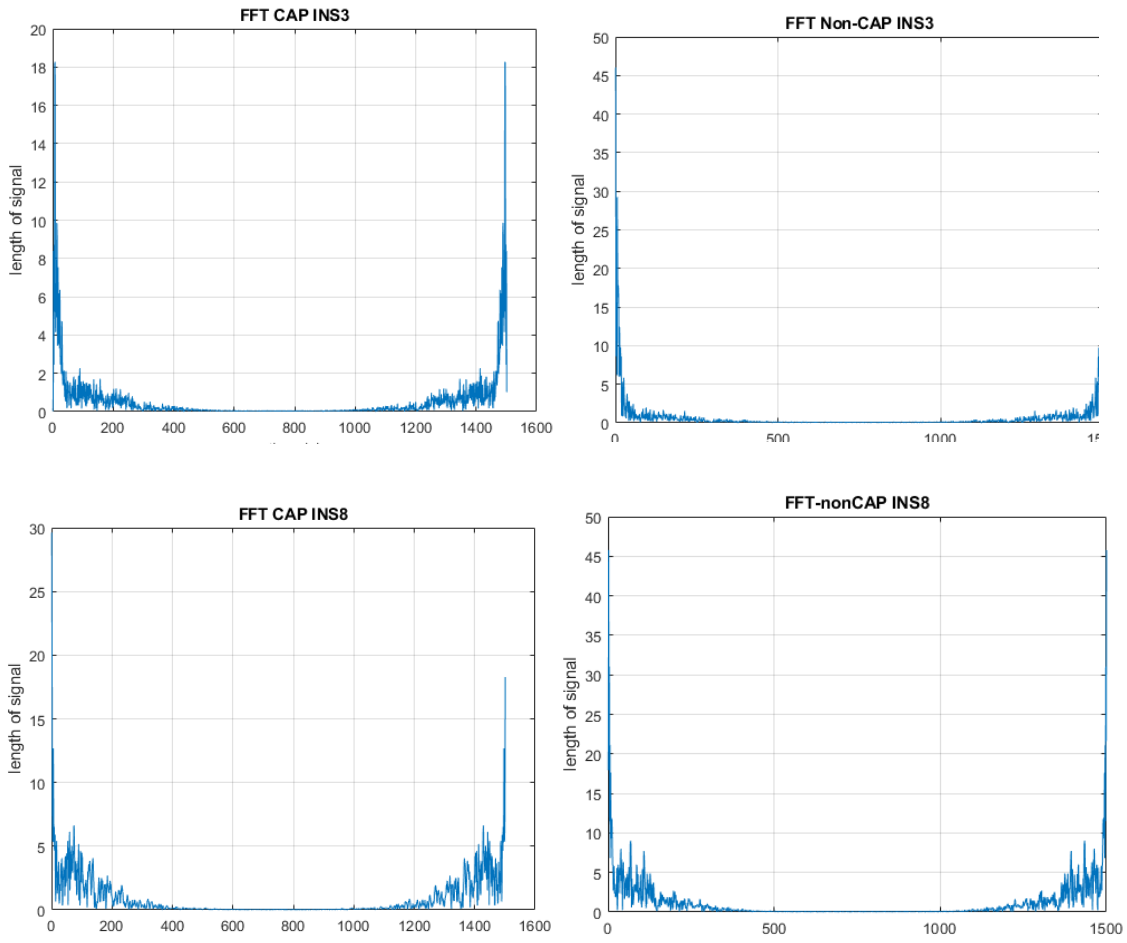

Figure 3-12 FFT features for INS subjects

3.5 Feature Extraction

The time and frequency-based characteristics described in section 3.6 measure the entropy along with the density of the EEG signal. There exists a 50% overlap of data in EEG signals, to exclude non-stationary signals. Shannon entropy measures impurity in the EEG signal. In order to determine the probability of CAP phase detection, Shannon entropy will be calculated over all the amplitudes of the EEG signal. Renyi's entropy is utilized in this study to compute the 2D frequency structure [50]. Renyi's entropy differs between EEG waveforms and CAP events within their equivalent frequency bands. Tsallis entropy is also used for feature extraction as this entropy is a generalized form of Shannon entropy and results in a low-resolution spectrum. Lastly, Sample entropy is also used to represent the roughness of the time series. HHT is applied in this study due to its recent application in biomedical and other fields. In addition, it is applied to nonlinear and non-

stationary signals. FFT is selected for feature extraction due to its speed over other available methods in real-time applications. The event to be extracted is specifically the CAP phase A event. This event is selected based on the information available for annotation data obtained from PhysioNet.

As previously mentioned, MATLAB codes are developed for each feature separately. Furthermore, results from the extracted features are kept if the time variable matches the time variable of the CAP event extracted from the annotations file. For instance, if a CAP event occurred between times a and b and lasted for 10 seconds, the results of the extracted features will be kept for times a and b and labeled as the CAP features that occurred in the EEG signal; this is later utilized in the classification step so that the extracted time features that match the CAP parameters are the true positives while the other values are the true negatives and so on. In Chapter 4, the approach of detecting CAP in EEG utilizing conventional and non-conventional features with the use of different classifiers is explored also the results and discussions are elaborated.

3.6 Data Classification

The importance of the classification step is to generate a confusion matrix that will result in true positive, as well as true negative (TN), false positive (FP), and false negative (FN) values. Furthermore, classifiers are evaluated by TP, TN, false, FP, and FN values. TP values indicate the number of data points that correspond to correctly classified CAP events. FP represents data points that point to non-CAP events as CAP events. TN represents the number of data points that correspond to non-CAP events in the signal and are correctly classified as non-CAP events. FN refers to the data points referring to CAP events as non-CAP events. The classification step results in CAP detection accuracy in EEG. Different classifiers are required in this study due to their varying approaches and abilities.

Prior to the analysis of the classifiers in the classification learner application, the data (i.e. the response CAP data, time, and feature results) need to be properly formatted into a table for input into the classification application. During the training process, the

algorithm learns to map the input EEG signals to the corresponding CAP or not CAP labels. Once the model is trained, it can classify newly discovered, unseen EEG signals as CAP or not CAP.

As shown in Figure 3.13, CAP response and features extracted from the sdb patient are prepared in a table that will be uploaded into the classification learner application.

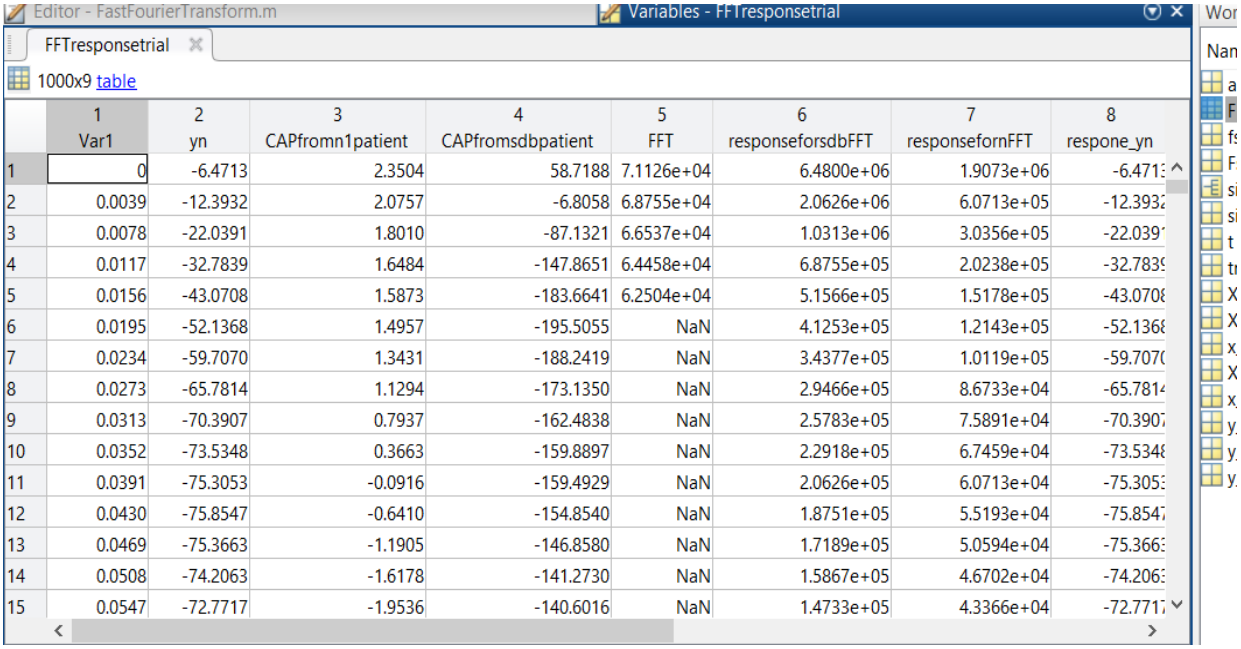
Editor - FastFourierTransform.m

Variables - FFTresponsetrial

FFTresponsetrial

1000x9 table

	1 Var1	2 yn	3 CAPfromn1patient	4 CAPfromsdbpatient	5 FFT	6 responseforsdbFFT	7 responsefornFFT	8 respone_yn
1	0	-6.4713	2.3504	58.7188	7.1126e+04	6.4800e+06	1.9073e+06	-6.471
2	0.0039	-12.3932	2.0757	-6.8058	6.8755e+04	2.0626e+06	6.0713e+05	-12.393
3	0.0078	-22.0391	1.8010	-87.1321	6.6537e+04	1.0313e+06	3.0356e+05	-22.039
4	0.0117	-32.7839	1.6484	-147.8651	6.4458e+04	6.8755e+05	2.0238e+05	-32.783
5	0.0156	-43.0708	1.5873	-183.6641	6.2504e+04	5.1566e+05	1.5178e+05	-43.070
6	0.0195	-52.1368	1.4957	-195.5055	NaN	4.1253e+05	1.2143e+05	-52.136
7	0.0234	-59.7070	1.3431	-188.2419	NaN	3.4377e+05	1.0119e+05	-59.707
8	0.0273	-65.7814	1.1294	-173.1350	NaN	2.9466e+05	8.6733e+04	-65.781
9	0.0313	-70.3907	0.7937	-162.4838	NaN	2.5783e+05	7.5891e+04	-70.390
10	0.0352	-73.5348	0.3663	-159.8897	NaN	2.2918e+05	6.7459e+04	-73.534
11	0.0391	-75.3053	-0.0916	-159.4929	NaN	2.0626e+05	6.0713e+04	-75.305
12	0.0430	-75.8547	-0.6410	-154.8540	NaN	1.8751e+05	5.5193e+04	-75.854
13	0.0469	-75.3663	-1.1905	-146.8580	NaN	1.7189e+05	5.0594e+04	-75.366
14	0.0508	-74.2063	-1.6178	-141.2730	NaN	1.5867e+05	4.6702e+04	-74.206
15	0.0547	-72.7717	-1.9536	-140.6016	NaN	1.4733e+05	4.3366e+04	-72.771

Figure 3-13 Snippet of the data column, such as the time, the response of the EEG signal, the CAP response for patient N1.

3.6.1 Linear Discriminant Analysis (LDA)

This method is statistical based and optimized the ratio of the covariance matrix, which means the probable space samples in each class develops a dense center and other samples separate by class fall away from that center [35,22,23]. This classification procedure performs well when each class is Gaussian like. It has been found that the LDA method behaves well with EEG signals.

3.6.2 Support Vector Machine (SVM)

Proposed by Vapnik, this classifier reduces the structural risk (any test errors). This classifier contains a user-selected bound that governs the margin width. This classifier is

categorized as linear binary, and can be applicable to inputted data with the leading SVM, which delivers a non-linear margin between different class models. The purpose of the method is to optimize the margins and minimize the risk; the Lagrange method is applicable for this method. A Lagrange coefficient is applied to each class, those classes that are within will have a non-zero Lagrange coefficient, while the other classes will be zero [35, ,23,23].

3.6.3 K-Nearest Neighbor (KNN)

This classifier is extremely flexible and performs best when the data distribution is multi module. This classifier utilizes a non-parametric approach to classify the signal. KNN makes choices for different class samples and acts as a local classifier. This classifier operates by finding the KNNs and labeling them based on the majority of KNNs found [1,10,14,22,23]. For signal classification, the KNN classifier needs the distance between the vectors, and this is obtained by utilizing equation 5.

$$d_{(x,y)} = \sqrt{\sum(x_i - y_i)^2} \tag{3-6}$$

3.6.4 Random Decision Trees

The random forest takes an average of predicted accuracies and best fits various decision trees. Decision trees are often utilized to categorize the various sleep stages utilizing a binary-tree method. Typically, random forest classifiers consist of many individual classification trees, the bagged (bootstrap-aggregated) decision trees mixes the results of the various decision trees with one another. This results in a reduction of the effects of over-fitting, in addition to improving generalization.

The training algorithm for random forests utilize general methodology of bootstrap aggregating, or bagging, to tree learners. For a given a training set X with responses Y, bagging repeatedly (B times) chooses a random sample with replacement of the training set and fits trees to these samples. Once training is complete, predictions for unseen samples x' can be made by averaging the predictions from all the individual regression

trees on x'. Equation 5 below represents the mathematical model for this methodology [50].

$$\hat{f} = \frac{1}{B}\sum_{b=1}^{B} f_b(x') \tag{3-7}$$

In order to classify an object from an input vector, the input vector must be classified under each tree in the forest. Each tree results in a classification, which results in "votes" for the particular class. The decision tree then selects the classification that receives the most votes. This is shown in Figure 3.14.

The following steps result in each tree classification as follows:

1. If the number of cases in the training set is N, sample N cases randomly - but with replacement, from the original data. This sample will be the training set for growing the tree.

2. If there are M input variables, a number m<<M is specified such that at each node, m variables are selected at random out of the M and the most optimal split of this m is used to split the node. The value of m is held constant during forest growth.

3. Each tree is grown to the greatest extent possible. There is no pruning [5].

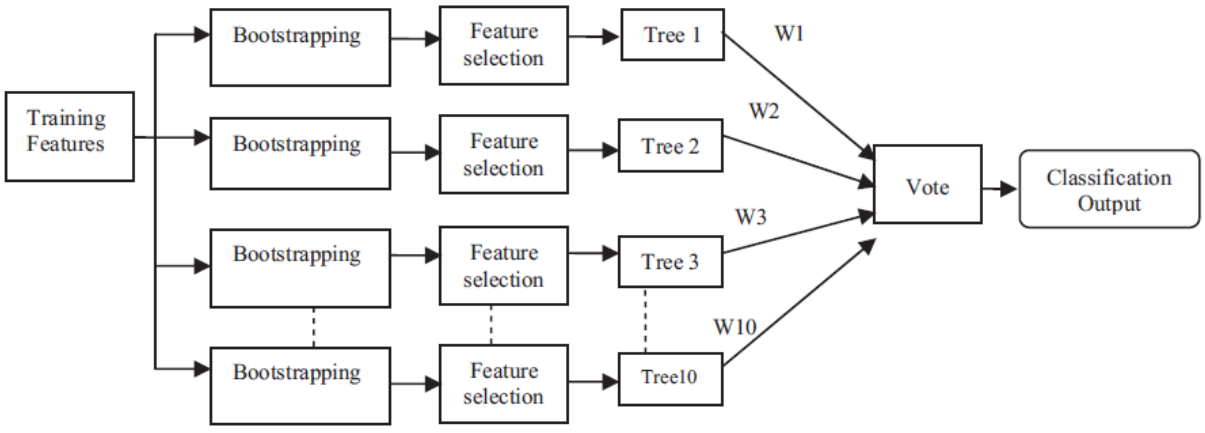

Figure 3-14 Structure of the random forest classifier [50]

The simulation results show more conservative results for CAP detection while using different classifiers in this study as opposed to the literature study.

Chapter 4 Results and Discussions

Chapter 4 of the thesis focuses on EEG CAP detection and performance evaluation. The study aims to develop a reliable method for the automated detection of CAPs in EEG signals. The study employed cross-validation techniques and evaluated the performance of four classification tools, Linear Discriminant Analysis, Support Vector Machine, K-Nearest Neighbor, and Random Forest.

4.1 – EEG CAP Detection and Motivation

The CAP EEG classification provides a more detailed and objective assessment of sleep quality than traditional measures such as total sleep time and sleep efficiency. CAP analysis can identify disturbances in sleep architecture and provide information on the underlying causes of sleep disorders such as insomnia, sleep apnea, and restless leg syndrome.

This thesis study aims to improve classification to achieve higher accuracy in detecting CAPs in EEG signals. Previously, Karimzadeh et al. Presented EEG Signals for Automatic CAP Detection in Sleep. A comparison of conventional and non-conventional characteristics was conducted using LDA, SVM, and KNN classifiers. The key was to use Sequential Forward Selection (SFS) proposed in [35] to select highly accurate features to detect CAP in EEG signals. The SFS begins by applying one feature to an empty feature sub-set; this will clearly show a desired function, then undergoes a second step; in this second step, a desired feature that can be compared to the first feature is identified. The SFS feature selection algorithm repeats the first and second steps until the best-performing features are selected.

In summary of later sections' findings, proposed entropy-based and frequency-based features are better suited for CAP detection in EEG than suggested conventional features in literature [35] and this is due to the degree of roughness accommodated in the entropy-based features. Figure 4.1 illustrates the accuracy results of SFS features for healthy and patient subjects. The literature study focuses on evaluating a family of entropy-based

features (i.e. Shannon, Sample, and Kolmogorov) through the use of different classifiers (SVM, LDA, and KNN) to achieve acceptable CAP detection accuracy in EEG [35]. The figure also shows the range of features selected for each classifier for example SFS= 81±1.6 performance of an SFS in selecting a subset of features so 81 is the accuracy score and ranged ±1.6 indicates the uncertainty or variance in the performance metric, which suggests that the performance of the algorithm could vary by up to ±1.6 depending on the specific dataset. The proposed features perform better than conventional features due to their ability to effectively quantify the change in brain activity as it transitions from a non-CAP to a CAP state [35].

SUGGESTED FEATURES FOR HEALTHY SUBJECTS (%)

Features	SVM	KNN	LDA
Shannon	70	71	70
Spectral	72	72	72
Kolmogorov	79	72	68
Sample	75	70	71
Tesallis	69	72	67
Higuchi	70	68	68
Features selected by SFS	81 ± 1.6	79 ± 1.5	79 ± 2.1

SUGGESTED FEATURES FOR PATIENTS (%)

Features	SVM	KNN	LDA
Shannon	67	63	62
Spectral	61	63	55
Kolmogorov	66	62	64
Sample	66	69	60
Tesallis	62	59	61
Higuchi	58	51	52
Features selected by SFS	76 ± 4.4	66 ± 2.3	74 ± 3.1

Figure 4-1: features for healthy & patients' subjects proposed in [35]

The features from the previous study [35] were used to train machine learning models on MATLAB to identify CAP/Non-CAP sequences in an EEG signal, along with additional proposed features for insomnia and sleep-disordered breathing disorders.

4.2 Cross Validation

Cross-validation, also known as out-of-sample testing, is a terminology used to refer to various model validation techniques to assess the generalization performance of a machine learning model. This is done by dividing the data into multiple folds and training the model on different subsets while evaluating it on the remaining part. This provides an estimate of how the model would perform on unseen data. It can be used to tune the model to hyperparameters, such as the regularization strength or the depth of a neural network. These techniques assess the results of a statistical analysis that results in an interdependent dataset. In k-fold cross-validation, the data is divided into k equally-sized subsets, and the model is trained on k-1 folds and tested on the remaining folds. This process is repeated k times, with each fold serving as a testing set once. The value of k can be chosen based on the dataset size and computational constraints.

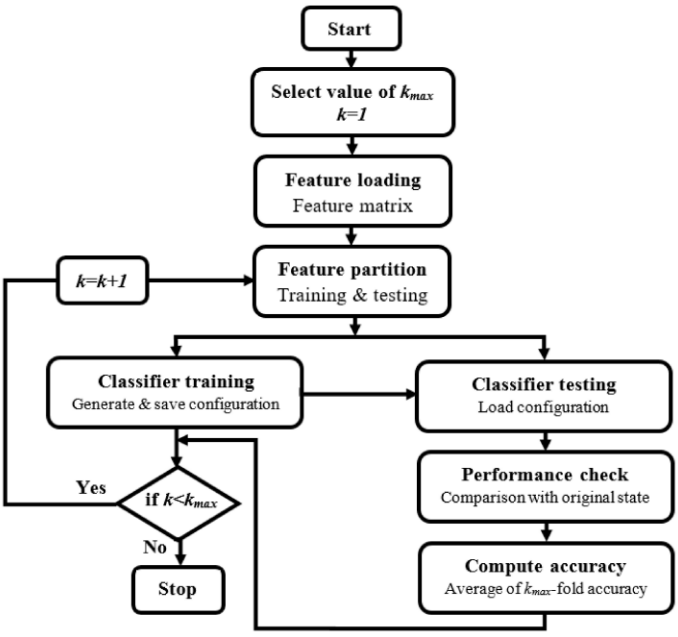

Figure 4-2 Methodology for k-fold cross-validation [60].

This is shown in Figure 4-2. In the classification learner application, in MATLAB, cross-validation is repeated for all combinations of k-1 to k sets, which include more parameters than can be accepted by the data. In this study, the cross-validation technique is applied

to evaluate certain predictive models and to approximate the out-of-sample error of a model. Once the error is approximated, the model is re-fitted with the full data set to fully exploit the information in the data set. In the MATLAB classification app, the dataset is divided into 5 equal parts or folds, with each fold containing 10% of the data. The following steps clarify the process of training, testing, and validating the data in the MATLAB Classifier App:

1. Data Splitting: When loading the CAP EEG dataset into the MATLAB Classification App, the app automatically divides the dataset into five equal parts, or "folds the process is as follows:
2. Cross-Validation Iterations: For each of the five iterations (folds), the process is as follows:
    - Training Data Selection: The app selects four out of the five folds (80% of the data) for training the classifier.
    - Validation/Testing Data Selection: The remaining one-fold (20% of the data) is used for testing and validation purposes. This fold will not be used during training.
3. Model Training: The chosen classifier will be trained using the four selected folds as training data
4. Validation/Testing: Using the trained classifier to predict labels for the data points in the validation/testing fold, performance metrics such as accuracy will be calculated based on the classifier's predictions on the validation/testing fold.

By completing the five iterations, performance metrics for each fold was obtained, helping assessing the classifier's performance more comprehensively. This approach allows to assess how well the classifier generalizes to new data and helps in estimating its real-world performance. MATLAB's Classification App streamlines this process, handling data splitting, training, validation, and metrics calculation automatically, also it enables

to visually explore results, compare different classifiers, and fine-tune model settings interactively.

4.3 Performance Evaluation

The processed data is classified in the classification learner application in MATLAB. This application explores supervised machine learning through feature selection, validation schemes, model training, and assessing results. Training of the model is automated to determine the most appropriate classifier for the data; this includes SVM, LDA, KNN, and Random Forest (RDT). The classification learner application evaluates the different classifiers by illustrating the confusion matrix or the Receiver Operating Characteristics (ROC) curve.

The classification learner application yields the confusion matrix, which is used for classifier classification. In this study, true positive (TP) values are utilized to determine if the patient fits the response curve and is expected to have a sleep-related illness. Furthermore, TP values are typically used for the sensitivity or recall formula. True negative (TN) values indicate that the patient does not have a sleep-related illness. False positive (FP) values, also known as Type I errors, predict that the sleep-related illness the patient is diagnosed with is inaccurate. False negative (FN) values, also known as Type II errors, predict that the sleep-associated illness not found is incorrect. The misclassification rate provides a rating for how often the classification is incorrect and is commonly referred to as the “Error Rate” [50]. Using the confusion matrix helps evaluate any classification model efficiently. Therefore, the confusion matrix along with the performance parameters will be utilized to evaluate the classification models. From the confusion matrix, the classifier's accuracy can be determined using Equation 4-1.

$$\text{Accuracy} = \frac{\text{TP}+\text{TN}}{\text{TP}+\text{TN}+\text{FP}+\text{FN}} \qquad (4\text{-}1)$$

$$\text{Recall} = \frac{\text{TP}+\text{TN}}{\text{TP}+\text{FN}} \qquad (4\text{-}2)$$

$$\text{Precision} = \frac{\text{TP}}{\text{TP+FP}} \quad (4\text{-}3)$$

$$\text{Misclassification} = \frac{\text{FP+FN}}{\text{Total}} \quad (4\text{-}4)$$

$$\text{Sensitivity} = \frac{\text{TP}}{\text{TP+Fn}} \quad (4\text{-}5)$$

The ROC curve can also be obtained from the classification learner application in MATLAB. By measuring the area under the curve, ROC is the ratio of TP values and FP values, as example shown in Figure 4-3.

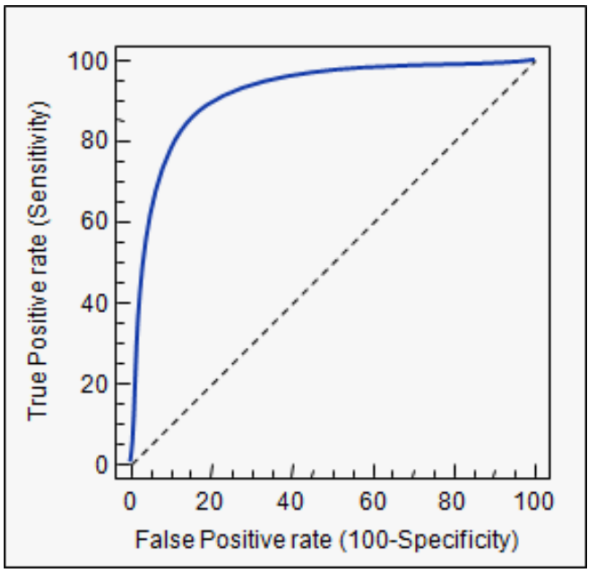

Figure 4-3: Illustration of ROC curve that MATLAB illustrates in the classification learner application

In addition, sensitivity and specificity are examples statistical measures of the performance of a binary classification test, that is commonly referred to as a classification function in statistics. It is worth noting that sensitivity measures the proportion of actual negatives that are correctly identified (e.g., the percentage of healthy people who are correctly identified as not having the condition) and specificity measures the proportion of actual negatives that are correctly identified such as (e.g., the percentage of healthy people who are correctly identified as not having the condition. To prepare the data table to be sent to the classification app. For example, for best results, table with the features

acting as predictors was created, the response being CAP data and observations being all other data.

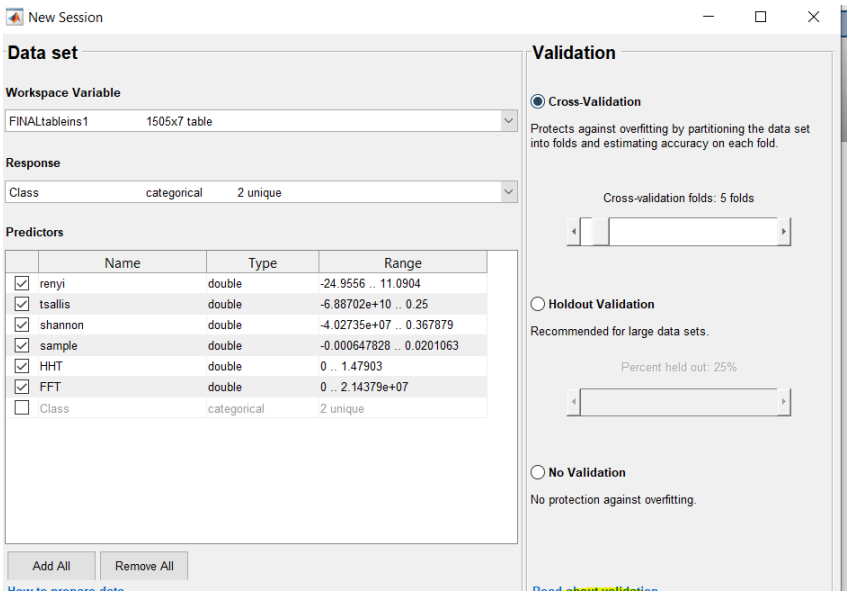

Figure 4-4: Example of features as predictors in the MATLAB classification App

In the Figures 4-4 and 4-5, it shows confusion matrix for a healthy subject result generated in the classifier app in MATLAB. This is repeated for the non-healthy patient, a bar graph showing the accuracy. These results are repeated for different response features. For example, to see how well one feature detects CAP and with which classifier it will achieve highest accuracy, that feature will be selected as the response class in the app classifier.

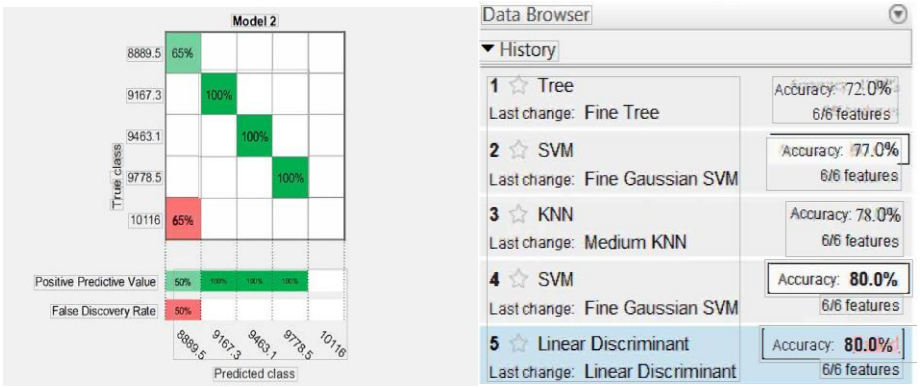

Figure 4-5: confusion matrix for a healthy subject in Classifier App

4.4 Case 1: Average Performance Evaluation for all patients

From MATLAB's classification learner app, the classifiers are evaluated by the true positive (TP), true negative (TN), false positive (FP) and false negative (FN) values. TP values represent the number of data points that refer to CAP events that are correctly classified. FP represents the data point that refer to non-CAP events as CAP events.TN represents the number of data points that refer to non-CAP events in the signal and are correctly classified as non-CAP events. FN represents the data points referring to CAP events as non-CAP events [50].

After analyzing different features and classifiers, the features detect the CAP peaks in the subjects using different domains, such as time, frequency or time frequency. The features then generate an output of data from the CAP input data provided for comparison. Training the data represents the ability of the predictor class (i.e. the feature tested) in locating similar CAP peaks. The higher the accuracy, the more data peaks the predictor class is able to find that are exact matches to the CAP peaks.

4.4.1 Observations

The results are obtained from the classification learner app, using 50% overlap, cross validation. Furthermore, the results shown are stored in a workspace variable via a code generated in MATLAB. Once the results of the features are available, the averages of the results for each patient set are taken. Rather than uploading all the data, sample from each subject data points are taken from each subset to create a scatter plot rather than uploading all of the data into the classification leaner app meaning a sample for each CAP response. For example, from the CAP annotations score reader Matlab file CAP starting times from 5 seconds to 25 minutes. From this time range will take a sample size (of a certain amount for example 20) from the first 5-30 seconds, from 1-10 minutes and from 10 – 30 minutes. In this way will have features and responses that cover the whole length of the time range without exceeding Matlab data limit.

By taking these steps, the classification results are enhanced (due to lower amount of data to be processed) and are classified on 10 seconds average. The SVM and KNN classifier classified the models the best and this is true for all patients (healthy, insomnia and sleep-disordered). In comparison between the three patients, CAP detection in sleep disorder patients presented slightly higher results than in insomnia patients when compared to a normal patient.

4.4.2 Results for average performance of the classifiers

The following results considered the various CAP events due to the provided annotations information. The results of the conventional time and frequency-based features that are classified utilizing SVM, LDA, Random Forest and KNN are illustrated in Tables 4-1, 4-3 and 4-5 below, for healthy patients, patients diagnosed with insomnia and patients with sleep disorder.

4.4.2.1 Patients with Insomnia Average Results

Features	Accuracy of LDA classifier (%)	Accuracy of KNN classifier (%)	Accuracy of SVM classifier (%)	Accuracy of RDT classifier (%)
Renyi entropy	82	82	85	84
Shannon entropy	83	85	87	82
Tsalli entropy	82	80	84	83
Sample entropy	84	79	83	80
HHT extraction	81	79.5	78	86
FFT extraction	79	80	82	82
Average accuracy of time-based entropy features	82.75	81.5	84.75	82.25

Average accuracy of frequency-based features	80	79.75	80	84

Table 4- 1 Average Results for CAP detection from the classification learner application in MATLAB for insomnia.

The results shown in this section illustrates the average results of chosen healthy patients (n1, n2, n3, n5), patients with sleep-disordered breathing (sdb1 – sdb4) and three patients with insomnia (ins1, ins3, ins8) and is meant to discuss the performance of the classifiers also to conduct comparisons with original results in the literature [35] and to show how accurately to classify the features that are detecting CAP events. Patients with Insomnia are added as new case to thesis study to compare the accuracy performance of the classifiers for different subjects.

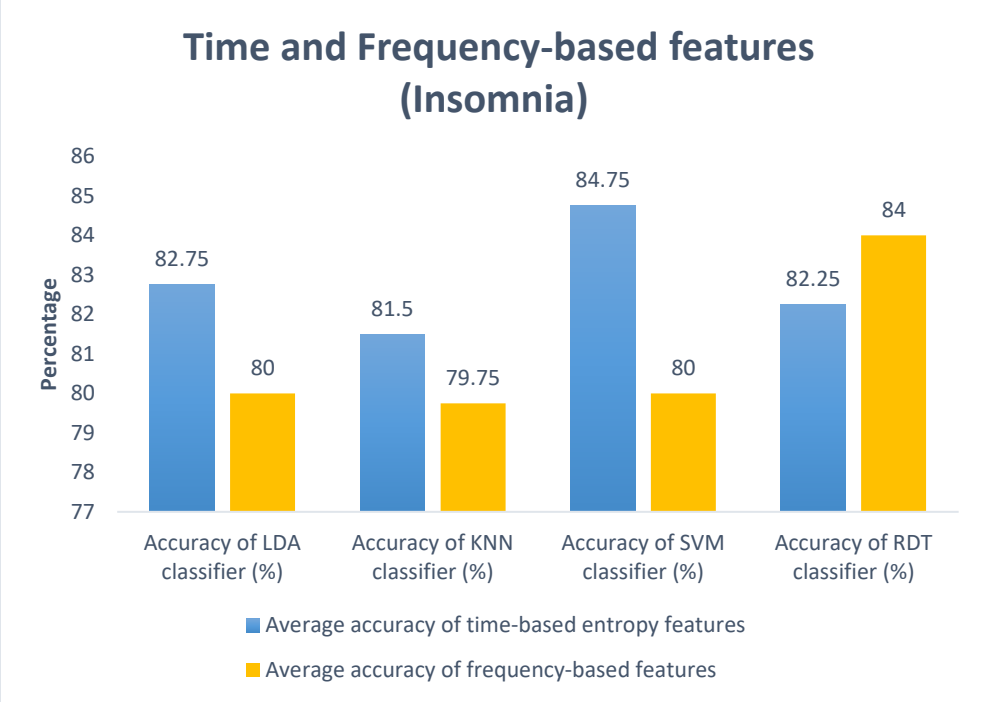

Figure 4-6 Comparison of performance of the classifiers for average accuracies between proposed time and frequency-based features for Insomnia patients.

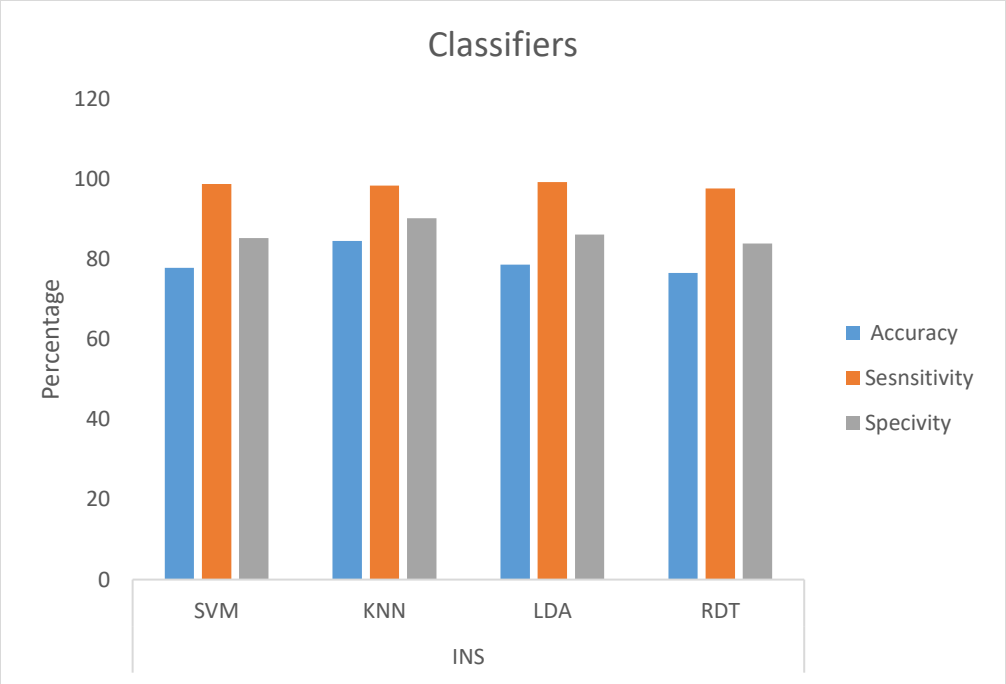

Figure 4-7: Results of accuracy, sensitivity and specivity utilizing LDA, KNN, SVM and RDT for CAP detection from the classification learner application in MATLAB for patients with insomnia.

Figure 4.6 represents the accuracy and sensitivity of LDA, SVM, KNN and RDT for patients diagnosed with insomnia. One observation worth noting is that the greater the number of samples, the greater the accuracy that is obtained. However, at a certain point, the amount of CAP samples extracted will cause the accuracy to converge as an optimized status is achieved. For example, for the SVM classifier: accuracy = (3.4 + 2.4) / (3.4 + 2.4 + 0.03 + 0.97) = 0.778 or 77.8% applying equation 4-1. Sensitivity is a measure of how well a classifier identifies positive instances for example from Table 4-2, for the SVM classifier sensitivity = 3.4 / (3.4 + 0.97) = 0.778 or 98.8% applying equation 4-5.

		Avg accuracy of classifier	Avg sesnsitivity of classifier%	Avg Tp	Avg specivity of classifier%	Avg Tn	Avg Fp	Avg Fn
INS	SVM	77.8	98.8	3.4	85.3	2.4	0.03	0.97
	KNN	84.6	98.3	5.1	90.2	4.1	0.07	0.93
	LDA	78.6	99.2	3.6	86.1	2.6	0.02	0.98
	RDT	76.5	97.7	3.1	83.8	2.1	0.05	0.95

Table 4- 2 All average values obtained for Tp, Fp, Fn, Tn from confusion matrix for insomnia subjects

4.4.2.2 Healthy Patients Average Results

Features	Accuracy of LDA classifier (%)	Accuracy of KNN classifier (%)	Accuracy of SVM classifier (%)	Accuracy of RDT classifier (%)
Renyi entropy	85	85	88	87
Shannon entropy	86	88	90	85
Tsalli entropy	85	83	87	86
Sample entropy	87	82	86	83
HHT extraction	84	82.5	81	89
FFT extraction	82	83	85	85
Average accuracy of time-based entropy features	85.75	84.5	87.75	85.25
Average accuracy of frequency-based features	83	82.75	83	87

Table 4-3 Average Results of time and frequency-based features utilizing LDA, KNN, SVM and RDT for CAP detection from the for normal patients.

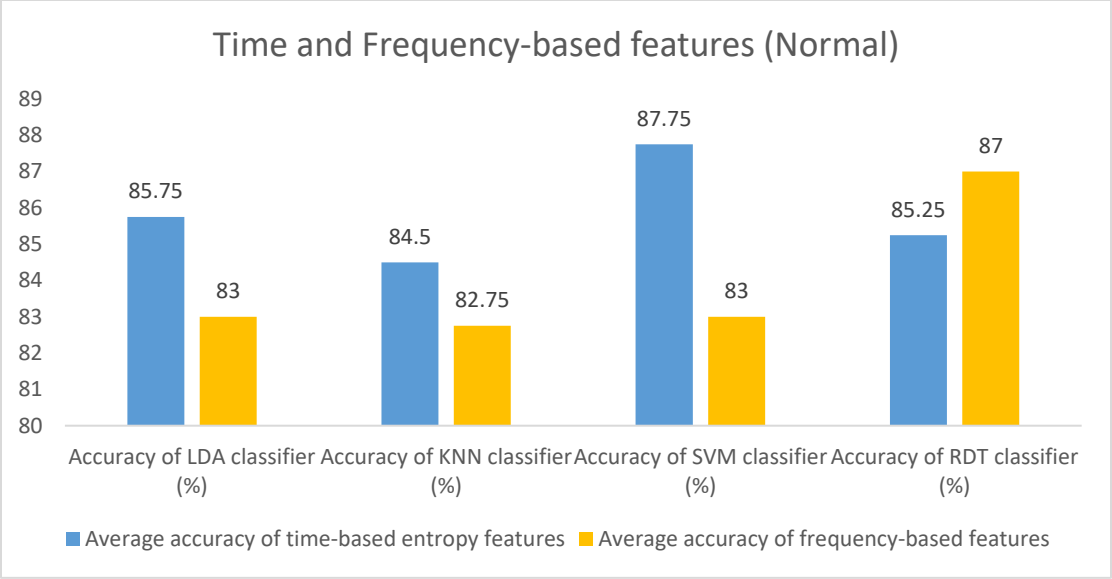

Figure 4-8 Comparison of performance of the classifiers for average accuracies between proposed time and frequency-based features for normal patients.

		Avg accuracy of classifier	Avg sesnsitivity of classifier%	Avg specivity of classifier%	Avg Tp	Avg Tn	Avg Fp	Avg Fn
Healthy (Normal)	SVM	90.1	99.7	94.4	9	8	0.02	0.98
	KNN	89.2	99.5	93.8	8	7	0.033	0.967
	LDA	84.2	98.5	90	5	4	0.06	0.94
	RDT	81.4	98.8	88.1	4.2	3.2	0.04	0.96

Table 4- 4 All average values obtained for Tp, Fp, Fn, Tn from confusion matrix for Normal subjects

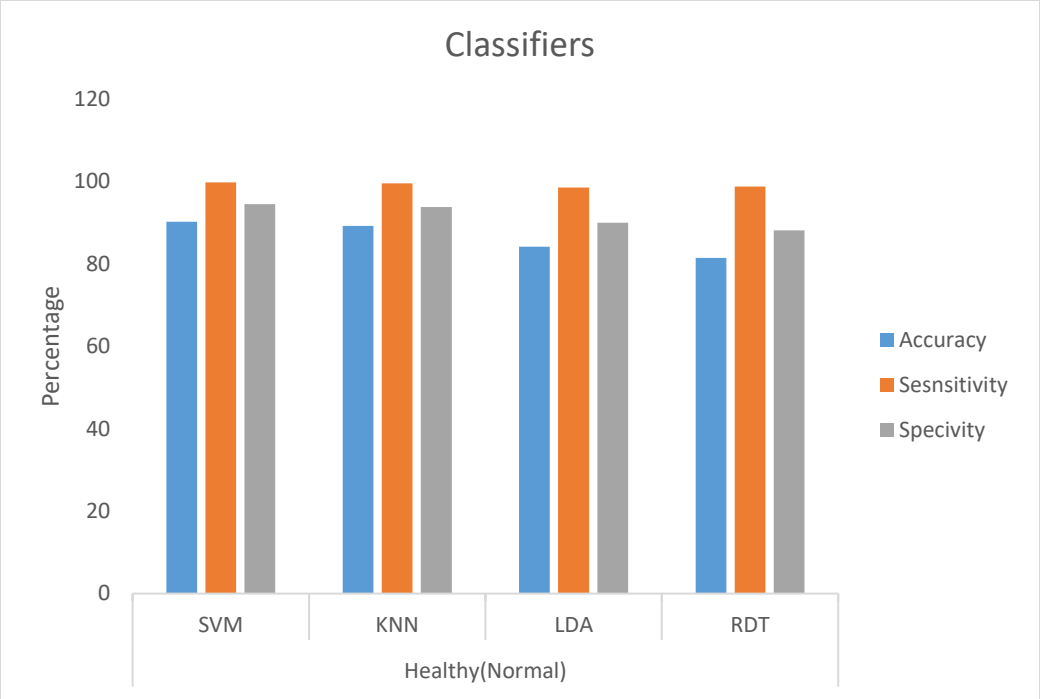

Figure 4-9: Average Results of accuracy, sensitivity and specivity utilizing LDA, KNN, SVM and RDT for CAP detection from the classification learner application in MATLAB for healthy patients.

For both the healthy patients and those diagnosed with insomnia, the SVM classifier is best for classifying the CAP events from extracted feature results. SVM achieves better results when comparing multi-class data or classifying various features at once. Meaning for classifying various features reflecting CAP and non-CAP events in the classification learner app, SVM presented the highest in accuracy, sensitivity and specivity followed by KNN, which is also a reliable classifier in CAP detection, then LDA and finally RDT.

4.4.2.3 Patients with Sleep-disordered Breathing Average Results

Features	Accuracy of LDA classifier (%)	Accuracy of KNN classifier (%)	Accuracy of SVM classifier (%)	Accuracy of RDT classifier (%)
Renyi entropy	84	84	87	86
Shannon entropy	85	87	89	84
Tsalli entropy	84	82	86	85
Sample entropy	86	81	85	82

HHT extraction	83	81.5	80	88
FFT extraction	81	82	84	84
Average accuracy of time-based entropy features	84.75	83.5	86.75	84.25
Average accuracy of frequency-based features	82	81.75	82	86

Table 4- 5 Average Results of time and frequency-based features utilizing LDA, KNN, SVM and RDT for CAP detection from the classification learner application in MATLAB for patients diagnosed with sleep-disordered breathing.

Figure 4.9 represents the accuracy, sensitivity and specivity of LDA, SVM, KNN and RDT for healthy patients. The sensitivity, which is called the TP rate, measures the ratio of actual CAP events that are correctly classified. The specivity of the classifiers, which is called the true negative rate, measure the ratio of non-CAP events that are classified correctly.

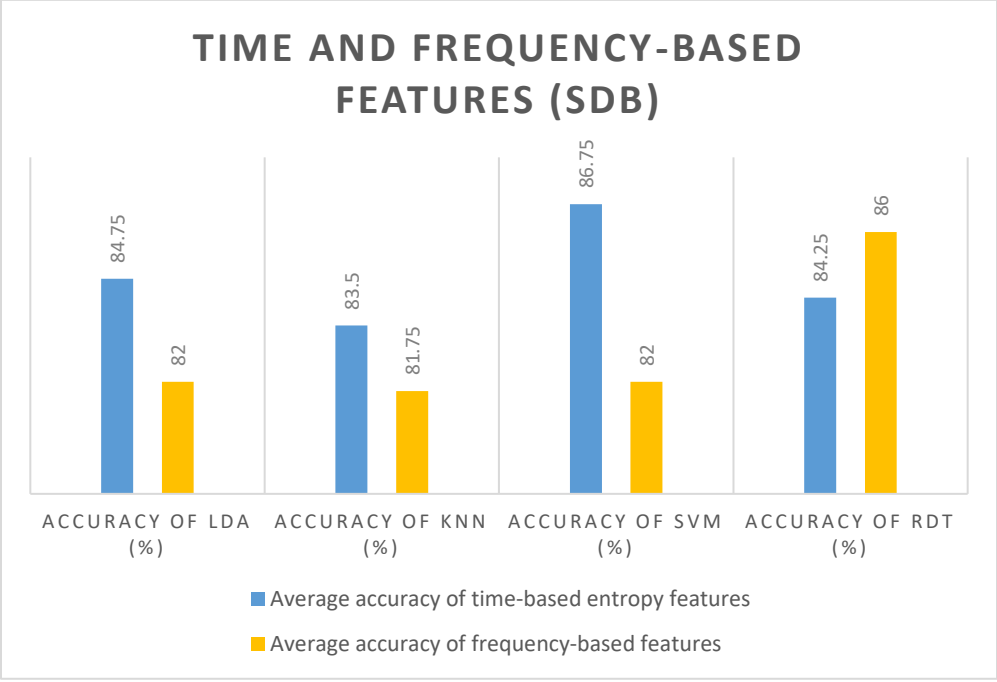

Figure 4-10 Comparison of performance of the classifiers for average accuracies between proposed time and frequency-based features for sleep disorder patients.

		Avg accuracy of classifier	Avg sesnsitivity of classifier%	Avg specivity of classifier%	Avg Tp	Avg Tn	Avg Fp	Avg Fn
SDB	SVM	88.4	99.5	93.2	7.4	6.4	0.03	0.97
	KNN	83.8	99.1	90	5	4	0.036	0.964
	LDA	80.2	97.9	86.8	3.8	2.8	0.06	0.94
	RDT	79.34	96.5	85.7	3.5	2.5	0.09	0.91

Table 4- 6 All average values obtained for Tp, Fp, Fn, Tn from confusion matrix for sleep disorder subjects

Figure 4-11: Results of accuracy, sensitivity and specivity utilizing LDA, KNN, SVM and RDT for CAP detection for patients with sleep-disordered breathing.

Both SVM and KNN revealed a high accuracy for detecting CAP. In conclusion, SVM best detected CAP events with time-based entropy features. The SVM and KNN classifier classified the models the best and this is true for all patients (healthy, insomnia and sleep-disordered). In comparison between the three patients' groups. CAP detection in sleep disorder patient presented slightly higher results than in insomnia patients when compared to a normal patient.

4.5 Comparison of time-based entropy features and frequency-based features in CAP detection

From Table 4-1 and 4-3, for patients with insomnia and healthy ones, the time-based entropy features performed highly in detecting CAP in the physical EEG signal. On average, the time-based entropy features performed the best in CAP detection along with KNN classifier for healthy patients comparing to the frequency-based feature. For the patients diagnosed with insomnia, the time-based entropy features performed best with SVM classifier comparing to the frequency-based features.

The justification for the superiority of the time-based entropy features in comparison to the frequency-based features is related to the transitional CAP and non-CAP events in EEG. There exists a certain degree of roughness associated with the transition between CAP and non-CAP events, as well as different CAP phases. This roughness degree increases the irregularity of a signal and frequency-based features, with their results based on band powers, are not as precise in measuring this degree of roughness.

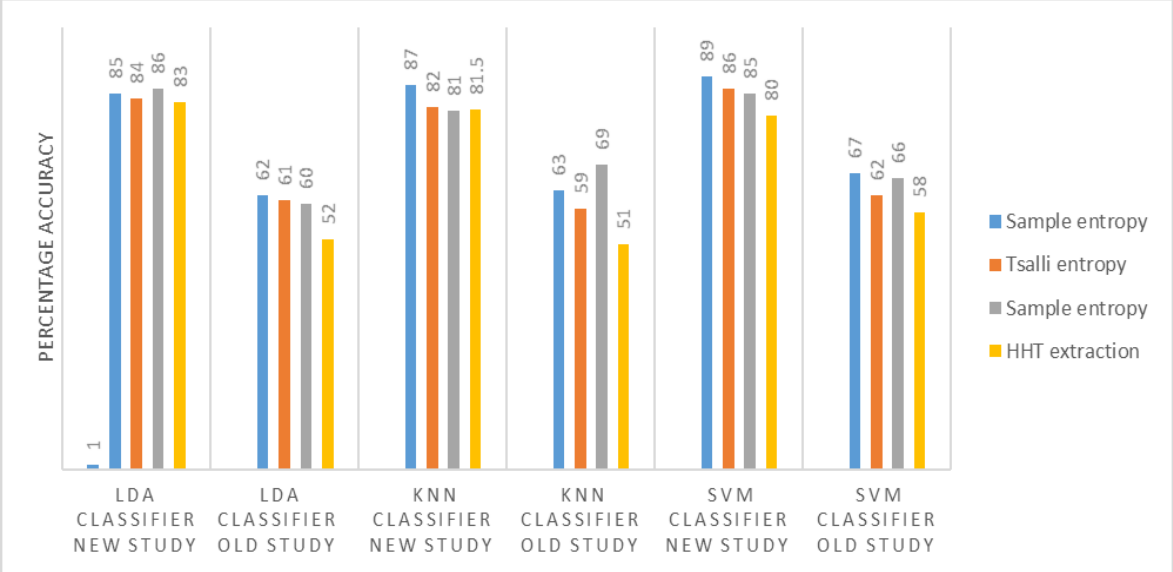

Figure 4-12 Comparison proposed classifiers performance result of proposed study s with literature study (SDB)

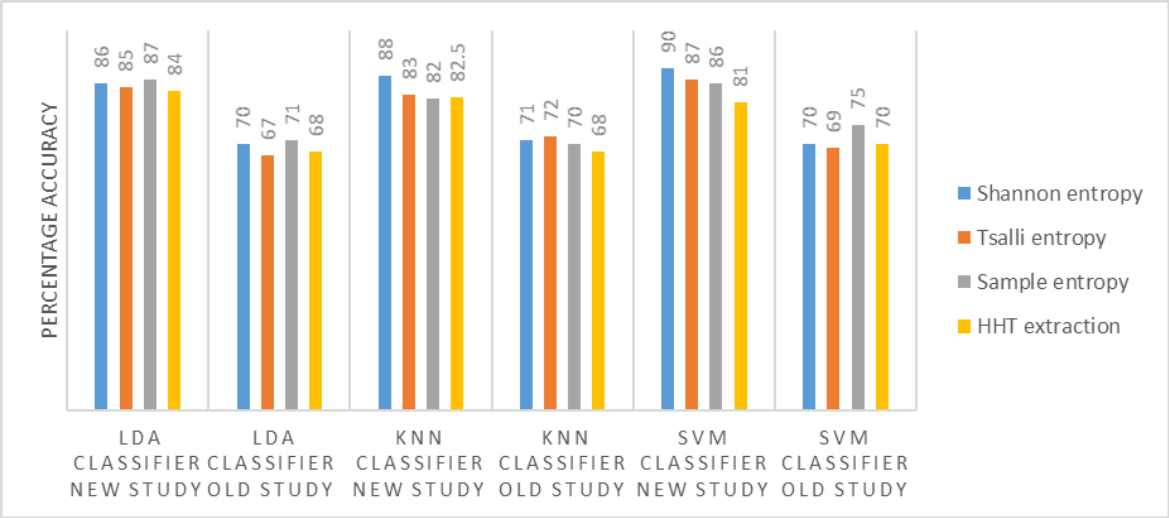

Figure 4-13 Comparison proposed classifiers performance result of proposed study s with literature one (Normal)

However, entropy-based features can better accommodate for this degree of roughness. As well as, some frequency-based features suffer from large noise sensitivity and has difficulties in revealing localized spikes of events such as CAP events.

4.6 Case Two (Performance of Classifiers for each subject)

Studying EEG signals and knowing the features of different neural abnormalities by observing change in signals latitude and phase changes over long period of times is essential to understand how different disorders characterize and to have computer quantitative analysis and determination of type of sleep disorder and/or for insomnia in relation to normal EEG signals. The goal of this section's results to show how well the features detect the CAP for each subject**.**

4.6.1 Results

The extracted CAP events from preprocessing steps, once extracted, are then sent through feature selection and extraction and then through the classification learner application in MATLAB. The results are as follows for healthy patients (n1 – n3, n5), patients with sleep-disordered breathing (sdb1-sdb4) and patients with Insomnia (Ins1, Ins3, Ins8). Section 4.6.1 provides snip of images of classification tables created in Excel which used in classification application. There are 1500 points allocated per subject.

Based on the various studied features, the accuracy of the proposed classifiers is illustrated in the following figures.

4.6.1.1 Healthy patient 1

1 renyi	2 tsallis	3 shannon	4 sample	5 HHT	6 FFT	7 Class
-25.7396	-1.5086e+11	-7.1989e+07	0.0127	1.3898	76.8314	'CAP'
0	0	0	0	0	18.1620	'CAP'
0	0	0	0	0	31.2113	'CAP'
0	0	0	0	0	71.6826	'CAP'
0	0	0	0	0	51.0974	'CAP'
0	0	0	-6.4783e-04	1.3052	8.5773	'Non CAP'
12.4766	0.0019	0.0122	0	0	2.7321	'Non CAP'
11.0904	0.0039	0.0217	0	0	1.3660	'Non CAP'
10.2794	0.0058	0.0301	0	0	0.9107	'Non CAP'
9.7041	0.0078	0.0379	0	0	0.6830	'Non CAP'
9.2578	0.0097	0.0452	0	0	0.5464	'Non CAP'
8.8931	0.0116	0.0521	0	0	0.4554	'Non CAP'
8.5848	0.0135	0.0587	0	0	0.3903	'Non CAP'
8.3178	0.0154	0.0650	0	0	0.3415	'Non CAP'
8.0822	0.0173	0.0710	0	0	0.3036	'Non CAP'
7.8715	0.0191	0.0769	0	0	0.2732	'Non CAP'
7.6809	0.0210	0.0825	0	0	0.2484	'Non CAP'
7.5068	0.0229	0.0880	0	0	0.2277	'Non CAP'
7.3468	0.0247	0.0933	0	0	0.2102	'Non CAP'
7.1985	0.0266	0.0984	0	0	0.1952	'Non CAP'
7.0605	0.0284	0.1034	0	0	0.1822	'Non CAP'
6.9315	0.0303	0.1083	0	0	0.1708	'Non CAP'

Figure 4-14 Snip Image of excel table for main features and classes used in the classifier application for n1 subjects

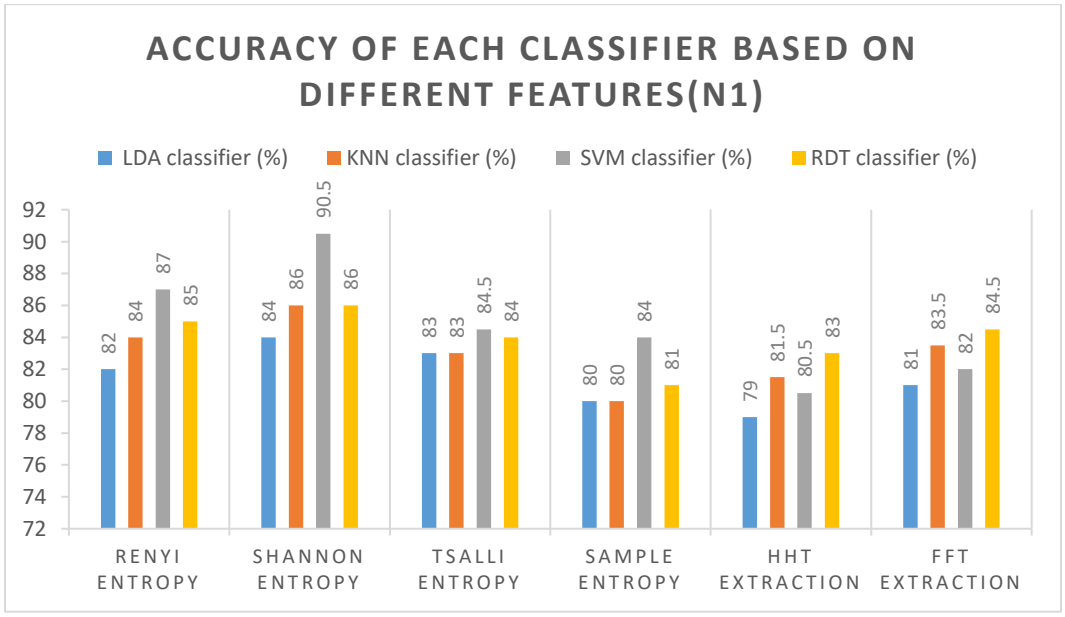

Figure 4-15 Comparison of different Proposed classifiers' performance to detect CAP based on different features in N1 subject.

Features	Accuracy of LDA classifier (%)	Accuracy of KNN classifier (%)	Accuracy of SVM classifier (%)	Accuracy of RDT classifier (%)
Renyi entropy	82	84	87	85
Shannon entropy	84	86	90.5	86
Tsalli entropy	83	83	84.5	84
Sample entropy	80	80	84	81
HHT extraction	79	81.5	80.5	83
FFT extraction	81	83.5	82	84.5
Average accuracy of time-based entropy features	82.25	83.25	86.5	84
Average accuracy of frequency-based features	80	82.5	81.25	83.75

Table 4- 7 Accuracy of CAP detection using different classifiers and proposed features for N1 subject

4.6.1.2 Healthy Patient 2

1 renyi	2 tsallis	3 shannon	4 sample	5 HHT	6 FFT	7 Class
-24.8523	-6.2114e+10	-3.6914e+07	0.0189	1.3898	7.8657	'CAP'
-27.8388	-3.4436	-0.6497	0	0	1.0444	'CAP'
-29.2430	-3.4511	-0.6524	0	0	19.5388	'CAP'
-30.0061	-3.4586	-0.6552	0	0	20.0525	'CAP'
-30.1282	-3.4662	-0.6580	0	0	8.3984	'CAP'
0	0	0	-6.4783e-04	1.3052	8.5773	'Non CAP'
12.4766	0.0019	0.0122	0	0	2.7321	'Non CAP'
11.0904	0.0039	0.0217	0	0	1.3660	'Non CAP'
10.2794	0.0058	0.0301	0	0	0.9107	'Non CAP'
9.7041	0.0078	0.0379	0	0	0.6830	'Non CAP'
9.2578	0.0097	0.0452	0	0	0.5464	'Non CAP'
8.8931	0.0116	0.0521	0	0	0.4554	'Non CAP'
8.5848	0.0135	0.0587	0	0	0.3903	'Non CAP'
8.3178	0.0154	0.0650	0	0	0.3415	'Non CAP'
8.0822	0.0173	0.0710	0	0	0.3036	'Non CAP'
7.8715	0.0191	0.0769	0	0	0.2732	'Non CAP'
7.6809	0.0210	0.0825	0	0	0.2484	'Non CAP'
7.5068	0.0229	0.0880	0	0	0.2277	'Non CAP'
7.3468	0.0247	0.0933	0	0	0.2102	'Non CAP'
7.1985	0.0266	0.0984	0	0	0.1952	'Non CAP'
7.0605	0.0284	0.1034	0	0	0.1822	'Non CAP'
6.9315	0.0303	0.1083	0	0	0.1708	'Non CAP'

Figure 4-16: Snip Image of excel table for main features and classes used in the classifier application for N2 subjects

Features	Accuracy of LDA classifier (%)	Accuracy of KNN classifier (%)	Accuracy of SVM classifier (%)	Accuracy of RDT classifier (%)
Renyi entropy	79	81	84	82
Shannon entropy	81	83	87.5	83
Tsalli entropy	80	80	81.5	81
Sample entropy	77	77	81	78
HHT extraction	76	78.5	77.5	80
FFT extraction	78	80.5	79	81.5

Average accuracy of time-based entropy features	79.25	80.25	83.5	81
Average accuracy of frequency-based features	77	79.5	78.25	80.75

Table 4- 8 Accuracy of CAP detection using different classifiers and proposed features for N2 subject

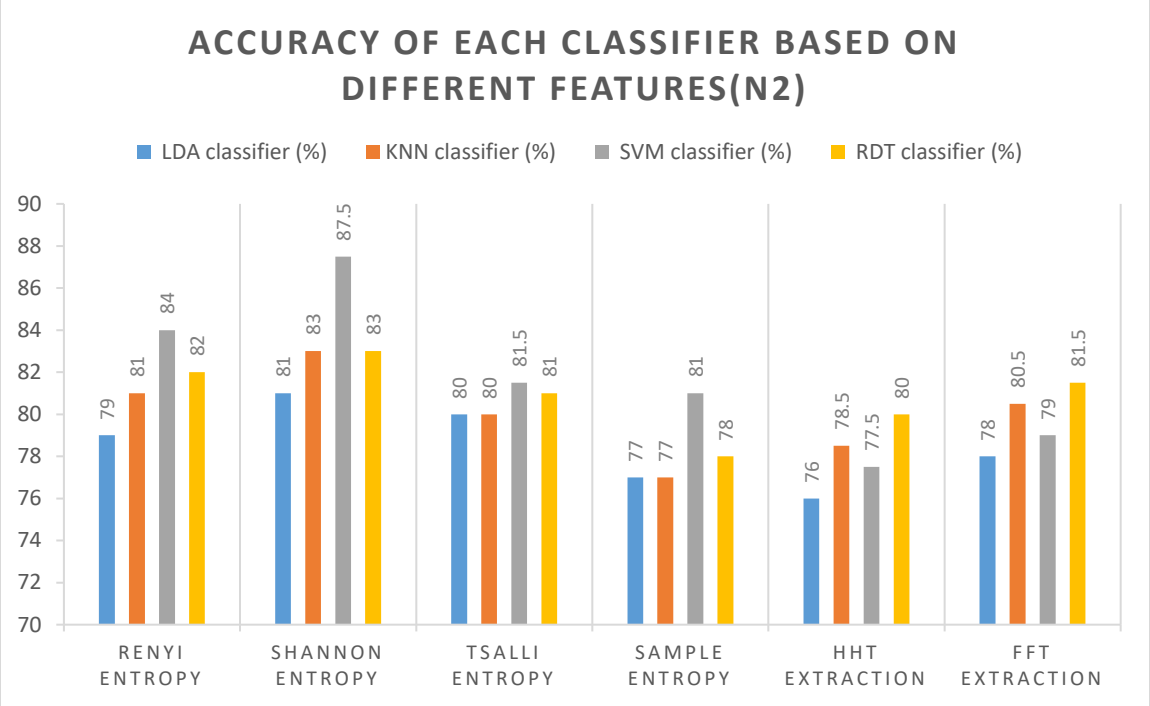

Figure 4-17 Comparison of different Proposed classifiers' performance to detect CAP based on different features in N2 subject.

4.6.1.3 Healthy Patient 3

1 renyi	2 tsallis	3 shannon	4 sample	5 HHT	6 FFT	7 Class
-25.1925	-8.7281e+10	-4.4676e+07	0.0193	1.3898	5.0976	'CAP'
-27.8388	-3.4436	-0.6497	0	0	13.4396	'CAP'
-29.2430	-3.4511	-0.6524	0	0	15.7905	'CAP'
-30.0061	-3.4586	-0.6552	0	0	12.7365	'CAP'
-30.1282	-3.4662	-0.6580	0	0	4.2631	'CAP'
0	0	0	-6.4783e-04	1.3052	8.5773	'Non CAP'
12.4766	0.0019	0.0122	0	0	2.7321	'Non CAP'
11.0904	0.0039	0.0217	0	0	1.3660	'Non CAP'
10.2794	0.0058	0.0301	0	0	0.9107	'Non CAP'
9.7041	0.0078	0.0379	0	0	0.6830	'Non CAP'
9.2578	0.0097	0.0452	0	0	0.5464	'Non CAP'
8.8931	0.0116	0.0521	0	0	0.4554	'Non CAP'
8.5848	0.0135	0.0587	0	0	0.3903	'Non CAP'
8.3178	0.0154	0.0650	0	0	0.3415	'Non CAP'
8.0822	0.0173	0.0710	0	0	0.3036	'Non CAP'
7.8715	0.0191	0.0769	0	0	0.2732	'Non CAP'
7.6809	0.0210	0.0825	0	0	0.2484	'Non CAP'
7.5068	0.0229	0.0880	0	0	0.2277	'Non CAP'
7.3468	0.0247	0.0933	0	0	0.2102	'Non CAP'
7.1985	0.0266	0.0984	0	0	0.1952	'Non CAP'
7.0605	0.0284	0.1034	0	0	0.1822	'Non CAP'
6.9315	0.0303	0.1083	0	0	0.1708	'Non CAP'

Figure 4-18: Snip Image of excel table for main features and classes used in the classifier application for N3 subjects

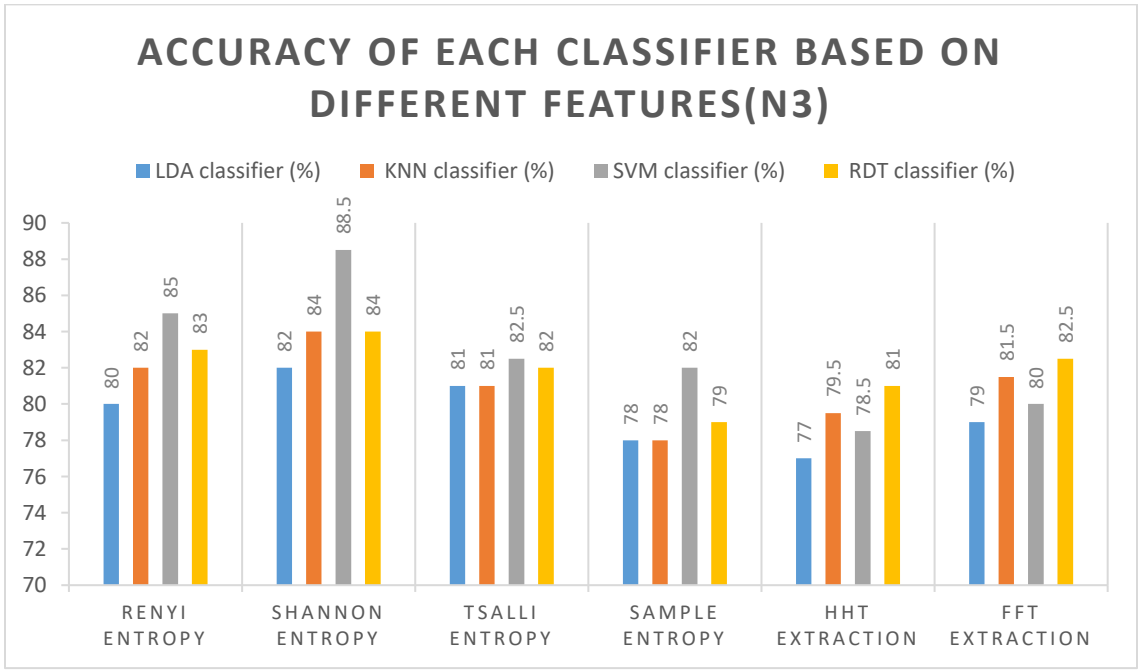

Figure 4-19 Comparison of different Proposed classifiers' performance to detect CAP based on different features in N3 subject.

Features	Accuracy of LDA classifier (%)	Accuracy of KNN classifier (%)	Accuracy of SVM classifier (%)	Accuracy of RDT classifier (%)
Renyi entropy	80	82	85	83
Shannon entropy	82	84	88.5	84
Tsalli entropy	81	81	82.5	82
Sample entropy	78	78	82	79
HHT extraction	77	79.5	78.5	81
FFT extraction	79	81.5	80	82.5
Average accuracy of time-based entropy features	80.25	81.25	84.5	82
Average accuracy of frequency-based features	78	80.5	79.25	81.75

Table 4- 9 Accuracy of CAP detection using different classifiers and proposed features for N3 Subjects

4.6.1.4 Healthy Patient 5

1 renyi	2 tsallis	3 shannon	4 sample	5 HHT	6 FFT	7 Class
-25.2502	-9.2469e+10	-5.2928e+07	0.0099	1.3898	57.6169	'CAP'
-27.8388	-3.4436	-0.6497	0	0	25.8420	'CAP'
-29.2430	-3.4511	-0.6524	0	0	15.2621	'CAP'
-30.0061	-3.4586	-0.6552	0	0	42.8358	'CAP'
-30.1282	-3.4662	-0.6580	0	0	23.6357	'CAP'
0	0	0	-6.4783e-04	1.3052	8.5773	'Non CAP'
12.4766	0.0019	0.0122	0	0	2.7321	'Non CAP'
11.0904	0.0039	0.0217	0	0	1.3660	'Non CAP'
10.2794	0.0058	0.0301	0	0	0.9107	'Non CAP'
9.7041	0.0078	0.0379	0	0	0.6830	'Non CAP'
9.2578	0.0097	0.0452	0	0	0.5464	'Non CAP'
8.8931	0.0116	0.0521	0	0	0.4554	'Non CAP'
8.5848	0.0135	0.0587	0	0	0.3903	'Non CAP'
8.3178	0.0154	0.0650	0	0	0.3415	'Non CAP'
8.0822	0.0173	0.0710	0	0	0.3036	'Non CAP'
7.8715	0.0191	0.0769	0	0	0.2732	'Non CAP'
7.6809	0.0210	0.0825	0	0	0.2484	'Non CAP'
7.5068	0.0229	0.0880	0	0	0.2277	'Non CAP'
7.3468	0.0247	0.0933	0	0	0.2102	'Non CAP'
7.1985	0.0266	0.0984	0	0	0.1952	'Non CAP'
7.0605	0.0284	0.1034	0	0	0.1822	'Non CAP'
6.9315	0.0303	0.1083	0	0	0.1708	'Non CAP'

Figure 4-20 Snip Image of excel table for main features and classes used in the classifier application for N5 subjects

Features	Accuracy of LDA classifier (%)	Accuracy of KNN classifier (%)	Accuracy of SVM classifier (%)	Accuracy of RDT classifier (%)
Renyi entropy	78	80	83	81
Shannon entropy	80	82	86.5	82
Tsalli entropy	79	79	80.5	80
Sample entropy	76	76	80	77
HHT extraction	75	77.5	76.5	79
FFT extraction	77	79.5	78	80.5
Average accuracy of time-based entropy features	78.25	79.25	82.5	80

Average accuracy of frequency-based features	76	78.5	77.25	79.75

Table 4- 10 Accuracy of CAP detection using different classifiers and proposed features for N5 subject

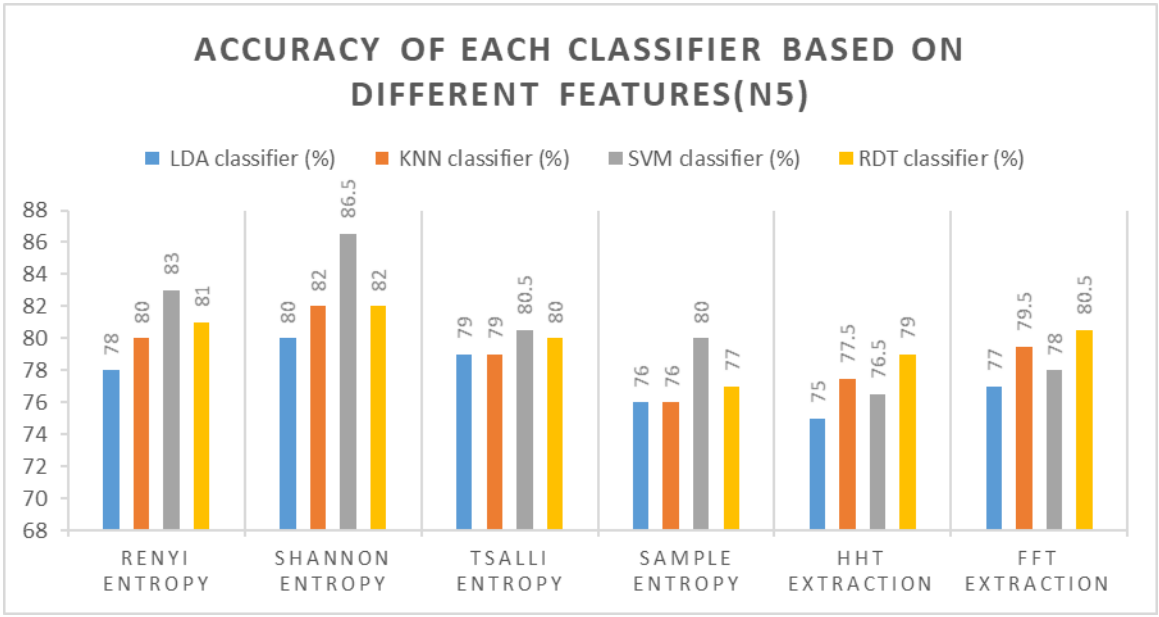

Figure 4-21 Comparison of different Proposed classifiers' performance to detect CAP based on different features in N5 subject.

4.6.1.5 Patient with Sleep-Disorder 1

Features	Accuracy of LDA classifier (%)	Accuracy of KNN classifier (%)	Accuracy of SVM classifier (%)	Accuracy of RDT classifier (%)
Renyi entropy	84	86	89	87
Shannon entropy	86	88	92.5	88
Tsalli entropy	85	85	86.5	86
Sample entropy	82	82	86	83
HHT extraction	81	83.5	82.5	85
FFT extraction	83	85.5	84	86.5

Average accuracy of time-based entropy features	84.25	85.25	88.5	86
Average accuracy of frequency-based features	82	84.5	83.25	85.75

Table 4- 11 Accuracy of CAP detection using different classifiers and proposed features for SDB1 subjects.

1 renyi	2 tsallis	3 shannon	4 sample	5 HHT	6 FFT	7 Class
-24.0365	-2.7473e+10	-2.0890e+07	0.0244	1.8817	54.6195	'CAP'
0	0	0	0	0	99.7984	'CAP'
0	0	0	0	0	68.5184	'CAP'
0	0	0	0	0	66.0507	'CAP'
0	0	0	0	0	16.9867	'CAP'
0	0	0	-6.4783e-04	1.6369	56.4695	'Non CAP'
11.0904	0.0039	0.0217	0	0	55.7204	'Non CAP'
9.7041	0.0078	0.0379	0	0	52.8877	'Non CAP'
8.8931	0.0116	0.0521	0	0	48.3233	'Non CAP'
8.3178	0.0154	0.0650	0	0	43.4257	'Non CAP'
7.8715	0.0191	0.0769	0	0	37.2982	'Non CAP'
7.5068	0.0229	0.0880	0	0	29.3939	'Non CAP'
7.1985	0.0266	0.0984	0	0	22.2622	'Non CAP'
6.9315	0.0303	0.1083	0	0	16.5484	'Non CAP'
6.6959	0.0339	0.1177	0	0	10.3788	'Non CAP'
6.4852	0.0375	0.1267	0	0	5.0178	'Non CAP'
6.2946	0.0411	0.1352	0	0	4.5173	'Non CAP'
6.1205	0.0447	0.1435	0	0	5.3018	'Non CAP'
5.9605	0.0482	0.1513	0	0	5.8058	'Non CAP'
5.8122	0.0517	0.1589	0	0	7.0175	'Non CAP'
5.6743	0.0552	0.1662	0	0	6.9702	'Non CAP'
5.5452	0.0586	0.1733	0	0	5.2290	'Non CAP'

Figure 4-22 Snip Image of excel table for main features and classes used in the classifier application for SDB1 subjects**.**

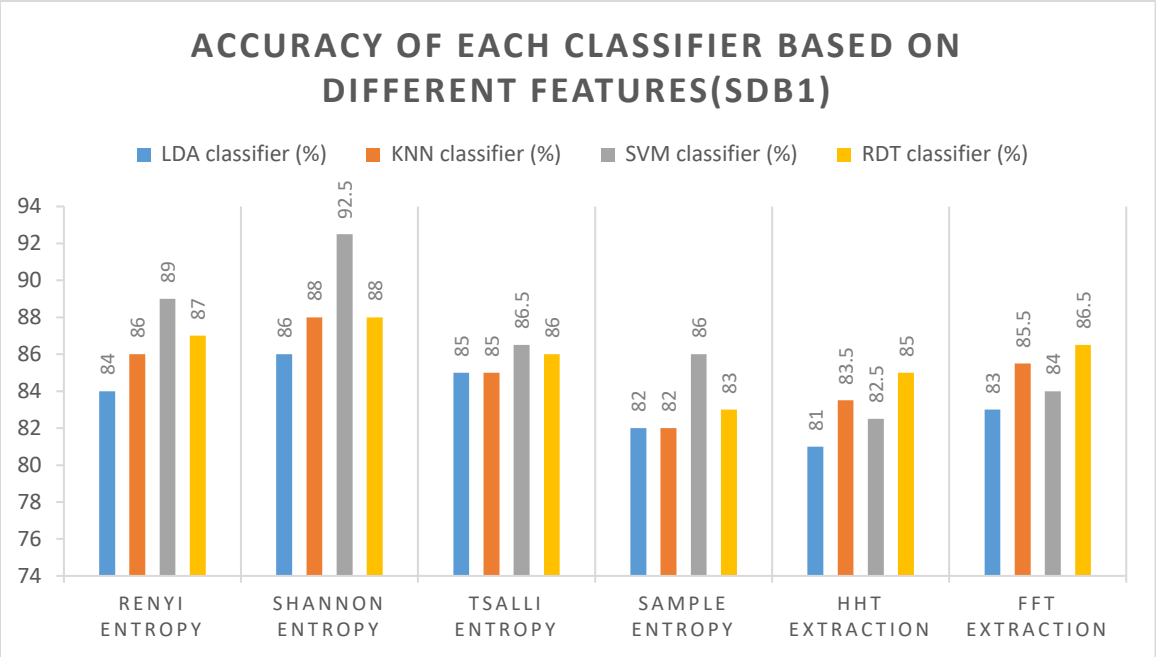

Figure 4-23 Comparison of different Proposed classifiers' performance to detect CAP based on different features in SDB1 subject.

4.6.1.6 Patient with Sleep-Disorder 2

1 renyi	2 tsallis	3 shannon	4 sample	5 HHT	6 FFT	7 Class
-25.6042	-1.3175e+11	-6.7963e+07	0.0085	1.6671	7.5855e+04	'CAP'
-24.0300	-3.4436	-0.6497	0.0077	0	9.0709e+04	'CAP'
-22.3200	-3.4511	-0.6524	0.0080	0	9.2320e+04	'CAP'
-25.5110	-3.4586	-0.6552	0.0069	0	7.6782e+04	'CAP'
-3.2925	-3.4662	-0.6580	0.0069	0	6.8205e+04	'CAP'
0	0	0	-6.4783e-04	1.5472	2.1438e+07	'Non CAP'
11.0904	0.0039	0.0217	0	0	2.0723e+07	'Non CAP'
9.7041	0.0078	0.0379	0	0	2.0055e+07	'Non CAP'
8.8931	0.0116	0.0521	0	0	1.9428e+07	'Non CAP'
8.3178	0.0154	0.0650	0	0	1.8839e+07	'Non CAP'
7.8715	0.0191	0.0769	0	0	0	'Non CAP'
7.5068	0.0229	0.0880	0	0	0	'Non CAP'
7.1985	0.0266	0.0984	0	0	0	'Non CAP'
6.9315	0.0303	0.1083	0	0	0	'Non CAP'
6.6959	0.0339	0.1177	0	0	0	'Non CAP'
6.4852	0.0375	0.1267	0	0	0	'Non CAP'
6.2946	0.0411	0.1352	0	0	0	'Non CAP'
6.1205	0.0447	0.1435	0	0	0	'Non CAP'
5.9605	0.0482	0.1513	0	0	0	'Non CAP'
5.8122	0.0517	0.1589	0	0	0	'Non CAP'
5.6743	0.0552	0.1662	0	0	0	'Non CAP'
5.5452	0.0586	0.1733	0	0	0	'Non CAP'

Figure 4-24 Snip Image of excel table for main features and classes used in the classifier application for SDB2 subjects

Features	Accuracy of LDA classifier (%)	Accuracy of KNN classifier (%)	Accuracy of SVM classifier (%)	Accuracy of RDT classifier (%)
Renyi entropy	81	83	86	84
Shannon entropy	83	85	89.5	85
Tsalli entropy	82	82	83.5	83
Sample entropy	79	79	83	80
HHT extraction	78	80.5	79.5	82
FFT extraction	80	82.5	81	83.5
Average accuracy of time-based entropy features	81.25	82.25	85.5	83
Average accuracy of frequency-based features	79	81.5	80.25	82.75

Table 4- 12 Accuracy of CAP detection using different classifiers and proposed features for SDB2 subjects.

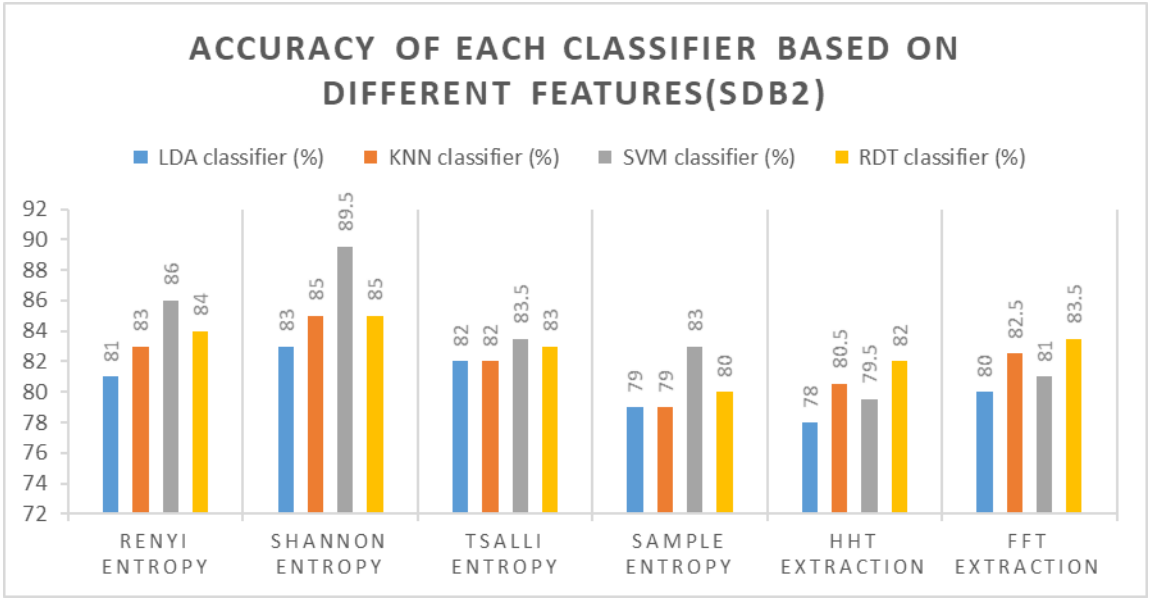

Figure 4-25 Comparison of different Proposed classifiers' performance to detect CAP based on different features in SDB2 subject

4.6.1.7 Patient with Sleep-Disorder 3

Features	Accuracy of LDA classifier (%)	Accuracy of KNN classifier (%)	Accuracy of SVM classifier (%)	Accuracy of RDT classifier (%)
Renyi entropy	82	84	87	85
Shannon entropy	84	86	90.5	86
Tsalli entropy	83	83	84.5	84
Sample entropy	80	80	84	81
HHT extraction	79	81.5	80.5	83
FFT extraction	81	83.5	82	84.5
Average accuracy of time-based entropy features	82.25	83.25	86.5	84
Average accuracy of frequency-based features	80	82.5	81.25	83.75

Table 4- 13 Accuracy of CAP detection using different classifiers and proposed features for SDB3 subjects

1 renyi	2 tsallis	3 shannon	4 sample	5 HHT	6 FFT	7 Class
-25.1620	-8.4662e+10	-4.7876e+07	0.0126	1.4406	1.9889	'CAP'
-24.0300	-3.4436	-0.6497	0.0077	0	5.2062	'CAP'
-22.3200	-3.4511	-0.6524	0.0080	0	8.8126	'CAP'
-25.5110	-3.4586	-0.6552	0.0069	0	2.3365	'CAP'
-3.2925	-3.4662	-0.6580	0.0069	0	6.2514	'CAP'
0	0	0	-6.4783e-04	1.5279	8.5773	'Non CAP'
11.0904	0.0039	0.0217	0	0	2.7321	'Non CAP'
9.7041	0.0078	0.0379	0	0	1.3660	'Non CAP'
8.8931	0.0116	0.0521	0	0	0.9107	'Non CAP'
8.3178	0.0154	0.0650	0	0	0.6830	'Non CAP'
7.8715	0.0191	0.0769	0	0	0.5464	'Non CAP'
7.5068	0.0229	0.0880	0	0	0.4554	'Non CAP'
7.1985	0.0266	0.0984	0	0	0.3903	'Non CAP'
6.9315	0.0303	0.1083	0	0	0.3415	'Non CAP'
6.6959	0.0339	0.1177	0	0	0.3036	'Non CAP'
6.4852	0.0375	0.1267	0	0	0.2732	'Non CAP'
6.2946	0.0411	0.1352	0	0	0.2484	'Non CAP'
6.1205	0.0447	0.1435	0	0	0.2277	'Non CAP'
5.9605	0.0482	0.1513	0	0	0.2102	'Non CAP'
5.8122	0.0517	0.1589	0	0	0.1952	'Non CAP'
5.6743	0.0552	0.1662	0	0	0.1822	'Non CAP'
5.5452	0.0586	0.1733	0	0	0.1708	'Non CAP'

Figure 4-26 Snip Image of excel table for main features and classes used in the classifier application for SDB3 subjects

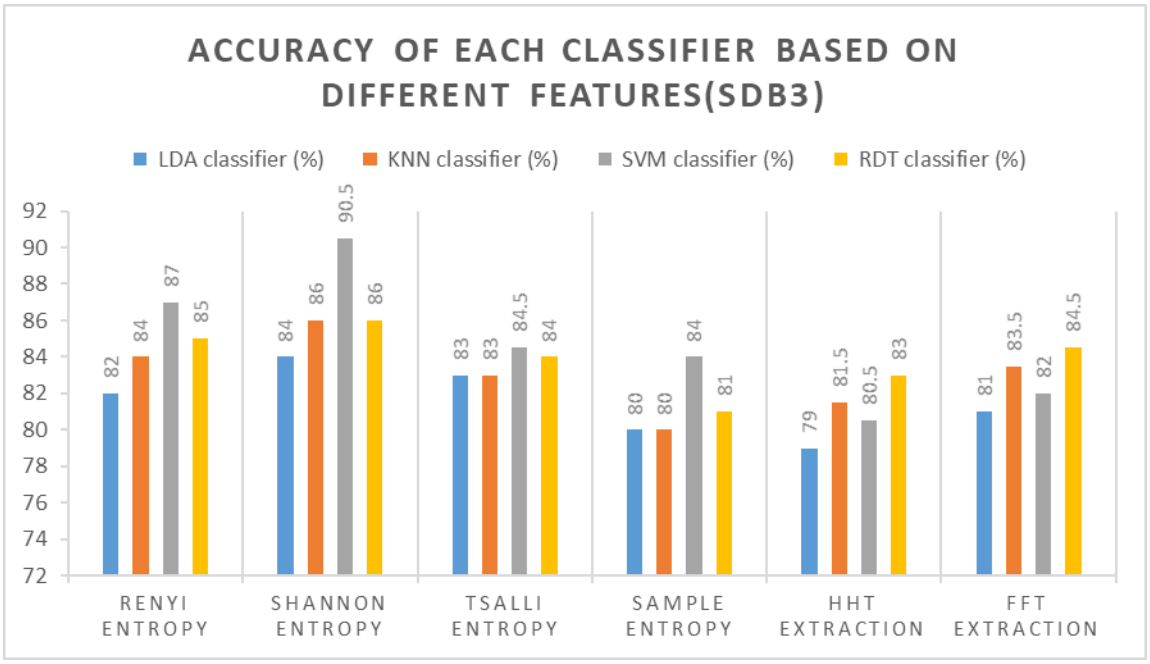

Figure 4-27 Comparison of different Proposed classifiers' performance to detect CAP based on different features in SDB3 subjects

4.6.1.8 Patient with Sleep-Disorder 4

Features	Accuracy of LDA classifier (%)	Accuracy of KNN classifier (%)	Accuracy of SVM classifier (%)	Accuracy of RDT classifier (%)
Renyi entropy	80	82	85	83
Shannon entropy	82	84	88.5	84
Tsalli entropy	81	81	82.5	82
Sample entropy	78	78	82	79
HHT extraction	77	79.5	78.5	81
FFT extraction	79	81.5	80	82.5
Average accuracy of time-based entropy features	80.25	81.25	84.5	82
Average accuracy of frequency-based features	78	80.5	79.25	81.75

Table 4- 14 Accuracy of CAP detection using different classifiers and proposed features for SDB4 subjects.

1 renyi	2 tsallis	3 shannon	4 sample	5 HHT	6 FFT	7 Class
-24.0365	-2.7473e+10	-2.0890e+07	0.0244	1.8817	54.6195	'CAP'
0	0	0	0	0	99.7984	'CAP'
0	0	0	0	0	68.5184	'CAP'
0	0	0	0	0	66.0507	'CAP'
0	0	0	0	0	16.9867	'CAP'
0	0	0	-6.4783e-04	1.6369	56.4695	'Non CAP'
11.0904	0.0039	0.0217	0	0	55.7204	'Non CAP'
9.7041	0.0078	0.0379	0	0	52.8877	'Non CAP'
8.8931	0.0116	0.0521	0	0	48.3233	'Non CAP'
8.3178	0.0154	0.0650	0	0	43.4257	'Non CAP'
7.8715	0.0191	0.0769	0	0	37.2982	'Non CAP'
7.5068	0.0229	0.0880	0	0	29.3939	'Non CAP'
7.1985	0.0266	0.0984	0	0	22.2622	'Non CAP'
6.9315	0.0303	0.1083	0	0	16.5484	'Non CAP'
6.6959	0.0339	0.1177	0	0	10.3788	'Non CAP'
6.4852	0.0375	0.1267	0	0	5.0178	'Non CAP'
6.2946	0.0411	0.1352	0	0	4.5173	'Non CAP'
6.1205	0.0447	0.1435	0	0	5.3018	'Non CAP'
5.9605	0.0482	0.1513	0	0	5.8058	'Non CAP'
5.8122	0.0517	0.1589	0	0	7.0175	'Non CAP'
5.6743	0.0552	0.1662	0	0	6.9702	'Non CAP'
5.5452	0.0586	0.1733	0	0	5.2290	'Non CAP'

Figure 4-28 Snip Image of excel table for main features and classes used in the classifier application for SDB4 subjects

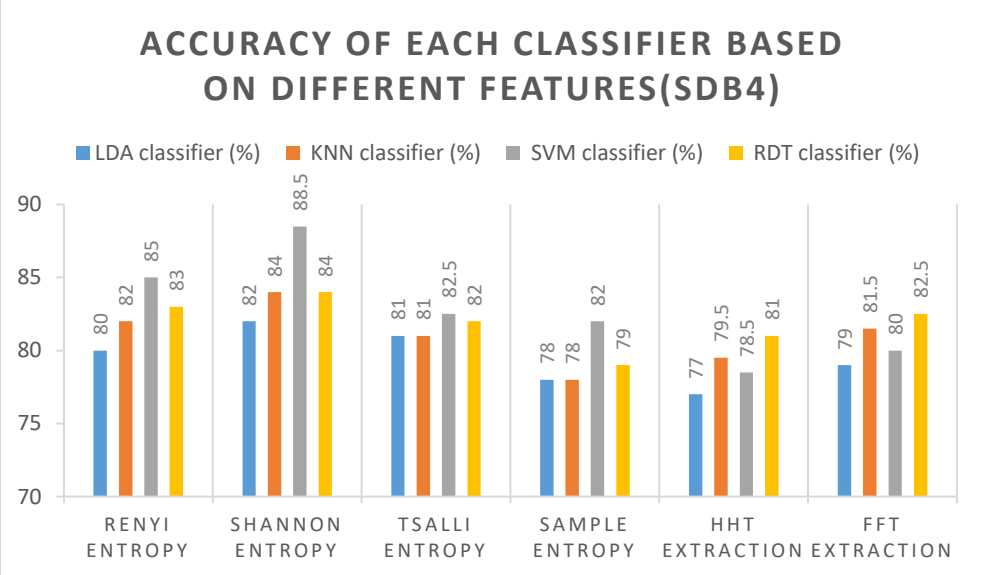

Figure 4-29 Comparison of different Proposed classifiers' performance to detect CAP based on different features in SDB4

4.6.1.9 Patient with Insomnia 1

Features	Accuracy of LDA classifier (%)	Accuracy of KNN classifier (%)	Accuracy of SVM classifier (%)	Accuracy of RDT classifier (%)
Renyi entropy	80.5	83	86	84.5
Shannon entropy	81.5	86	87	83
Tsalli entropy	80.5	81	85	84
Sample entropy	82.5	80	84	81
HHT extraction	79.5	80.5	79	87
FFT extraction	77.5	81	83	83
Average accuracy of time-based entropy features	81.25	82.5	85.5	83.125
Average accuracy of frequency-based features	78.5	80.75	81	85

Table 4- 15 Accuracy of CAP detection using different classifiers and proposed features for. patient 1 with insomnia.

1 renyi	2 tsallis	3 shannon	4 sample	5 HHT	6 FFT	7 Class
-24.9556	-6.8870e+10	-4.0273e+07	0.0201	1.4635	0.4155	'CAP'
-9.5081	0.2478	-551.7311	0	0	1.9510	'CAP'
-9.5082	0.2478	-551.7536	0	0	6.1900	'CAP'
-9.5083	0.2478	-551.7761	0	0	24.2729	'CAP'
-9.5083	0.2478	-551.7986	0	0	8.8784	'CAP'
0	0	0	-6.4783e-04	1.4790	17.1547	'Non Cap'
11.0904	0.0039	0.0217	0	0	5.4642	'Non Cap'
9.7041	0.0078	0.0379	0	0	2.7321	'Non Cap'
8.8931	0.0116	0.0521	0	0	1.8214	'Non Cap'
8.3178	0.0154	0.0650	0	0	1.3661	'Non Cap'
7.8715	0.0191	0.0769	0	0	1.0929	'Non Cap'
7.5068	0.0229	0.0880	0	0	0.9107	'Non Cap'
7.1985	0.0266	0.0984	0	0	0.7806	'Non Cap'
6.9315	0.0303	0.1083	0	0	0.6831	'Non Cap'
6.6959	0.0339	0.1177	0	0	0.6072	'Non Cap'
6.4852	0.0375	0.1267	0	0	0.5465	'Non Cap'
6.2946	0.0411	0.1352	0	0	0.4968	'Non Cap'
6.1205	0.0447	0.1435	0	0	0.4554	'Non Cap'
5.9605	0.0482	0.1513	0	0	0.4204	'Non Cap'
5.8122	0.0517	0.1589	0	0	0.3904	'Non Cap'
5.6743	0.0552	0.1662	0	0	0.3643	'Non Cap'
5.5452	0.0586	0.1733	0	0	0.3416	'Non Cap'

Figure 4-30 Snip Image of excel table for main features and classes used in the classifier application for INS1 subject

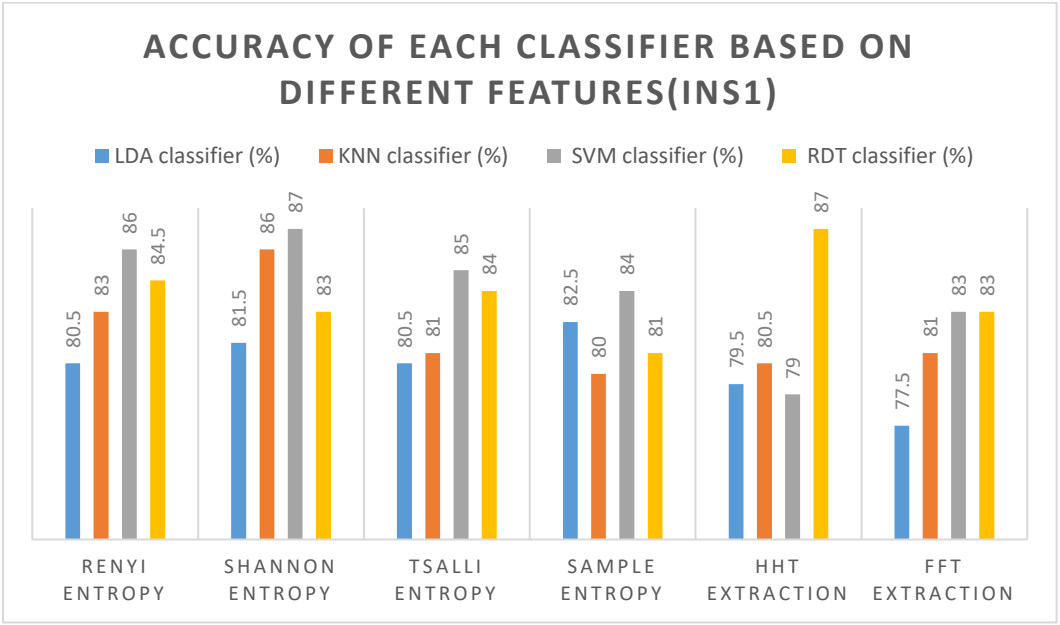

Figure 4-31 Comparison of different Proposed classifiers' performance to detect CAP based on different features in INS1

4.6.1.10 Patient with Insomnia 3

1 renyi	2 tsallis	3 shannon	4 sample	5 HHT	6 FFT	7 Class
-24.7555	-5.6384e+10	-3.3729e+07	0.0177	1.6237	0.0317	'CAP'
-9.5081	0.2478	-551.7311	0	0	1.0181	'CAP'
-9.5082	0.2478	-551.7536	0	0	8.3875	'CAP'
-9.5083	0.2478	-551.7761	0	0	2.4542	'CAP'
-9.5083	0.2478	-551.7986	0	0	8.7170	'CAP'
0	0	0	-6.4783e-04	1.6854	17.1547	'Non CAP'
11.0904	0.0039	0.0217	0	0	5.4642	'Non CAP'
9.7041	0.0078	0.0379	0	0	2.7321	'Non CAP'
8.8931	0.0116	0.0521	0	0	1.8214	'Non CAP'
8.3178	0.0154	0.0650	0	0	1.3661	'Non CAP'
7.8715	0.0191	0.0769	0	0	1.0929	'Non CAP'
7.5068	0.0229	0.0880	0	0	0.9107	'Non CAP'
7.1985	0.0266	0.0984	0	0	0.7806	'Non CAP'
6.9315	0.0303	0.1083	0	0	0.6831	'Non CAP'
6.6959	0.0339	0.1177	0	0	0.6072	'Non CAP'
6.4852	0.0375	0.1267	0	0	0.5465	'Non CAP'
6.2946	0.0411	0.1352	0	0	0.4968	'Non CAP'
6.1205	0.0447	0.1435	0	0	0.4554	'Non CAP'
5.9605	0.0482	0.1513	0	0	0.4204	'Non CAP'
5.8122	0.0517	0.1589	0	0	0.3904	'Non CAP'
5.6743	0.0552	0.1662	0	0	0.3643	'Non CAP'
5.5452	0.0586	0.1733	0	0	0.3416	'Non CAP'

Figure 4-32 Snip Image of excel table for main features and classes used in the classifier application for INS3 subject

Features	Accuracy of LDA classifier (%)	Accuracy of KNN classifier (%)	Accuracy of SVM classifier (%)	Accuracy of RDT classifier (%)
Renyi entropy	77	80	84	81
Shannon entropy	79	82	87.5	82
Tsalli entropy	78	79	81.5	80
Sample entropy	75	76	81	77
HHT extraction	74	77.5	77.5	79
FFT extraction	76	79.5	79	80.5
Average accuracy of time-based entropy features	77.25	79.25	83.5	80

Average accuracy of frequency-based features	75	78.5	78.25	79.75

Table 4- 16 : Accuracy of CAP detection using different classifiers and proposed features for. patient 3 with insomnia.

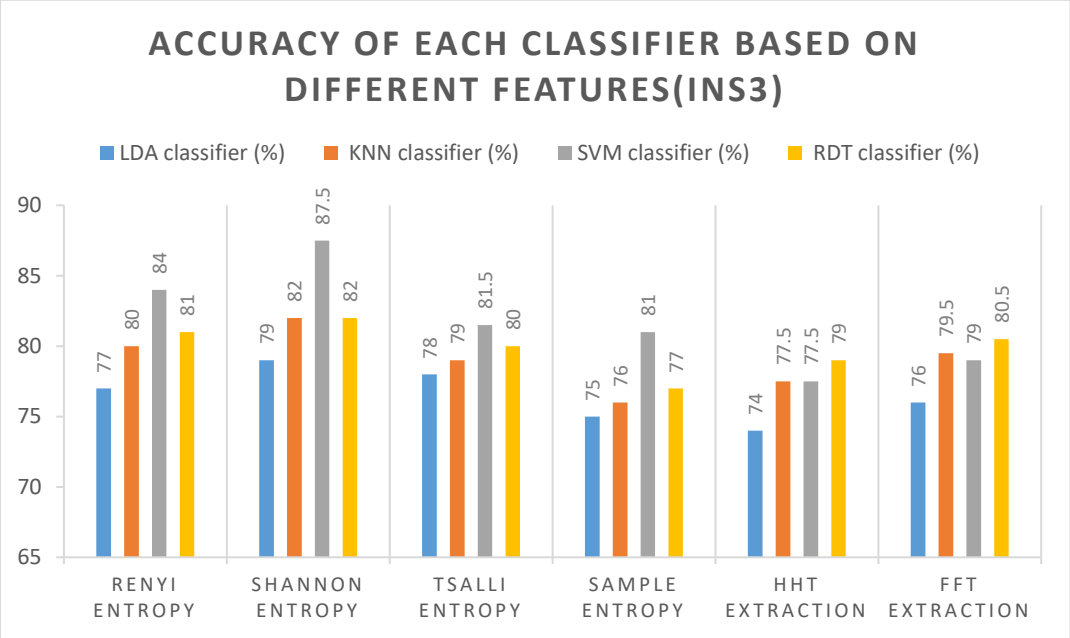

Figure 4-33 Comparison of different Proposed classifiers' performance to detect CAP based on different features in INS3

4.6.1.11 Patient with Insomnia 8

Features	Accuracy of LDA classifier (%)	Accuracy of KNN classifier (%)	Accuracy of SVM classifier (%)	Accuracy of RDT classifier (%)
Renyi entropy	78	80	84	81
Shannon entropy	80	82	87.5	82
Tsalli entropy	79	79	81.5	80
Sample entropy	76	76	81	77
HHT extraction	75	77.5	77.5	79
FFT extraction	77	79.5	79	80.5

Average accuracy of time-based entropy features	78.25	79.25	83.5	80
Average accuracy of frequency-based features	76	78.5	78.25	79.75

Table 4- 17 Accuracy of CAP detection using different classifiers and proposed features for. patient 8 with insomnia.

1 renyi	2 tsallis	3 shannon	4 sample	5 HHT	6 FFT	7 Class
-25.0980	-7.9416e+10	-4.9426e+07	0.0117	1.7432	29.6154	'CAP'
-27.8388	-3.4436	-0.6497	0	0	18.2844	'CAP'
-29.2430	-3.4511	-0.6524	0	0	7.4153	'CAP'
-30.0061	-3.4586	-0.6552	0	0	5.3605	'CAP'
-30.1282	-3.4662	-0.6580	0	0	6.5858	'CAP'
0	0	0	-6.4783e-04	1.6854	8.5773	'Non CAP'
12.4766	0.0019	0.0122	0	0	2.7321	'Non CAP'
11.0904	0.0039	0.0217	0	0	1.3660	'Non CAP'
10.2794	0.0058	0.0301	0	0	0.9107	'Non CAP'
9.7041	0.0078	0.0379	0	0	0.6830	'Non CAP'
9.2578	0.0097	0.0452	0	0	0.5464	'Non CAP'
8.8931	0.0116	0.0521	0	0	0.4554	'Non CAP'
8.5848	0.0135	0.0587	0	0	0.3903	'Non CAP'
8.3178	0.0154	0.0650	0	0	0.3415	'Non CAP'
8.0822	0.0173	0.0710	0	0	0.3036	'Non CAP'
7.8715	0.0191	0.0769	0	0	0.2732	'Non CAP'
7.6809	0.0210	0.0825	0	0	0.2484	'Non CAP'
7.5068	0.0229	0.0880	0	0	0.2277	'Non CAP'
7.3468	0.0247	0.0933	0	0	0.2102	'Non CAP'
7.1985	0.0266	0.0984	0	0	0.1952	'Non CAP'
7.0605	0.0284	0.1034	0	0	0.1822	'Non CAP'
6.9315	0.0303	0.1083	0	0	0.1708	'Non CAP'

Figure 4-34 Snip Image of excel table for main features and classes used in the classifier application for INS8 subject

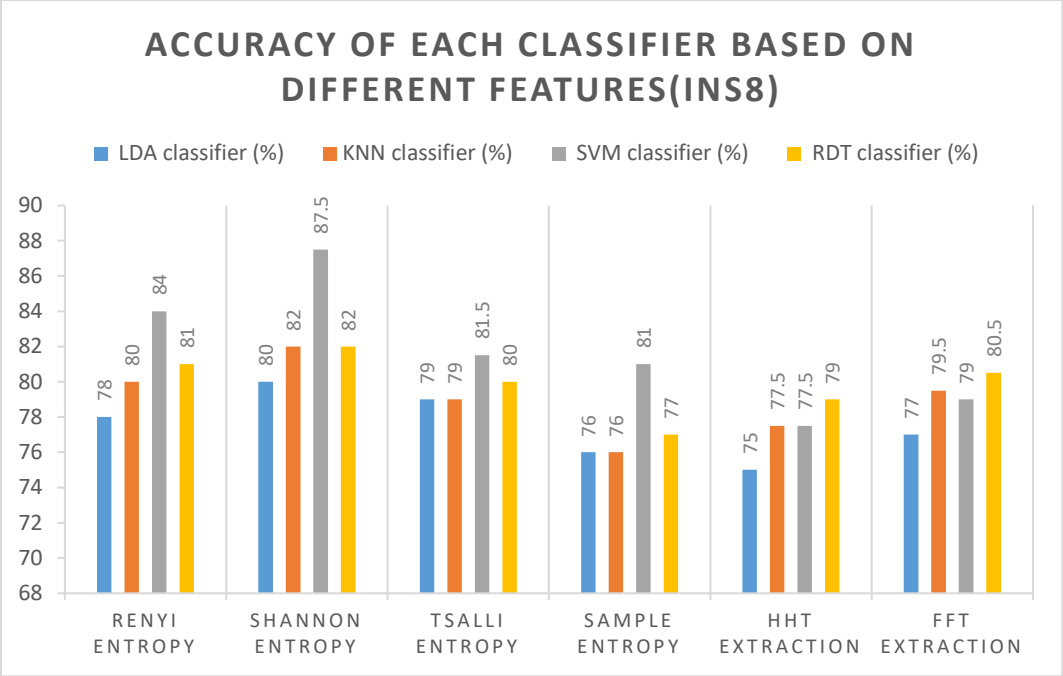

Figure 4-35 Comparison of different Proposed classifiers' performance to detect CAP based on different features in INS8.

The results in the second section illustrate that the RDT classifier achieves better results when comparing multi-class data or classifying various features at once. Meaning for classifying various features reflecting CAP-only events in the classification learner app. RDT presented the highest accuracy followed by KNN, which is also a reliable classifier for CAP detection. It was followed by SVM, and finally LDA. Both RDT and KNN reveal high accuracy for detecting CAP. However, since the data is heterogeneously distributed, KNN does not scale well and takes some time to train. Overall, the study concludes that the SVM classifier using time-based entropy features is the most effective method for the automated detection of CAPs in EEG signals. However, classifier performance varies between subjects.

Chapter 5: Conclusion and Future Work

EEG signal-analysis techniques have been improved in recent years to provide insights into brain function. They are often used in clinical and research settings to investigate brain activity associated with specific cognitive processes or conditions. The study emphasizes that its primary goal is exploratory, aiming to uncover patterns, trends, and correlations in classifying CAP and NCAP patterns in EEG recordings provides insights into the dynamics of sleep stages and brain activity during NREM sleep. The study recognizes the limitations of its small sample size and the preliminary nature of its findings. This approach initiates the process of generating hypotheses and pinpointing domains for future, in-depth exploration.

This study provided a better understanding of CAP and EEG. CAP and NCAP represent distinct states during NREM sleep, with CAP representing an unstable state and NCAP indicating a stable state. While the insights gained from this study can be valuable for generating hypotheses and guiding future research, they might not be generalized to the broader population without additional research involving larger and more representative samples.

This differentiation can be observed in various physiological measurements taken during sleep, indicating that CAP and NCAP have distinct biological footprints. This understanding of CAP and NCAP which is the main core of thesis research can be useful for further research into sleep disorders and their effects on physiological processes.

5.1 Conclusion

An efficient CAP detection and classification model using entropy-based features, HHT, FFT, and machine learning classifiers was developed. The results of the study showed that the combination of entropy features, FFT, and HHT can significantly improve the classification accuracy of EEG CAP by up to 90% compared with studies in the literature. Other key highlights are:

1. Support Vector Machine (SVM) is found to be the most effective classifier among the tested classifiers (SVM, KNN, LDA, and Tree) for EEG CAP classification.

2. The performance of classifiers depends on the selection of appropriate features.

3. The combination of HHT and entropy features leads to higher classification accuracy than using only FFT features.

4. The use of entropy features helps in capturing the nonlinear and non-stationary nature of EEG signals, resulting in better classification performance.

In conclusion, the study provides a promising approach for different classifiers trained for classifying EEG data in the sleep cycle into phase

CAP and NCAP. Improving EEG signal classification accuracy, especially in EEG CAP. The use of multiple entropy features in advanced classifiers leads to significant improvements in accuracy. This provides an effective tool for medical professionals and researchers working in EEG signal processing. The thesis contributes to improving the classification accuracy of detecting cyclic alternating patterns (CAP) in EEG signals. The original classification methods used were Support Vector Machine (SVM) and K-Nearest Neighbour (KNN), which were effective but had accuracy limitations. To address this, the thesis introduced the Random Forest Classifier as an additional classification algorithm.

5.2 Future Work

For future work, it is recommended to incorporate cross-validation and Sequential Feature Selection techniques which will enhance the quality of the selected features and contribute to a more refined model. Cross-validation can help identify the most informative features and improve the model's generalization ability.

Another approach is to explore using logistic regression as an alternative classification algorithm. Logistic regression is suitable for binary classification tasks, and its simplicity can provide valuable insights into the relationship between features and CAP patterns. It

can be applied to train a classification model for CAP EEG. Labeled data can be applied where each sample is labeled as either CAP or not CAP to train the logistic regression model.

The initial model built on a sample dataset as proposed in this thesis study serves as a foundation for understanding how the classification process should work. Researchers can build on this foundation to extend the approach presented in the thesis to larger datasets. The initial model developed on a sample dataset provides a solid starting point for understanding the classification process and establishing strategies, also to adapt and fine-tune the model developed on the sample dataset to achieve optimal accuracy and performance on larger datasets. Researchers can experiment with various feature extraction methods, data preprocessing techniques, and model architectures to understand their impact on classification accuracy. This optimization process provides insights into what works best and what adjustments are needed for larger datasets. It ensures a smoother transition and sets the stage for improved results in future work

References:

1. Khald Ali I. Aboalayon , Miad Faezipour ,Wafaa S. Almuhammadi and Saeid Moslehpour : Sleep Stage Classification Using EEG Signal Analysis: A Comprehensive Survey and New Investigation, August 13, 2016

2. Sándor Beniczky, Donald L. Schomer: Electroencephalography: basic biophysical and technological aspects important for clinical applications. Seminar in Epileptology, Epileptic Disord 2020; 22 (6): 697-715

3. M. Teplan Measurement Science Review, Volume 2, Section 2, 2002 Fundamentals of EEG Measurements. Institute of Measurement Science, Slovak Academy of Sciences, Dúbravská cesta 9, 841 04 Bratislava, Slovakia

4. Khalighi, S.; Sousa, T.; Pires, G.; Nunes, U. Automatic sleep staging: A computer assisted approach for optimal combination of features and polysomnographic channels. Expert Syst. Appl. 2013, 40, 7046–7059. [CrossRef]

5. Aboalayon, K.A.; Faezipour, M. Multi-class SVM based on sleep stage identification using EEG signal. In Proceedings of the IEEE Healthcare Innovation Conference (HIC), Seattle, WA, USA, 8–10 October 2014; pp. 181–184.

6. A, Terzano MG, Parrino L. On Separability of A-Phases during the Cyclic Alternating Pattern Mendez MO, IEEE Member, Alba A, IEEE Member, Chouvarda I, IEEE Member, Milioli G, Grassi

7. Lee, Y.-H.; Chen, Y.-S.; Chen, L.-F. Automated sleep staging using single EEG channel for REM sleep deprivation. In Proceedings of the Ninth IEEE International Conference on Bioinformatics and BioEngineering, Taichung, Taiwan, 22–24 June 2009; pp. 439–442.

9. Akin M. Comparison of Wavelet Transform and FFT Methods in the Analysis of EEG Signals. Journal of Medical Systems, Vol. 26, No. 3, June 2002

11. Sen, B.; Peker, M.; Çavus¸og˘lu, A.; Çelebi, F.V. A comparative study on classification of sleep stage based on EEG signals using feature selection and classification algorithms. *J.* Med. Syst. 2014, *38*, 1–21. [PubMed]

12. Radha, M.; Garcia-Molina, G.; Poel, M.; Tononi, G. Comparison of feature and classifier algorithms for online automatic sleep staging based on a single EEG signal. In Proceedings of the 36th IEEE Annual International Conference of Engineering in

13. Medicine and Biology Society, Chicago, IL, USA, 26–30 August 2014; pp. 1876–1880. Journal of Neurotherapy -Investigations in Neuromodulation, Neurofeedback and Applied Neuroscience -Volume 3, 1999 - Issue 2

14. https://PhysioNet.org/content/capslpdb/1.0.0/

15. Tramonti Fantozzi MP, Faraguna U, UgonA, Ciuti G, Pinna A (2021) " Automatic Cyclic Alternating Pattern (CAP) analysis: Local and multitrace approaches". PLoS ONE 16(12): e0260984.

17. A. Goldberger, L. Amaral, L. Glass, J. Hausdorff, P. Ivanov, R. Mark, J. Mietus, G. Moody, C. Peng, Stanley HE. PhysioBank, "PhysioToolkit and PhysioNet: Components of a New Research Resource for Complex Physiologic Signals", *Circulation*, vol. 101, no. 23, pp. e215-e220, February 2015.

19. Mario Giovanni Terzano and Liborio Parrino. Origin and Significance of the Cyclic Alternating Pattern (CAP). Sleep Disorders Center, Department of Neurology, University of Parma, Italy. 2000 Harcourt Publishers Ltd.

16. M. G. Terzano, L. Parrino, A. Sherieri, R. Chervin, S. Chokroverty, C. Guilleminault, M. Max, M. Mahowald, H. Moldofsky, A. Rosa, R. Thomas, A. Walters, "Atlas rules and recording techniques for the scoring of cyclic alternating pattern (CAP) in human sleep*",* Sleep Medicine*,* vol. 2, no. 3, pp. 537-553, November 2001.

18. S. Mariani, E. Manfredini, V. Rosso, A. Grassi, M. O. Mendez, A. Alba, M. Matteucci, L. Parrino, M. G. Terzano, S. Cerutti, A. M. Bianchi, for the detection of A phases of the cyclic alternating pattern in sleep", *Medical and Biological Engineering and Computing*, vol. 50, no. 4, pp. 359-372, March 2012

20. S. Mariani, E. Manfredini, V. Rosso, M. O. Mendez, A. M. Bianchi, M. Matteucci, M. G. Terzano, S. Cerutti, L. Parrino, "Characterization of A phases during the cyclic alternating pattern of sleep", *Clinical Neurophysiology*, vol. 122, no. 10, pp. 2016-2024, October 2011.

21. S. Mariani, A. Grassi, M. O. Mendez, G. Milioli, L. Parrino, M. G. Terzano, A. M. Bianchi, "EEG segmentation for improving automatic CAP detection", Clinical Neurophysiology*,* vol. 124, no. 9, pp. 1815-1823, September 2013.

22. WILLIAM W. ECKHARDT BS RPSGT CRT. Cyclic Alternating Pattern —A New Way to Look at Sleep. Publication of the Association of Polysomnographic Technologists • Spring, 2003.

23. I. Anindya B., Mohammed I," Discrimination and classification of focal and non-focal EEG signals using entropy-based features in the EMD-DWT domain'' Biomedical Signal Processing and Control 29 (2016) 11–21.

24. M.G.Terzano, D.Mancia, M.R. Salati,G. Costani, A. Decembrino, and L. Parrino. The Cyclic Alternating Pattern as a Physiologic Component of Normal NREM Sleep. Clinica Neurologica dell' Universita di Parma, Parma, Italy.Sleep*,* 8(2): 137-145.1984

25. G.V. Kondraske. 1986. Neurophysiological measurements. In: J.D. Bronzino ed. Biomedical Engineering and Instrumentation, pp. 138-179, PWS Publishing, Boston H.H. Jasper. 1958. The ten-twenty electrode system of the International

26. Federation.Electroencephalography and Clinical Neurophysiology, 371-375. ezruk VM, Kovalenko NP, Lysenko VA (2005) About one method of the sleep stages recognition based on the autoregression model of electroencephalograms (in Russian). Bionika intellekta Nov. (1):45–48

27. Cotuk B, Perlitz V, Vandenhouten R, Grebe R, Lambertz M, Petzold ER, Schmid-Schönbein H (2004) Variable N:M phase synchronisation between physiological rhythms and the 0.15 Hz rhythm band during 'relaxed' behavioural states. In: Proceedings of the International Congress on Modeling Mental Processes and Disorders, 24–29 May 2004, Kuşadası, Turkey

28. Holzheimer K (2014a) Dataplore – Analysis of signals and time series data. https://www.ixellence.com/index. php/en/products/dataplore. Accessed 25 Aug 2014

29. Holzheimer K (2014b) ixTrend – recording vital signs from Philips IntelliVue patient monitors. https:// www.ixellence.com/index.php/en/products/ixtrend. Accessed 25 Aug 2014

30. Jose L., Alejandro O. David C. Eva C. Automatic Sleep Stages Classification Using EEG Entropy Features and Unsupervised Pattern Analysis Techniques. Entropy 2014, 16, 6573-6589; doi:10.3390/e16126573

31. Guldemır, H., & Sengur, A. (2006). Comparison of clustering algorithms for analog modulation classification. Expert Systems with Applications, 30(4), 642–649.

32. Latifog lu, F., Polat, K., Kara, S., & Güneßs, S. Medical diagnosis of atherosclerosis from carotid artery Doppler signals using principal component analysis (PCA), k-NN based weighting pre-processing and artificial immune recognition system (AIRS). Journal of Biomedical Informatics, 41(1), 15–23(2008).

33. MacQueen, B. (1967). Some Methods for classification and analysis of multivariate observations. In Proceedings of 5th Berkeley symposium on mathematical statistics and probability (Vol. 1, pp. 281–297). Berkeley: University of California Press.

34. Aditya C., Abhijeet A., Aakash., Kedar D., Pranav S. A machine learning model for identifying cyclic alternating patterns in the sleeping brain.[stat.ML] 23 Apr 2018

35. Foroozan Karimzadeh; Esmaeil Seraj; Reza Boostani ; Mohammad Torabi-Nami, Presenting efficient features for automatic CAP detection in sleep EEG signals, July 9, 2015

36. M. Sharanreddy, P. K. Kulkarni Automated EEG signal analysis for identification of epilepsy seizures and brain tumor, Journal of Medical Engineering & Technology Volume 37, 2013 - Issue 8

37. Liborio Parrino, Mirella Boselli, Maria Cristina Spaggiari, Arianna Smerieri, Mario Giovanni Terzano. Cyclic alternating pattern (CAP) in normal sleep: polysomnographic parameters in different age groups, Istituto di Neurologia, Universita` degli Studi, Via del Quartiere 4, 43100 Parma, Italy, 23 July 1998.

38. Luana Novelli, Raffaele Ferri, Oliviero Bruni Sleep cyclic alternating pattern and cognition in children: A review, International Journal of Psychophysiology, August 2013, Pages 246-251

39. Smerieri A, Parrino L, Agosti M, Ferri R, Terzano MG. Cyclic alternating pattern sequences and non-cyclic alternating pattern periods in human sleep. Clin Neurophysiol 2007;118(10):2305-13.

40. Sara Mariani, Anna M., Elena ManfrediniBianchi. Automatic Detection of A phases of the Cyclic Alternating Pattern during sleep.

41. Mathematical Modeling and Data Analysis of Electroencephalographic Signals: A Review Varsha K. Harpale1, Dr. Vinayak K. Bairagi2 International Journal of Emerging Technology and Advanced Engineering Website: www.ijetae.com (ISSN 2250-2459, ISO 9001:2008 Certified Journal, Volume 5, Issue 3, March 2015).

42. Mingyang Li , Wanzhong Chen ''FFT-based deep feature learning method for EEG classification'' College of Communication Engineering, Jilin University, Changchun, 130012, China

43. Parrino L, Ferri R, Bruni O, Terzano MG. Cyclic alternating pattern (CAP): the marker of sleep instability. Sleep Med Rev 2012a;16(1):27-45.

46. F´atima Machado1, C´esar Teixeira1, Clara Santos2, Conceic¸A-phases subtype detection using different classification methods˜ao Bento3, Francisco Sales3 and Ant´onio Dourado1, Member IEEE,2016

47. Hamid Niknazar, Saman Seifpour, Anahita KhorramiA Novel Method to Detect the A Phases of Cyclic Alternating Pattern (CAP) Using Similarity Index, 2015 23rd Iranian Conference on electrical Engineering IEEE.

48. Reza Boostani , Foroozan Karimzadeh , Mohammad Nami , A comparative review on sleep stage classification methods in patients and healthy individuals, Computer Methods and Programs in Biomedicine 140 (2017) 77–91.

49. Amjed S Al-Fahoum , Ausilah A Al-Fraihat, Methods of EEG signal features extraction using linear analysis in frequency and time-frequency domains, 2014 Feb 13;2014:730218

50. Luay Fraiwana, Khaldon Lweesyb,1, Natheer Khasawnehc, Heinrich Wenzd, Hartmut Dickhause. Automated sleep stage identification system based on time–frequency analysis of a

single EEG channel and random forest classifier computer methods and programming biomedicine 1 0 8 (2 0 1 2) 10–19

51. Alaleh Rabie1, Ahmed Al-Ani1, Bram Van Dun2, Harvey Dillon2. Detection of alertness states using electroencephalogram and cortical auditory evoked potential responses, Conference Paper · November 2013 DOI: 10.1109/NER.2013.6696213

52. D. Puthankattil Subha, Paul K. Joseph,Rajendra Acharya U ,Choo Min Lim EEG Signal Analysis: A Survey. Paper 6 December 2008 Springer J Med Syst (2010) 34:195–212 DOI 10.1007/s10916-008-9231-z

53 Anna Krakovska∗, Kristina Mezeiova. Automatic sleep scoring: A search for an optimal combination of measures. Institute of Measurement Science, Slovak Academy of Sciences, Dúbravská cesta 9, 842 19 Bratislava, Slovak Republic. Artificial Intelligence in Medicine 53 (2011) 25– 33

54. Processing Turky Alotaiby1*, Fathi E Abd El-Samie2,3, Saleh A Alshebeili4 and Ishtiaq Ahmad5, Alotaiby et al. A review of channel selection algorithms for EEG signal. EURASIP Journal on Advances in Signal Processing (2015) 2015:66 DOI 10.1186/s13634-015-0251-9

55. W. R. Klemm Why does REM sleep occur? A wake-up hypothesis Texas A&M University Article in Frontiers in Systems Neuroscience · September 2011 DOI: 10.3389/fnsys.2011.00073 · Source: PubMed

56. Swati Vaid, Preeti Singh, Chamandeep Kaur. EEG Signal Analysis for BCI Interface: A Review. 2015 Fifth International Conference on Advanced Computing & Communication Technologies. 2327-0659/15 2015 IEEE DOI 10.1109/ACCT.2015.72

57. Khalid A., Massudi M., Ramy H., Amr M.: Performance Evaluation for Compression Accuracy trade off using Compressive Sensing for EEG based Epileptic Seizure Detection in Wireless Tele-monitoring. Department of Computer Science & Engineering, College of Engineering, Qatar University. Qatar Awang Had Salleh Graduate School of Arts and Science, Utara Malaysia, Malaysia Conference Paper.July 2013 DOI: 10.1109/IWCMC.2013.6583564

58. Antoine Kass-iliyya, Hashim Hashim: Nocturnal polyuria: Literature review of definition, pathophysiology, investigations and treatment. Journal of Clinical Urology · February 2018 DOI: 10.1177/2051415818756792.

59. Qiang Pan; Damien Brulin; Eric Campo: Current Status and Future Challenges of Sleep Monitoring Systems: Systematic Review, LAAS-CNRS, University of Toulouse, Toulouse, France; http://biomedeng.jmir.org/2020/1/e20921/

60. Alturki, F.A.; AlSharabi, K.; Aljalal, M.; Abdurraqeeb, A.M. A DWT-Band power-SVM Based Architecture for Neurological Brain Disorders Diagnosis Using EEG Signals. In Proceedings of

the 2019 2nd International Conference on Computer Applications & Information Security (ICCAIS), Riyadh, Saudi Arabia, 1–3 May 2019.

Appendix A (Code Scripts)

Convert to physical signal (for Normal Patinets)

```
% plot of the patient with respect to time
%normal subjects
data_n1  = 'n1_edfm';
[tm,signal,Fs,siginfo]=rdmat(data_n1);
time_sec1n = tm;
sig_response_sec1n = signal;
figure(1)
plot(time_sec1n,sig_response_sec1n);
title('N subjects with respect to time');
xlabel('seconds');
ylabel('signal response');
grid on

hold on

data_n2  = 'n2_edfm';
[tm,signal,Fs,siginfo]=rdmat(data_n2);
time_sec2n = tm;
sig_response_sec2n = signal;
figure(1)
plot(time_sec2n,sig_response_sec2n);

data_n3  = 'n3_edfm';
[tm,signal,Fs,siginfo]=rdmat(data_n3);
time_sec3n = tm;
sig_response_sec3n = signal;
figure(1)
plot(time_sec3n,sig_response_sec3n);

data_n5  = 'n5_edfm';
[tm,signal,Fs,siginfo]=rdmat(data_n5);
time_sec5n = tm;
sig_response_sec5n = signal;
figure(1)
plot(time_sec5n,sig_response_sec5n);

hold off

% %%% plot of the patient with respect to samples
[tm,signal,Fs,siginfo]=rdmat(data_n1);
time_sample1n = (tm/Fs);
sig_sample1n = signal;
figure(2)
plot(time_sample1n,sig_sample1n);
title('N subjects with respect samples');
xlabel('samples');
```

```
ylabel('signal response');
grid on

hold on

[tm,signal,Fs,siginfo]=rdmat(data_n2);
time_sample2n = (tm/Fs)*3600/7;
sig_sample2n = signal;
figure(2)
plot(time_sample2n,sig_sample2n);

[tm,signal,Fs,siginfo]=rdmat(data_n3);
time_sample3n = (tm/Fs)*3600/7;
sig_sample3n = signal;
figure(2)
plot(time_sample3n,sig_sample3n);

[tm,signal,Fs,siginfo]=rdmat(data_n5);
time_sample5n = (tm/Fs)*3600/7;
sig_sample5n = signal;
figure(2)
plot(time_sample5n,sig_sample5n);
hold off

%FOR OTHER PATIENTS - PHYSICAL SIGNAL
[tm,signal,Fs,siginfo]=rdmat('n1_edfm');
x_p = tm;
y_p = signal;
F_p = Fs;
figure(1)
plot(x_p,y_p);
title('n patient (n1)');
xlabel('time in seconds');
ylabel('Response n1 Signal');
grid on
% FOR N PATIENTS - PHYSICAL SIGNAL
[tm,signal,Fs,siginfo]=rdmat('n1_edfm');
x_n = tm;
y_n = signal;
F_n = Fs;
figure(2)
plot(x_n,y_n);
title('N Patient (N1)');
xlabel('time in seconds');
ylabel('Response signal');
grid on
```

plotting CAP for N1 Subject

```
%******************
% y_p = signal response for patient
% x_n = time response for patient
% x_n = time response for normal patient
% y_n = signal response for normal patient
```

```
%initializing counter for patient
event_count_p=0;

for k=2:length(y_p(1:10000))
    if(y_p(k)>y_p(k-1) & y_p(k)>y_p(k+1) & y_p(k)>1)
        k;
        disp('dominant peak found');
        event_count_p=event_count_p+1;
       end
    CAP_y_p(k) = y_p(k); %to store CAP signal response whenever the
event is indicated by k
    CAP_x_p(k) = x_p(k); %to store CAP time response whenever the event
is indicated by k
end
event_count_p;
N_p=length(y_p);
peak_duration_p= N_p/F_p;  %this event duration is in seconds -
dividing the samples (N) and frequency results in the time
CAP_event_p = event_count_p/peak_duration_p;

figure(3)
title('Physical CAP response in patient(n1)');
xlabel('time in seconds');
ylabel('Response signal');
grid on
hold on
plot(CAP_x_p,CAP_y_p,'ro');


%initializing counter for normal patient
event_count_n=0;

for k_n=2:length(y_n(1:10000))
    if(y_n(k_n)>y_n(k_n-1) && y_n(k_n)>y_n(k_n+1) && y_n(k_n)>1)
        k_n;
        disp('dominant peak found');
        event_count_n=event_count_n+1;

       end
    CAP_y_n(k_n) = y_n(k_n); %to store CAP signal response whenever the
event is indicated by k
    CAP_x_n(k_n) = x_n(k_n); %to store CAP time response whenever the
event is indicated by k
end
event_count_n;
N_n=length(y_n);
 peak_duration_n= N_n/F_n;  %this event duration is in seconds -
dividing the samples (N) and frequency results in the time
 CAP_event_n = event_count_n/peak_duration_n;

figure(4)
title('Physical CAP response in normal(N1)');
xlabel('time in seconds');
ylabel('Response signal');
grid on
```

```
hold on
plot(CAP_x_n,CAP_y_n,'ro');
```

Main Code to retrieve the accuracy results For N1

```
run ScoringReader %this is to obtain the cap events starting time and
durations in the physical signal response
run convert_to_physical_signal_n %this is to get the physical signal
response

%declaring nonCAP and CAP specific variables
data_n1_nonCap = time_sec1n(1:1700);%chose a sample size of data points
for similar comparison of the CAP events value obtained from scoring
reader variable (time_total)
data_n1_CAP = time_tot; %the starting time of the CAP events
sig_response_n1_sec_CAP = sig_response_sec1n(1632:5000); %need to
obtain the y responses of only CAP data points for FFT function

%running entropy features for CAP and nonCAP time values
[y_renyi_n1_nonCap] = renyi_entro(data_n1_nonCap,2);
[y_renyi_n1_Cap] = renyi_entro(data_n1_CAP,2);

[y_tsallis_n1_nonCap] = Tsallis_entro(data_n1_nonCap,2);
[y_tsallis_n1_Cap] = Tsallis_entro(data_n1_CAP,2);

[y_shannon_n1_nonCap] = shannon_entro(data_n1_nonCap);
[y_shannon_n1_CAP] = shannon_entro(data_n1_CAP);

[y_sample_n1_nonCap] =
sample_entropy(data_n1_nonCap,2,0.2,'chebychev');
[y_sample_n1_CAP] = sample_entropy(data_n1_CAP,2,0.2,'chebychev');

[y_HHT_n1_nonCap] = HHT(sig_response_sec1n,32); %32 represents the Kmax
for ins1 because that is the gain (ins1 info txt file) of the signal
from PhysioNet
[y_HHT_n1_Cap] = HHT(sig_response_n1_sec_CAP,32);

%Here, utilized time and response data for ins1_edfm (CAP/nonCAP)
run FastFourierTransform_nonCap_n1
y_FFT_nonCap_n1 = ans;

run FastFourierTransform_Cap_n1
y_FFT_Cap_n1 = ans;

%once all feature results are available, create an excel spreadsheet
for record keeping.

ClassifierTable_N1_ALL =
readtable('FINAL_table_n1.xlsx','Range','A1:G1506'); %here to select
the size of the imported table
```

```
[RDT_trainedClassifier_FFT, RDT_validationAccuracy_FFT] =
RDT_trainClassifier_FFTn1(ClassifierTable_N1_ALL);
[RDT_trainedClassifier_HHT, RDT_validationAccuracy_HHT] =
RDT_trainClassifier_HHTn1(ClassifierTable_N1_ALL);
[RDT_trainedClassifier_tsallis, RDT_validationAccuracy_tsallis] =
RDT_trainClassifier_tsallisn1(ClassifierTable_N1_ALL);
[RDT_trainedClassifier_sample, RDT_validationAccuracy_sample] =
RDT_trainClassifier_samplen1(ClassifierTable_N1_ALL);
[RDT_trainedClassifier_shannon, RDT_validationAccuracy_shannon] =
RDT_trainClassifier_shannonn1(ClassifierTable_N1_ALL);
[RDT_trainedClassifier_renyi, RDT_validationAccuracy_renyi] =
RDT_trainClassifier_renyin1(ClassifierTable_N1_ALL);

Accuracy_RDT_all_features =
table(RDT_validationAccuracy_renyi,RDT_validationAccuracy_shannon,RDT_v
alidationAccuracy_tsallis,RDT_validationAccuracy_sample,RDT_validationA
ccuracy_HHT,RDT_validationAccuracy_FFT);

[LDA_trainedClassifier_FFT, LDA_validationAccuracy_FFT] =
LDA_trainClassifier_FFTDn1(ClassifierTable_N1_ALL);
[LDA_trainedClassifier_HHT, LDA_validationAccuracy_HHT] =
LDA_trainClassifier_HHTDn1(ClassifierTable_N1_ALL);
[LDA_trainedClassifier_tsallis, LDA_validationAccuracy_tsallis] =
LDA_trainClassifier_tsallisDn1(ClassifierTable_N1_ALL);
[LDA_trainedClassifier_sample, LDA_validationAccuracy_sample] =
LDA_trainClassifier_sampleDn1(ClassifierTable_N1_ALL);
[LDA_trainedClassifier_shannon, LDA_validationAccuracy_shannon] =
LDA_trainClassifier_shannonDn1(ClassifierTable_N1_ALL);
[LDA_trainedClassifier_renyi, LDA_validationAccuracy_renyi] =
LDA_trainClassifier_renyiDn1(ClassifierTable_N1_ALL);

Accuracy_LDA_all_features =
table(LDA_validationAccuracy_renyi,LDA_validationAccuracy_shannon,LDA_v
alidationAccuracy_tsallis,LDA_validationAccuracy_sample,LDA_validationA
ccuracy_HHT,LDA_validationAccuracy_FFT);

[KNN_trainedClassifier_FFT, KNN_validationAccuracy_FFT] =
KNN_trainClassifier_FFTn1(ClassifierTable_N1_ALL);
[KNN_trainedClassifier_HHT, KNN_validationAccuracy_HHT] =
KNN_trainClassifier_HHTn1(ClassifierTable_N1_ALL);
[KNN_trainedClassifier_tsallis, KNN_validationAccuracy_tsallis] =
KNN_trainClassifier_tsallisn1(ClassifierTable_N1_ALL);
[KNN_trainedClassifier_sample, KNN_validationAccuracy_sample] =
KNN_trainClassifier_sampleDn1(ClassifierTable_N1_ALL);
[KNN_trainedClassifier_shannon, KNN_validationAccuracy_shannon] =
KNN_trainClassifier_shannonn1(ClassifierTable_N1_ALL);
[KNN_trainedClassifier_renyi, KNN_validationAccuracy_renyi] =
KNN_trainClassifier_renyin1(ClassifierTable_N1_ALL);

Accuracy_KNN_all_features =
table(KNN_validationAccuracy_renyi,KNN_validationAccuracy_shannon,KNN_v
alidationAccuracy_tsallis,KNN_validationAccuracy_sample,KNN_validationA
ccuracy_HHT,KNN_validationAccuracy_FFT);

[SVM_trainedClassifier_FFT, SVM_validationAccuracy_FFT] =
SVM_trainClassifier_FFTn1(ClassifierTable_N1_ALL);
```

```
[SVM_trainedClassifier_HHT, SVM_validationAccuracy_HHT] =
SVM_trainClassifier_HHTn1(ClassifierTable_N1_ALL);
[SVM_trainedClassifier_tsallis, SVM_validationAccuracy_tsallis] =
SVM_trainClassifier_tsallisn1(ClassifierTable_N1_ALL);
[SVM_trainedClassifier_sample, SVM_validationAccuracy_sample] =
SVM_trainClassifier_samplen1(ClassifierTable_N1_ALL);
[SVM_trainedClassifier_shannon, SVM_validationAccuracy_shannon] =
SVM_trainClassifier_shannonn1(ClassifierTable_N1_ALL);
[SVM_trainedClassifier_renyi, SVM_validationAccuracy_renyi] =
SVM_trainClassifier_renyin1(ClassifierTable_N1_ALL);

Accuracy_SVM_all_features =
table(SVM_validationAccuracy_renyi,SVM_validationAccuracy_shannon,SVM_v
alidationAccuracy_tsallis,SVM_validationAccuracy_sample,SVM_validationA
ccuracy_HHT,SVM_validationAccuracy_FFT);

allCLASSIFIER_accuracies_n1 =
table(Accuracy_LDA_all_features,Accuracy_KNN_all_features,Accuracy_SVM_
all_features,Accuracy_RDT_all_features);
```

FastFourierTransform_Cap_n1

```
% to get length of signal fs* time

fs = 512; %sampling frequency
t = 0: 1/fs : 10 - 1/fs;

%now apply FFT function
X= fft(sig_response_sec1n(1632:3132)); %(X stores time domain (x) function)

 %z= length (x_sdb);%return samples
%lenght (X) = zt; %returns bin values not samples

X_mag = abs(X);

X_mag(30:34);

 plot(X_mag, sig_response_sec1n(1632:3132)); %spikes correspond to a frequency component
(mirror image left and right hand side)

%frequency on x axis = fs/2
format long
%get f1. f2 and f3 corresponds to lowest - middle- highest frequency
X_phase = angle(X);
plot(X_mag/(fs/2)); %results to time %display lower half of output to better see CAP

Cap=X_mag/(fs/2);

figure(1)
grid on
xlabel('time (s)')
ylabel('length of signal')
```

FastFourierTransform_nonCap_n1

```
% to get length of signal fs* time


fs = 512; %sampling frequency
t = 0: 1/fs : 10 - 1/fs;

plot(time_sec1n(1:1500),sig_response_sec1n(1:1500)); %here we are passing X and Y of sdb - shown in the workspace


%now apply FFT function
X= fft(sig_response_sec1n(1:1500)); %(X stores time domain (x) function)

 %z= length (x_sdb);%return samples
%lenght (X) = zt; %returns bin values not samples

X_mag = abs(X);

X_mag(30:34);

 plot(X_mag, sig_response_sec1n(1:1500)); %spikes correspond to a frequency component (mirror image left and right hand side)

%frequency on x axis = fs/2
format long
%get f1. f2 and f3 corresponds to lowest - middle- highest frequency
X_phase = angle(X);
plot(X_mag/(fs/2)); %results to time %display lower half of output to better see CAP

nonCap=X_mag/(fs/2);

figure(1)
grid on
xlabel('time (s)')
ylabel('length of signal')
```